DOWNSCALING METEOROLOGICAL PREDICTIONS FOR SHORT-TERM HYDROLOGIC FORECASTING

DOWNSCALING METEOROLOGICAL PREDICTIONS FOR SHORT-TERM HYDROLOGIC FORECASTING

By

XIAOLI LIU

Master of Science (Chinese Academy of Sciences)

A Thesis

Submitted to the School of Graduate Studies

in Partial Fulfillment of the Requirements

for the Degree

Master of Applied Science

McMaster University

Department of Civil Engineering

MASTER OF APPLIED SCIENCE (2007) McMaster University
(Civil Engineering) Hamilton, Ontario

TITLE: Downscaling Meteorological Predictions for Short-Term Hydrologic Forecasting

AUTHOR: Xiaoli Liu
M.S. (Chinese Academy of Science)
B.S. (Nankai University)

SUPERVISOR: Dr. Paulin Coulibaly

NUMBER OF PAGES: xi, 110

Abstract

This study investigates the use of large scale ensemble weather predictions provided by the National Centers for Environmental Prediction (NCEP) medium range forecast (MRF) modeling system, for short-term hydrologic forecasting. The weather predictors are used to downscale daily precipitation and temperature series at two meteorological stations in the Saguenay watershed in northeastern Canada. Three data-driven methods, namely, statistical downscaling model (SDSM), time lagged feedforward neural network (TLFN), and evolutionary polynomial regression (EPR), are used as downscaling models and their downscaling results are compared. The downscaled results of the best models are used as additional inputs in two hydrological models, Hydrologiska Byråns Vattenbalansavdelning (HBV) and Bayesian neural networks (BNN), for up to 14 day ahead reservoir inflow and river flow forecasting. The performance of the two hydrological forecasting models is compared, the ultimate objective being to improve 7 to 14 day ahead forecasts.

The downscaling results show that all the three models have good performance in downscaling temperature time series, the correlation between the observed and downscaled data is more than 0.90, however the downscaling results are less accurate for precipitation, the correlation coefficient is no more than 0.62. TLFN and EPR models have quite close performance in most cases, and they both perform better than SDSM.

Therefore the TLFN downscaled meteorological data are used as predictors in the HBV and BNN hydrological models for up to 14 day ahead reservoir inflow and river flow forecasting, and the forecasting results are compared with the case where no downscaled data is included. The results show that for both reservoir inflow and river flow, HBV models have better performance when including downscaled meteorological data, while there is no significant improvement for the BNN models. When comparing the performance of HBV and BNN models through scatter plots, it can be found that BNN models perform better in low flow forecasting than HBV models, while less good in peak flow forecasting.

Acknowledgements

I would hereby express my appreciation to my supervisor, Dr. Paulin Coulibaly, for his patience and valuable suggestions in my thesis study. When I am confused and talk with him, he always tries to help in time. I benefit a lot and I could not have completed this thesis without his help.

I also appreciate the help I received from my friends in the lab, Ashok, Getnet, and Tarana. During the thesis study, I learned a lot from them.

Here I can not ignore the great support I received from my family, especially from my parents. They always understand my decisions and support me ever since.

I also want to say thanks to my boyfriend, Lin. Whenever I meet with any problems, he is always there to help me.

Table of Contents

List of Tables

List of Figures

List of Symbols

m	The size of the hidden layer in a network
n	Time steps
w_j	The weight vector for the connection between the hidden and output layers
k	The memory depth
w_{ji}	The weight matrix for the connection between the input and hidden layers
b_j	Network biases
$Y_{Nx1}(\theta,Z)$	The least squares estimate vector of the N target values
Z_{Nxd}	A matrix formed by vectors of bias and vectors of bariables
I	The unitary vector for bias
N	The number of target values
z_j	A transformed variable
a_j	An adjustable parameter in a polynomial term
a_0	An optional bias in polynomials
θ	The vector of parameters in the polynomial terms
h	The number of the parameters in the polynomial terms
d	$d=h+1$
p	The number of predictors in SDSM models
x_i	The predictor in SDSM models
α_i	The coefficient in SDSM models

Chapter 1: Introduction

1.1 Background

Rapid population growth and economic development, along with changing social demands on freshwater resources, have imposed new challenges on water management in many regions around the world. Managers must balance the need to retain enough water in reservoirs to meet the needs of irrigation, hydropower generation, and domestic consumption, along with needs such as ensuring an adequate supply of water for recreational uses, as well as meeting stringent water quality standards, regulations for maintenance of aquatic ecosystems. In order to improve water resources management in various areas (e.g. reservoir operation, water supply, and flood or drought mitigation, etc.), accurate site-specific forecast of reservoir inflow and river flow is needed with adequate lead time.

Many studies have sought to examine the potential of hydrologic models for longer lead time (up to 2 weeks ahead) forecasting of hydrologic variables for efficient management of water resource systems. In most of the previous studies on river flow forecasts, the forecast lead time was less than 7 days ahead because usually when the lead time increases, the model performance deteriorates (Goswami, and O'Connor, 2007; Sivakumar at al., 2002; Karunasinghe, and Liong, 2006; Coulibaly et al, 2000; Coulibaly et al, 2001a). A number of recent studies have attempted to link hydrologic models with downscaled outputs from large scale climate or weather forecasting models (Leung et al., 1999; Hay et al., 2000; Bergström et al., 2001). It is observed that daily temperature and precipitation are the principal atmospheric forcing parameters required for hydrologic modeling, and a spatial resolution of 0.125° is generally sufficient to simulate the flows. Climate or weather forecasting models, however, are run at much coarser resolutions (typically 2° or more) and do not resolve important mesoscale processes and surface features that control the regional precipitation. Thus, downscaling methods have been developed to generate local/regional scale data from the climate or weather models.

Downscaling methods were initially developed for generating high resolution data from global climate models (GCMs) outputs. Kalnay et al. (1996) suggested that National Centers for Environmental Prediction–National Center for Atmospheric Research (NCEP–NCAR) predictions shall be used as the large-scale predictor fields in an analogous manner to which a general circulation model (GCM) would be used in a climate change study. It is observed that precipitation is determined entirely by the large-scale model. Wilby et al. (1999) examined the hydrological response in the Animas River basin of Colorado to dynamically and statistically downscaled output from NCEP–NCAR. A distributed hydrological model was then applied to the downscaled data. Relative to raw NCEP output, downscaled climate variables provided more realistic simulations of basin-scale hydrology. However, the results highlight the sensitivity of modeled processes to the choice of downscaling techniques, and point to the need for caution when interpreting future hydrological scenarios. Given the large systematic biases and the poor skill present in NCEP precipitation and temperature estimates in some regions, it is necessary to explore methods that may improve upon these global-scale models (Hay and Clark, 2003). It is observed from the study that hydrologic models based on the downscaled output have a significant role in better understanding as well as to forecast the model outputs over longer lead time.

In this study downscaling methods are used to generate high resolution (i.e local scale) ensemble weather predictions from data provided by the National Centers for Environmental Prediction (NCEP) medium range forecast (MRF) modeling system, which has a resolution of 2.5°. This study can be divided into two major parts: downscaling large-scale meteorological prediction and short-term hydrological forecasting. In the first part, precipitation and temperature time series data of Saguenay watershed is downscaled from the large-scale meteorological forecast using three downscaling methods. Time lagged feedforward neural networks (TLFN) have temporal processing capability without resorting to complex and costly training methods. Evolutionary polynomial regression (EPR) is another data-driven method based on hybrid evolutionary paradigm. The results of these two models are compared with the well-known multiple regression based downscaling tool, namely the statistical downscaling model (SDSM). The downscaling model performances of TLFN and EPR are compared and the downscaled daily meteorological data of the best model results are selected as inputs in hydrological models to improve short-term hydrologic forecasting. The downscaled results of SDSM are also used as inputs in the hydrological models as a benchmark for comparison.

In the second part, two hydrological models, namely, the data-driven model Bayesian neural network (BNN) and the widely used conceptual HBV model, are applied for short term reservoir inflow and river flow forecasting. This study is aimed at improving up to 14 day ahead reservoir inflow and river flow forecasts including up to 14 day ahead precipitation and temperature downscaled from meteorological predictions. The hydrological model results are compared with the results of the models where no downscaled data is included.

1.2 Research Objectives

The overall purpose of this study is to derive local scale meteorological information from the 3-D large scale MRF ensemble predictions, and to include these local or downscaled meteorological forecasts in up to 14 day ahead reservoir inflow and river flow forecasts in Saguenay watershed. In order to accomplish this purpose, the specific objectives are listed as follows:

- Investigate and identify an optimal approach for using the large scale MRF ensemble data in downscaling daily precipitation and temperature data.
- Identify optimal downscaling models that can capture the complex relationship between selected large-scale predictors and locally observed meteorological variables using three different data-driven methods (i.e. linear regression method, ANNs, and Genetic Programming).

- Increase the performance of hydrological models specially for 7 to 14 day ahead forecasting using the downscaled meteorological predictions.
- Compare the performance of two different hydrological models for hydrologic forecasts up to 14 day ahead and assess the impact of the downscaled weather predictions on the hydrologic model forecast results.

1.3 Structure of Thesis

This thesis consists of 6 chapters including this introduction, which is Chapter 1. Chapter 2 describes the study area and data used. In Chapter 3, downscaling methods are reviewed and the two methods applied in this study are especially described. Chapter 4 presents the results of downscaling the MRF ensemble predictions, in which there are two major parts. In the first part, the MRF predictions are explored to identify the best way of using the ensemble predictors for downscaling local precipitation and temperature data. In the second part, the downscaling results from the three different models are analyzed and compared. In Chapter 5, up to 14 day ahead hydrological forecasting is performed using HBV and BNN. In this chapter, the hydrologic forecasting models are firstly introduced, then the input data of the two models are selected, and finally the forecasting results are presented and discussed. In the last Chapter (Chapter 6), the conclusions and recommendation are given.

Chapter 2: Study Area and Data

2.1 Study Area

The study area selected in this research for applying and evaluating downscaling methods and hydrological models is the Chute-du-Diable basin and the Serpent River basin located in the Saguenay-Lac-Saint Jean watershed (Figure 1), which is a well-known flood prone region in Canada. There are a large number of reservoirs and dams in the Saguenay watershed and most of the large reservoirs are managed by the Aluminum Company of Canada (ALCAN) for hydroelectric power production. The sub-basin Chute-du-Diable has an area of 9700 km^2 and is located in the eastern part of the Saguenay watershed. Serpent River basin is located at the middle of the watershed and has an area of 1760 km^2.

2.2 Data Collection

The study area was chosen because of the availability of hydro-meteorological records for a long period in those particular basins. Twenty-three years (1979-2001) of historical total daily precipitation (Prec., in mm), mean maximum temperature (Tmax, in °C) and mean minimum temperature (Tmin, in °C) series for the two particular basins were obtained from the ALCAN hydro-meteorological network and used as predictands in the downscaling models, and as predictors in the hydrological forecasting models. For the Serpent River basin, the precipitation and temperature data were obtained from the Chute-des-Passes meteorological station (station ID 7061541) located near the Serpent basin with latitude and longitude of 49.9°N and 71.25°W respectively. For the Chute-du-Diable basin, the precipitation and temperature data were obtained from both the Chute-des-Passes and the Chute-du-Diable meteorological stations. The latter station is located at 48.75°N and 71.7°W with ID 7061560.

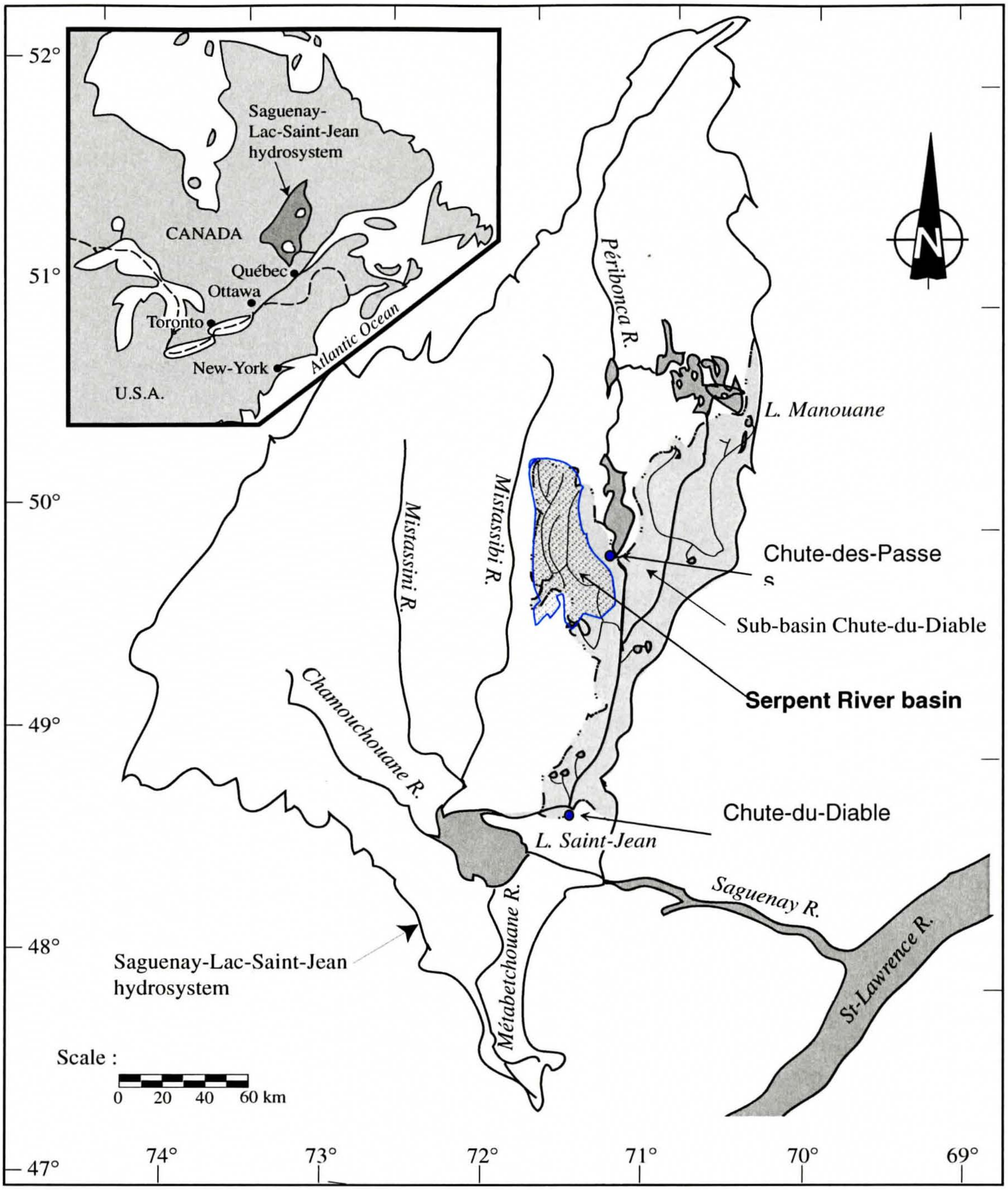

Figure 1: Location map of the Serpent River sub-basin and the Chute-du-Diable sub-basin within the Saguenay –Lac-Saint-Jean watershed

In the downscaling part of this study, the predictors are collected from NCEP. The NOAA-CIRES Climate Diagnostic Center has undertaken a reforecasting project providing retrospective numerical ensemble forecasts. An unchanged version of National Centers for Environmental Prediction's Global Forecast System (NCEP GFS, formely known as MRF) at T62 resolution is used to generate 15-day real-time forecast scenarios (30 time steps of 12 hours each). Forecasts are run every day from 0000 UTC initial conditions from 1979 to present. There are 15-member ensemble forecasts that are generated from 15 initial conditions consisting of a reanalysis and seven pairs of bred modes (Hamill et al., 2004). The global lat-lon (latitude-longitude) grid has a large-scale resolution of 2.5° both in longitude and latitude and contains 144×73 grid points. The map of the NOAA ensemble forecast grid points and the local meteorological station is shown in Figure 2, where the blue points are the grid points, and the two red stars are the meteorological stations.

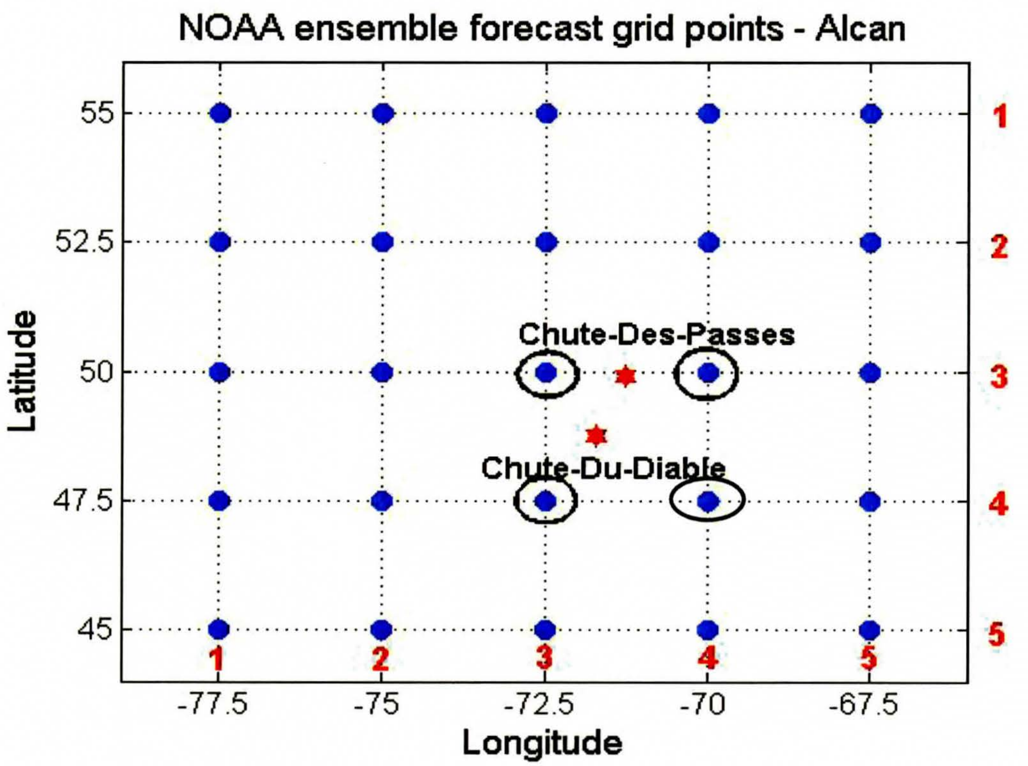

Figure 2: Map of meteorological stations (red stars) and NOAA ensemble forecast grid points (blue points)

The global data were collected directly from the reforecast project ftp server. There are 12 files for 12 variables per day. These files are netCDF (network Common Data Format) files. The 3-D ensemble data for each file is more clearly described in Figure 3. In this figure each sheet contains the data for one forecast range (Fr) or time delay, and there are 15 delays for each variable. In each sheet, there are 15 members data shown in time series for that delay.

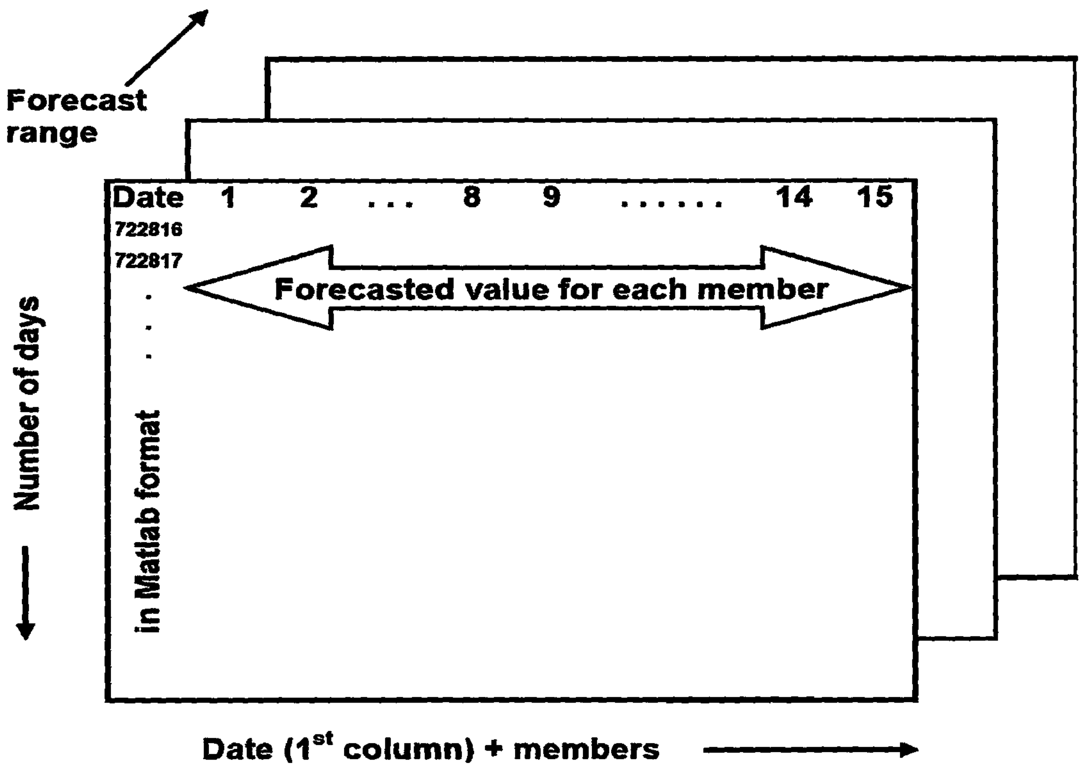

Figure 3: Description of 3-D ensemble meteorological data (courtesy Dr. Evora)

In order to get geographical subsets of grid points over a region of interest, an operator named "ncks" (netCDF Kitchen Sink) from NCO (netCDF Operators) is used. This operator is executed through a Matlab Graphical User Interface that has been developed. Geographical subsets are produced by "ncks" only from a global latlon grid. So, we have been able to process only the first eight variable fields shown on Table 1. The geographical subsets files are also netCDF files. So a second operation was necessary to transform the netCDF files for the geographical subsets into Matlab files using MexCDF conversion utilities. MexCDF is a mex-file interface between NetCDF and MATLAB.

In the hydrological forecasting part, the precipitation and temperature data from the two meteorological stations described above are used as predictors to forecast the short-term Serpent river flows and forecast the reservoir inflows in Chute-du-Diable respectively. The observed flow data for the Serpent river basin are obtained from a hydrometric station (station ID 062214) located at 49.41°N and 71.22°W. For this station, 11 years of observed river flow data is available, from 1991 to 2001, among which the first 8 years (1991-1998) of data are used to calibrate the hydrologic models, and the last 3 years (1999-2001) of data are used to validate the models. The observed reservoir inflow data are for the whole Chute-du-Diable catchment, and 23 years of inflow data (1979-2001) are used in the study, the first 18 years (1979-1996) data are used for calibration, and the last 5 years (1997-2001) data are used for validation.

Table 1: NOAA reforecast ensemble variable fields

Variable Field	Description	Surface level (mb)
apcp	Accumulated precipitation (mm)	Surface
heating	Vertically integrated diabatic heating (K/s/mb)	Vertical average
pwat	Precipitable water	Surface
prmsl	Pressure reduced to mean sea-level (Pa)	Surface
t2m	Temperature at 2 meters (K)	Surface
rhum	Relative humidity (%)	700 mb
u10m	Zonal wind at 10 meters (m/s)	Surface
v10m	Meridional wind at 10 meters (m/s)	Surface

mb: millibar

Chapter 3: Downscaling methods

3.1 Downscaling Methods Review

There are varieties of downscaling techniques, but they can be identified as two major approaches, namely, dynamic approaches (in which physical dynamics are solved explicitly) and empirical approaches (the so-called 'statistical downscaling') (Burger and Chen, 2005, Coulibaly et al, 2005).

3.1.1 Dynamical Downscaling

The dynamical downscaling approach is to embed a higher-resolution limited-area climate model into the GCMs over an area of interest, using the GCM data as the boundary conditions. The dynamic downscaling is achieved by developing and using limited-area models (LAMs) or regional climate models (RCMs). Regional Climate Models are run at finer horizontal resolution than the global-scale models, and thus provide a more accurate depiction of important model components. The main advantage of RCMs is that they can resolve smaller-scale atmospheric features such as orographic precipitation or low-level jets better than the host GCM. Furthermore, RCMs can be used to explore the relative significance of different external forcings such as terrestrial-ecosystem or atmospheric chemistry changes (Wilby et al, 2002). However, there are several limitations of RCMs. The main limitation is that they require considerable computing resources and they are as expensive to run as GCMs. RCMs also suffer from similar bias problems as the global-scale models (Hay et al. 1991, Hay and Clark, 2003), and the scenarios produced by RCMs are sensitive to the choice of boundary conditions used to initiate experiments. RCM errors are still too large, especially over complex terrain, for a direct coupling to hydrologic models (Giorgi and Mearns, 1999). Besides, they are inflexible in the sense that expanding the region or moving to a slightly different region requires redoing the entire experiment, which is expensive to apply (Crane and Hewitson, 1998).

3.1.2 Empirical Downscaling

Empirical downscaling methods seek to derive the local-scale information from the larger scale data through inference from the cross-scale relationship, using some random and/or deterministic functions (Coulibaly et al., 2005). The concept of regional climate being conditioned by the large-scale state may be written as

$$R=F\,(L) \qquad (1)$$

where R represents the predictand (a regional or local climate variable), L is the predictor (a set of large-scale climate variables), and F is a deterministic/stochastic function conditioned by L and has to be found empirically from observation or modeled datasets. When using downscaling for assessing regional climate change, three implicit assumptions are made: 1) the predictors are variables of relevance and are realistically modeled by the GCM; 2) the predictors that are employed fully represent the climate change signal; 3) the relationship is valid also under altered climate conditions.

Empirical downscaling methods have enjoyed a rapid development over the last few years with many different statistical methods employed: multiple regression (Karl et al., 1990; Wigley et al., 1990), canonical correlation, neural networks or stochastic simulation (Cannon and Whitfield, 2002; Dibike and Coulibaly, 2006; Coulibaly et al., 2005). All the methods, however, translate the large-scale GCM information into a high resolution distribution based on empirically derived relationships (Landman et al., 2001).

There are several advantages and limitations in using statistics to derive spatially more detailed climate scenarios. The biggest advantages are that these models are less computer-intensive and are able to produce long time series of climate variables for climate impact studies. Once the methodology has been established and tested it can be applied relatively easily to other GCMs, regions, and parameters. Assuming observed data are available, a statistical model can be used to derive parameters which are not explicitly simulated by the GCM.

A limitation of statistical models is that they always need long and homogeneous time series of observations for model training and testing. Hence, in data-sparse regions, this technique is unsuitable. Another disadvantage arises from the assumption that the underlying scale interactions will remain constant under changed climate conditions (Schubert and Henderson, 1997). Statistical downscaling methods can be classified according to the techniques used or according to the chosen predictor variables (Wilby and Wigley, 1997). In Wilby and Wigley's study (1997), statistical downscaling techniques are described using three categories, namely: regression methods; weather pattern-based approaches (Wilby, 1995); and stochastic weather generators (Katz, 1996). Because in this study, only regression methods are applied, they are described in the following section.

3.1.3 Regression Methods

Regression-based downscaling methods rely on direct quantitative relationship between the local scale climate variable (predictand) and the variables containing the larger scale climate information (predictors) through some form of regression functions (Wilby et al., 2002). Individual downscaling schemes differ according to the choice of mathematical transfer function, predictor variables or statistical fitting procedure. To date, linear and nonlinear regression, artificial neural networks, canonical correlation and principal component analysis have all been used to derive predictor–predictand relationships (Conway et al., 1996; Dibike and Coulibaly, 2005). The procedures include: 1) identify a large-scale predictor G, which controls the local parameter L; 2) find a statistical relationship between L and G, and validate the relationship with independent data; 3) if the relationship is confirmed, G can be derived from GCM experiments to estimate L.

The main strength of the regression downscaling is the relative ease of application, and simple, less computationally demanding. The main weakness is that the models often explain only a fraction of the observed climate variability (especially in precipitation series). Regression methods also assume validity of the model parameters under future climate conditions, and regression-based downscaling is highly sensitive to the choice of predictor variables and statistical transfer function. Application is limited to the sites, variables and seasons. Furthermore, downscaling future extreme events using regression methods is problematic since these phenomena tend to lie at the margins or beyond the range of the calibration data set (Dibike and Coulibaly, 2006; Coulibaly and Dibike, 2005; Wilby et al., 2002).

In this study, two main regression methods are used, i.e., artificial neural networks (ANNs) and genetic programming (GP), and they are described in the following. The interest in ANNs used for downscaling is nowadays increasing because of their high potential for complex, nonlinear, and time-varying input-output mapping. Artificial neural networks (ANNs) are multi-layer perceptrons used to map relationships between input variables and dependent output variables. An ANN is composed of an input layer, any number of hidden layers and an output layer. Although the weights of an ANN are similar to non-linear regression coefficients, the simple non-linear functions that send information between nodes in a neural network allow the network to approximate extremely non-linear functions. Also, ANNs allow the data to define the functional form. An ensemble ANN downscaling model was capable of predicting changes in stream flows using only large-scale atmospheric conditions as model input (Cannon and Whitfield, 2002). There are some categories of neural networks that have a memory structure to account for temporal relationships in the input-output mappings, and they appear more suitable for complex nonlinear system modeling (Coulibaly et al., 2001b; Coulibaly and Dibike, 2005).

However, there are some limitations of ANNs in climate downscaling. When it is used for downscaling daily precipitation, the performance of ANNs is generally somewhat worse than other methods, mainly owing to an inability of the ANNs to reproduce two key features of high-resolution precipitation time series: intermittency and variability. Intermittency refers to the incidence of both "wet" and ''dry'' time intervals, ANNs tend to generate small trace precipitation in actual dry intervals, thereby overestimating the observed zero-depth probability. Variability, on the other hand, is particularly manifested in sudden and short-lived extreme intensities of magnitudes many times the mean intensity; ANNs typically underestimate the observed extreme intensities (Olsson et al., 2004).

Genetic Programming (GP) is another well known data-driven technique that has showing promising potential for the downscaling of daily extreme temperatures (Coulibaly, 2004). It is an evolutionary computing method that generates a "transparent" and structured representation of the system being studied. The technique creates mathematical expressions to fit a set of data points using the evolutionary process of genetic programming (Giustolisi and Savic, 2004). However, no study has fully investigated and compared the selected data-driven methods for downscaling ensemble weather forecasts.

3.2 Time Lag Feedforword Neural Network (TLFN)

A neural network is characterized by its architecture, which is represented by the network topology and pattern of connections between the nodes, its method of determining the connection weights, and the activation functions that it employs (Khan and Coulibaly, 2006). Multi-layer perceptrons (MLPs), which probably constitute the most widely used network architecture, are composed of a hierarchy of processing units organized in a series of two or more mutually exclusive sets of neurons or layers. The information flow in the network is restricted to a flow, layer by layer, from the input to the output, hence also called feedforward network.

TLFN is a neural network that can be formulated by replacing the neurons in the input layer of an MLP with a memory structure, which is sometimes called a tap delay-line. The size of the memory layer (the tap delay) depends on the number of past samples that are needed to describe the input characteristics in time and it has to be determined on a case-by-case basis. TLFN uses delay-line processing elements, which implement memory by simply holding past samples of the input signal. The output (y) of such a network with one hidden layer is given by

$$y(n) = \varphi_1(\sum_{j=1}^{m} w_j y_j(n) + b_0)$$

$$= \varphi_1(\sum_{j=1}^{m} w_j \varphi_2(\sum_{j=0}^{k} w_{ji} x(n-1) + b_j) + b_0) \quad (2)$$

where m is the size of the hidden layer, n is the time step, w_j is the weight vector for the connection between the hidden and output layers, k is the memory depth, w_{ji} is the weight matrix for the connection between the input and hidden layers, 1 and 2 are transfer functions at the output and hidden layers respectively. b_j and b_0 are additional network parameters (often called biases) to be determined during training of the networks with observed input/output data sets. For the case of multiple inputs (of size p), the delay-line with a memory depth k can be represented by

$$\chi(\mathrm{n}) = [\mathrm{X(n), X(n-1), \ldots, X(n-k+1)}] \quad (3)$$

where $\mathrm{X(n) = (x_1(n), x_2(n), \ldots, x_p(n))}$ and represents the input pattern at time step n, xj(n) is an individual input at the nth time step and is the combined input matrix to the processing elements at time step n. Such delay-line only ‘remembers’ k samples in the past. The advantage of TLFNs is that they share some of the nice properties of feedforward neural networks, but they can capture the information present in the input time signals. An interesting feature of the TLFN is that the tap delay-line at the input does not have any free parameters; therefore the network can still be trained with the classical backpropagation algorithm. The TLFN topology has been successfully used in non-linear system identification, time series prediction, and temporal pattern recognition (Principe et al., 2000). A major advantage of the TLFN is that it is less complex than the conventional time delay and recurrent networks and has the similar temporal patterns processing capability (Coulibaly et al., 2001b; Khan and Coulibaly, 2006).

3.3 Evolutionary Polynomial Regression (EPR)

EPR is a hybrid evolutionary regression technique based on genetic programming (GP) introduced by Koza (1992). GP is a method for constructing populations of mathematical models using stochastic search methods namely evolutionary algorithms. For multivariate time series modeling using the GP approach, the ultimate objective of the evolutionary process is to discover an optimal equation (or model) for relating dependent variable (or predictand) and independent variables (or predictors). However, as the search space of all possible equations is extremely large particularly for multivariate time series, the heuristic search needs to be optimized in term of computational efficiency and parsimonious solution (i.e. model structure). The evolutionary polynomial regression (EPR) technique recently proposed by Giustolisi and Savic (Giustolisi and Savic, 2005) aims to provide an optimal solution by exploiting both numerical and symbolic regression. Essentially, EPR uses a GA to find the form of the polynomial expressions and least squares optimization to determine the values of the parameters in the expressions. The description of the EPR method is limited herein to the needs of the present study. For a more detailed description of the EPR method, readers are referred to other sources, such as Giustolisi and Savic 2003, 2004, 2005.

Although the EPR technique is similar to the rule-based symbolic regression (Davidson et al., 2000), there is a key difference in the search for model structure. While the latter uses rules to simplify symbolic expressions, the former employs a simple GA to search in the model structure space.

In gernaral, the rule-based symbolic regression limits the range of operators normally used in symbolic regression to a subset consisting of addition, multiplication and non-negative integer powers. The expressions that result from applying the limited set of operators are usually in the form of polynomials such as

$$y=\sum_{j=1}^{h}\mathrm{a}_{\mathrm{j}} * \mathrm{z}_{\mathrm{j}} + a_0 \tag{4}$$

where y is the least squares estimate of the target value, a_j is an adjustable parameter for the jth term, a_0 is an optional bias, m is the number of terms/parameters of the expression, and z_j is a transformed variable. In EPR method, it is useful to transform Eq. (4) into the following vector form (Giustolisi and Savic, 2005)

$$Y_{N\times1}(\theta,Z) = [I_{N\times1}\ Z^{j}{}_{N\times h}]\times[a_0\ a_1 \ldots a_h]^T = Z_{N\times d}\times\theta^T{}_{d\times1} \tag{5}$$

where $Y_{Nx1}(\theta,Z)$ is the least squares estimate vector of the N target values; θ_{1xd} is the vector of d=h+1 parameters a_j and a_0 (θ^T is the transposed vector); and Z_{Nxd} is a matrix formed by I, unitary vector for bias a_0, and m vectors of variables Z_j that for fixed j are a product of the independent predictor vectors of inputs, X =(X_1 X_2 … X_k). The key idea behind the EPR is to use evolutionary search for exponents of polynomial expressions by means of a GA engine (Giustolisi and Savic, 2004, 2005). This allows: (a) easy computational implementation of the algorithm; (b) efficient search for an expression (formula); (c) improved control of the complexity of the expression generated; and (d) a small number of search parameters to be pre-specified (Giustolisi and Savic, 2005).

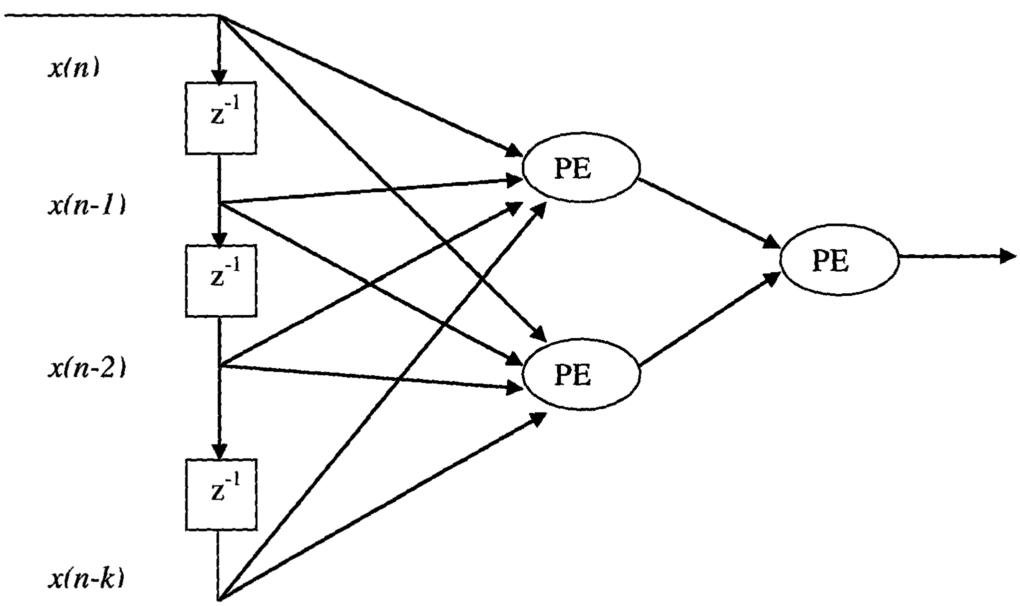

Figure 4: Schematization of the Time lagged feed-forward neural network (TLFN) with one hidden layer, one input variable and a delay-line with memory depth of k

3.4 Statistical DownScaling Model

The most common regression based technique used to map global climate models to individual sites or localities is the Statistical DownScaling Model (SDSM, Wilby et al., 2002). SDSM is best described as a hybrid of the stochastic weather generator and regression based methods. This is because large scale circulation patterns and atmospheric moisture variables are used to linearly condition local scale weather generator parameters (e.g., precipitation occurrence and intensity). Additionally, stochastic techniques are used to artificially inflate the variance of the downscaled daily time series to better accord with observations. To date, the downscaling algorithm of SDSM has been applied to a host of meteorological, hydrological and environmental assessments (Wilby et al., 2002). And hence, SDSM is usually used as a basis of comparison with other downscaling models.

The SDSM uses multiple linear regression (MLR) to model the linear relationship between a dependent variable and one or more independent variables. The dependent variable is also called the predictand, and the independent variables, the predictors. The model expresses the value of a predictand variable as a linear function of one or more predictor variables:

$$\hat{y} = \alpha_0 + \alpha_1 x_1 + \ldots + \alpha_p x_p \tag{6}$$

Where $\hat{y}$ is the predictand (estimation of dependent variables), x_i is the i^{th} predictor, p is the number of predictors, and α_i is the i^{th} coefficient.

The model is fit to a period, called calibration period. In the process of fitting or estimating, the model statistics are computed. The performance of the model on independent data is usually checked in some way by a process called validation (test period). Finally, in the prediction, the regression model is applied to generate estimates of the predictand variable outside the period used to fit the data.

Chapter 4: Downscaling MRF Ensemble Predictions

4.1 Exploration of MRF Ensemble Data for Downscaling

4.1.1 Correlation Analysis

As described in Chapter 2, the predictor variables are derived from the 3-D ensemble forecasts generated by the MRF model. Each variable has 15 time delays, and in each delay, there are 15 members. First, the correlations between the predictands (prec., Tmax, and Tmin) and the predictors are calculated to find the predictors which are most correlated to the predictands. The correlation results are shown in Table 2. From the table we can see that among all the possible predictor variables for precipitation, apcp (predicted accumulated precipitation) appears the most correlated to precipitation. Similarly, t2m (predicted temperature at 2m) is most correlated to observed Tmax and Tmin.

Table 2: Correlation between meteorological observations and MRF predictors

Predictors / Observation	apcp	heating	prmsl	pwat	rhum	t2m	u10m	v10m
Prec.	**0.51**	0.49	-0.32	0.36	0.32	0.2	-0.08	0.19
Tmax	0.17	0.31	-0.19	0.78	-0.1	**0.96**	-0.12	0.18
Tmin	0.27	0.36	-0.3	0.79	0.01	**0.94**	-0.08	0.13

To further investigate the MRF data, the correlation between the observed precipitation and the first member (M1), the mean of the 15 members, and the total of the 15 members of the first delay from the variable apcp are compared. The correlation results are shown in Figure 5, from where we can see that the mean and the total of the members have quite similar correlation with the observed precipitation, and they are better than the correlation between M1 and observed precipitation. Similar analysis is done for Tmax and Tmin, correlations between the observed temperature (Tmax, Tmin) and M1 (of the 15 members of t2m) are compared with the correlations between the observed temperature and the mean of the 15 members of t2m. It appears from Figure 5 that the mean of the 15 members is most correlated with the observed values. Therefore, the mean of each predictor variable is preferred rather than using any single member from the ensembles.

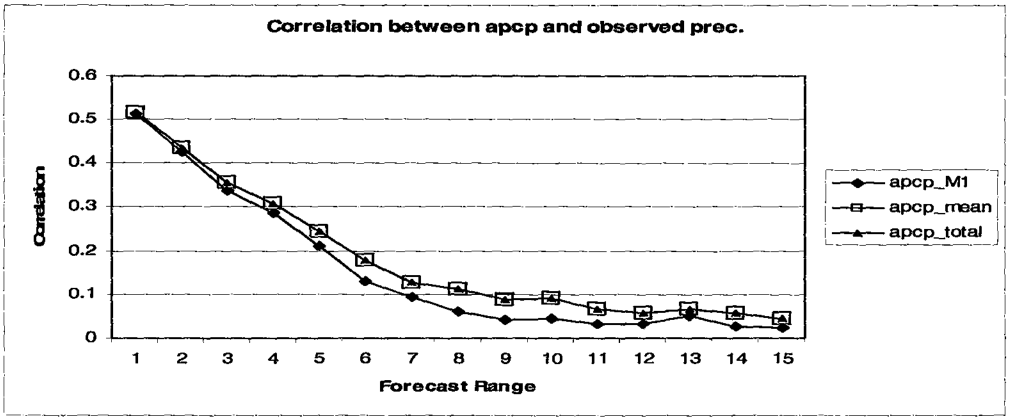

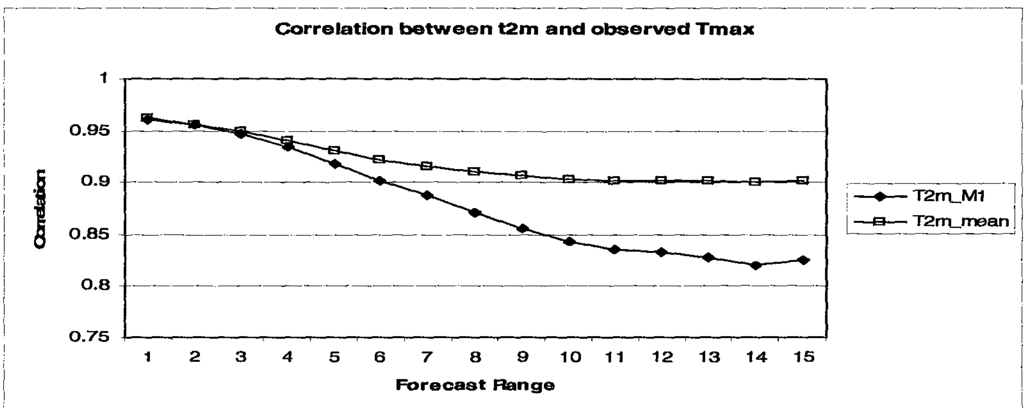

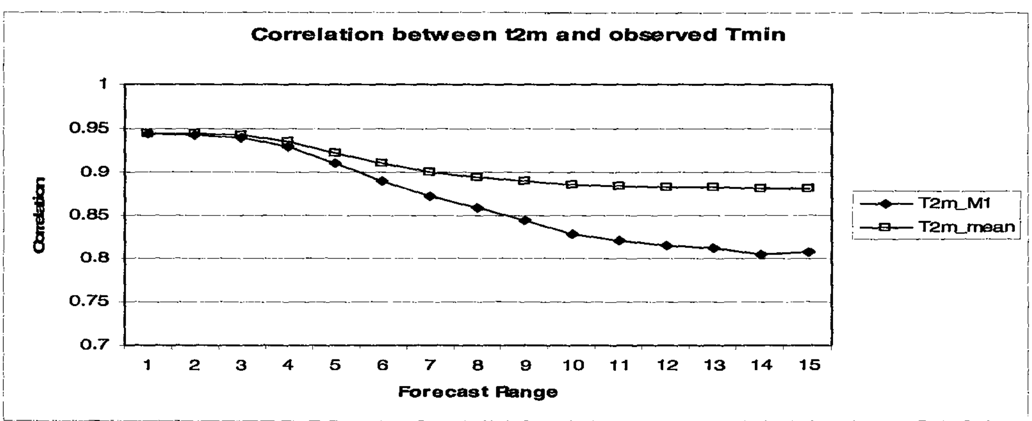

Figure 5: Correlation plots between predictors and observed Precipitation, Tmax, and Tmin at CDD station

4.1.2 Model Predictors Selection

In order to identify an appropriate way of using the ensemble data in the downscaling experiments, six cases of input data are explored and their results are compared. This analysis is performed for the CDD station. The first four cases apply the predictors only from grid point 4_3 (see Figure 2), and the fifth case applies predictors from all the four grid points around the station, and the sixth case includes the variables from grid point 4_3 and 3_3, which are the nearest to the station. The six cases are explained respectively as follows:

- Case 1: uses the first members (M1) of the first delays from each variable as predictors for downscaling.
- Case 2: uses the mean of the members of the first delay from each variable as predictors for downscaling.
- Case 3: principal component analysis (PCA) of the members of the first delay is performed, and the first principal components are used as predictors.
- Case 4: the mean of the members from each delay at grid point 4_3 are calculated for all of the eight variables, and then the predictors are screened through sensitivity analysis.
- Case 5: the same predictors selected in the fourth case as well as the corresponding predictors from all the other three grid points around the CDD station, namely, the predictors from grid point 4_3, 3_3, 3_4, and 4_4 are used (see Figure 2).
- Case 6: sensitivity analysis is applied to the means of the members of each delay for all the variables from grid point 4_3 and 3_3, then the significant predictors are selected and used as input predictors.

Sensitivity analysis provides a measure of the relative importance among the predictors by calculating how the model output varies in response to variation of an input. The relative sensitivity of the model to each input is calculated by dividing the standard deviation of the output by the standard deviation of the input, which is varied to create the output. The results provide a measure of the relative importance of each input (predictor) in the particular input–output transformation. In this study, sensitivity analysis is performed using TLFN models.

Based on sensitivity analysis results, the most relevant input variables are then selected. The final selected predictor variables used for the three models in case 4 are presented in Table 3. In case 5, the same predictors as in case 4 from all the four grid points are used. In case 6, the final selected predictors are listed in Table 4.

Then all the six cases of selected large scale predictors as well as the observed precipitation and temperature data are used to construct the downscaling models based on TLFN and SDSM methods respectively. By comparing the model performances, the best case of input data is selected and applied to further analyses.

4.1.3 Selection of Optimal Case of Model Input

Once the predictors for all the six cases are selected, they are used to construct downscaling models with SDSM and TLFN methods. All potential optimal combinations of the parameters of SDSM and TLFN models are tested to get the best performance for each model. The performance of the models is evaluated by three statistics: mean squared error (MSE), normalized mean squared error (NMSE, NMSE=MSE/variance of desired output), and correlation coefficient (*r*) between model output and desired output for test period. The SDSM and TLFN model performances for all six cases are shown in Table 5.

Table 3: Predictors selected in case 4 for downscaling at CDD station (Fr0, Fr1 denotes forecast range, t=0 (current), t=1 (lag 1) respetively)

Predictands	Downscaling Methods	selected lags of predictors							
		apcp	heating	pwat	prmsl	t2m	rhum	u10m	v10m
Prec.	SDSM	Fr0,1,2,3	Fr1,2,3	Fr0,1,2	\	\	Fr0,1	\	\
	TLFN	Fr0,1,2,3	Fr1,2,3,4,5,7,8,9,10,11,12	Fr0,1,2,3,5,6,7,9,10,11,12	Fr0,1,2,3	Fr0,1,2,3,4,5,6,8,9,10,11,12	Fr0,1,2	Fr0,1,2,3	Fr0,1,3
Tmax	SDSM	\	\	\	\	Fr0,1,2,3,4,5,6,7,8,9,10,12	\	\	\
	TLFN	Fr0,1,2,3	Fr0,1,2,3,4,6,7,8,9,10,11,12	Fr0,2,3,5,6,7,9,10,11,12	Fr0,1,2,3	Fr0,1,2,3,4,5,6,7,8,9,10,11,12	Fr0,1,2	Fr0,1,2,3	Fr0,1,2,3
Tmin	SDSM	\	\	\	\	Fr0,1,2,3,4,5,6,7,8,9,10,11	\	\	\
	TLFN	Fr0,1,2,3	Fr1,2,3,4,5,6,7,8,9,10,11,12	Fr0,1,2,3,4,5,6,7,8,9,10,11,12	Fr0,1,2,3	Fr0,1,2,3,4,5,6,7,8,9,10,11,12	Fr0,1,2	Fr0,1,2,3	Fr0,1,2,3

Table 4: Predictors selected in case 6 for downscaling at CDD station

Predictands	Downscaling Methods	selected lags of predictors							
		apcp	heating	pwat	prmsl	t2m	rhum	u10m	v10m
Prec.	SDSM	4_3Fr0	4_3Fr0	3_3Fr0,3,10,4 _3Fr0,5	\	3_3Fr0,4_3Fr10	\	\	4_3Fr0
	TLFN	4_3Fr0	4_3Fr0	3_3Fr0,3,10,4 _3Fr0,5	\	3_3Fr0,4_3Fr10	\	\	4_3Fr0
Tmax	SDSM	\	4_3Fr0	3_3Fr0	\	3_3Fr0,1,5,7,12, 4_3Fr0,1,6	\	\	\
	TLFN	\	4_3Fr0	3_3Fr0	\	3_3Fr0,1,5,7,12, 4_3Fr0,1,6	\	\	\
Tmin	SDSM	\	\	\	4_3Fr1	3_3Fr0,1,5,7,12, 4_3Fr0,2,8,12	\	\	\
	TLFN	\	\	\	4_3Fr1	3_3Fr0,1,5,7,12, 4_3Fr0,2,8,12	\	\	\

Table 5: Performance of downscaling models for Prec., Tmax, and Tmin for all 6 cases at CDD station

Predictands	Cases	TLFN-Testing			SDSM-Testing		
		MSE	NMSE	r	MSE	NMSE	r
Prec.	Case 1: Mean	20.47	0.65	0.61	42.78	1.35	0.03
	Case 2: Member 1	20.40	0.65	0.61	59.14	1.87	0.01
	Case 3: Pincipal Component	20.56	0.65	0.61	72.27	2.29	0.00
	Case 4: selected predictors from grid point 4_3	20.36	0.64	0.62	49.15	1.56	0.10
	Case 5: selected predictors from 4 grid points	20.33	0.64	0.62	48.87	1.55	0.06
	Case 6: selected predictors from 2 grid points	**20.65**	**0.65**	**0.61**	**49.52**	**1.57**	**0.26**
Tmax	Case 1: Mean	8.97	0.05	0.97	70.11	0.42	0.79
	Case 2: Member 1	9.52	0.06	0.97	72.91	0.44	0.79
	Case 3: Pincipal Component	8.99	0.05	0.97	71.34	0.43	0.79
	Case 4: selected predictors from grid point 4_3	9.49	0.06	0.97	65.01	0.39	0.80
	Case 5: selected predictors from 4 grid-points	36.98	0.22	0.88	62.95	0.38	0.81
	Case 6: selected predictors from 2 grid points	**8.65**	**0.05**	**0.97**	**13.49**	**0.08**	**0.96**
Tmin	Case 1: Mean	10.57	0.06	0.97	83.75	0.50	0.77
	Case 2: Member 1	11.58	0.07	0.97	86.62	0.52	0.77
	Case 3: Pincipal Component	11.39	0.07	0.97	84.06	0.50	0.76
	Case 4: selected predictors from grid point 4_3	12.04	0.07	0.96	21.97	0.13	0.94
	Case 5: selected predictors from 4 grid-points	28.71	0.17	0.91	19.01	0.11	0.94
	Case 6: selected predictors from 2 grid points	**9.69**	**0.06**	**0.97**	**18.49**	**0.11**	**0.95**

In downscaling Prec., the performance of TLFN models is better than that of SDSM models. When applying TLFN models in downscaling Prec., all the 6 cases have quite close results, the MSE are all around 20.5 and correlation are all around 0.61. This means all the 6 cases provide similar information in downscaling precipitation. When SDSM method is applied in downscaling Prec., based on the MSE, the results of Case 1, Case 4, Case 5, and Case 6 are similar and better than the other two cases. Among these 4 cases, the r of case 6 is a little bit better than the other cases.

For downscaling Tmax, TLFN models have quite good performance in almost all the cases except Case 5, where the MSE is 36 compared with around 9 or 8 in other cases. SDSM models have obviously better performance in Case 6, where the MSE is 13 compared with 60 or 70 in other cases. For Tmin, the downscaling results, the TLFN models have quite close performance with that in downscaling Tmax. The SDSM models perform better with Case 4, Case 5, and Case 6 data.

Considering better model performance and fewer predictors applied, Case 6 is selected for downscaling the local precipitation and temperature in the CDD and CDP stations using SDSM, TLFN, and EPR models. For CDD station, significant predictors from grid point 4_3 and 3_3 are selected. For CDP station, the same screening method is applied and significant predictors from grid points 3_4 and 3_3 (case 6) are selected. The selected predictors at CDP station are listed in Table 6 (note that selected predictors at CDD station are presented in Table 4). The downscaling results of the two stations using these three methods will be explained in the following section.

Table 6: Predictors selected for downscaling meteorological data at CDP station

Predictands	Downscaling Methods	selected lags of predictors							
		apcp	heating	pwat	prmsl	t2m	rhum	u10m	v10m
Prec.	SDSM	3_3Fr7	3_3Fr0,10,3_4Fr0	3_3Fr0,11,3_4Fr0	3_3Fr0	3_4Fr8	\	3_3Fr0	\
	TLFN	3_3Fr7	3_3Fr0,10,3_4Fr0	3_3Fr0,11,3_4Fr0	3_3Fr0	3_4Fr8	\	3_3Fr0	\
	EPR	3_3Fr7	3_3Fr0,10,3_4Fr0	3_3Fr0,11,3_4Fr0	3_3Fr0	3_4Fr8	\	3_3Fr0	\
Tmax	SDSM	\	3_4Fr0,12	3_3Fr0,3_4Fr3	\	3_3Fr0,10,3_4Fr0,1,6,12	3_4Fr0	\	3_4Fr1
	TLFN	3_3Fr12	3_3Fr0,3_4Fr0,9,12	3_3Fr0,1,3,5,11,3_4Fr3,6,11	\	3_3Fr0,1,2,10,3_4Fr0,1,6,8,12	3_4Fr0	\	3_4Fr1
	EPR	3_3Fr13	3_3Fr0,3_4Fr0,9,13	3_3Fr0,1,3,5,11,3_4Fr3,6,12	\	3_3Fr0,1,2,10,3_4Fr0,1,6,8,13	3_4Fr0	\	3_4Fr1
Tmin	SDSM	3_3Fr0,2	3_4Fr0,7	\	\	3_3Fr0,1,4,3_4Fr0,3	\	\	3_3Fr0,2
	TLFN	3_3Fr0,1,2	3_4Fr0,4,7	\	3_3Fr9	3_3Fr0,1,4,8,10,3_4Fr0,1,2,3,5,10	\	\	3_3Fr0,2
	EPR	3_3Fr0,1,3	3_4Fr0,4,8	\	3_3Fr10	3_3Fr0,1,4,8,10,3_4Fr0,1,2,3,5,11	\	\	3_3Fr0,3

4.2 Results of Downscaling MRF Data for Prec. and Temp

4.2.1 Downscaling Results at CDD station

Validation statistics in terms of MSE, NMSE, and *r* are used to evaluate the models performance. Table 7 shows all the performance statistics of SDSM, TLFN, and EPR models results in downscaling Prec., Tmax, and Tmin at CDD station. The model performance statistics show that the three models do not perform very well in downscaling Prec., the correlation between the downscaled data and the observed data is no more than 0.62, and the MSE are more than 20. However, TLFN and EPR much better perform than SDSM, considering their MSE is around 20 compared with 50 of SDSM models results. For Tmax and Tmin, all the three models pretty well perform in downscaling Tmax and Tmin, especially for TLFN and EPR, the NMSE is approximately 0.05, and the correlation is approximately 0.97. One surprising thing is that the comparative results indicate TLFN and EPR have very similar performance in downscaling precipitation, Tmax and Tmin, and they perform better than SDSM.

Table 7: Downscaling results for Prec., Tmax, Tmin at CDD station

Predictands	Downscaling Methods	Statistics		
		MSE	NMSE	r
Prec.	SDSM	49.52	1.57	0.26
	TLFN	20.65	**0.65**	**0.61**
	EPR	20.35	**0.64**	**0.62**
Tmax	SDSM	13.49	0.08	0.96
	TLFN	8.65	**0.05**	**0.97**
	EPR	8.34	**0.05**	**0.98**
Tmin	SDSM	18.49	0.11	0.95
	TLFN	9.69	**0.06**	**0.97**
	EPR	9.49	**0.06**	**0.97**

To further assess the downscaling models' performances, seasonal statistics are calculated. Seasonal downscaling results of the three models can be found in the Table 8, from which we can see that when downscaling precipitation, the TLFN and EPR perform well in winter, with lower MSE and higher r, and also in spring and autumn, while the results are not as good in the summer. This may be caused by heavier precipitation in the form of convective storms and thunderstorms that are difficult to model with large scale weather models. SDSM models perform badly in downscaling daily Prec. in all four seasons. When downscaling Tmax and Tmin, all three methods have better model results in Spring and Autumn than in Winter and Summer. For Tmin, the correlation from TLFN and EPR are above 0.9 in Spring and Autumn, while around 0.8 in Winter and Summer, and correlation from SDSM is more than 0.85 in Spring and Autumn, while around 0.75 in Winter and Summer. And there is very similar situation in Tmax downscaling results. This is because the temperature usually has higher variance in winter and summer, which makes it more difficult to simulate. Still TLFN and EPR have similar performances, and perform better than SDSM.

Table 8: Seasonal downscaling results for Prec., Tmax, Tmin at CDD Station

Predictands	**Models**	**Seasons**											
		Winter			**Spring**			**Summer**			**Autumn**		
		MSE	NMSE	r	MSE	NMSE	r	MSE	NMSE	r	MSE	NMSE	r
prec.	SDSM	32.89	1.86	0.03	27.09	1.33	0.09	78.77	1.66	0.04	56.48	1.47	0.04
	TLFN	9.51	0.54	**0.71**	12.17	0.60	0.64	34.17	0.72	**0.56**	25.13	0.65	0.61
	EPR	9.53	0.54	**0.71**	11.66	0.57	0.66	34.53	0.73	**0.55**	24.37	0.63	0.64
Tmax	SDSM	84.94	1.82	0.12	89.40	1.02	**0.62**	34.41	1.67	0.15	51.54	0.78	**0.70**
	TLFN	8.27	0.18	0.91	13.55	0.15	**0.94**	8.55	0.42	0.81	7.54	0.11	**0.94**
	EPR	9.17	0.20	0.91	15.60	0.18	**0.94**	8.60	0.42	0.81	7.64	0.12	**0.94**
Tmin	SDSM	43.08	0.53	0.75	25.26	0.31	**0.86**	8.49	0.55	0.71	11.36	0.24	**0.88**
	TLFN	22.68	0.28	0.85	11.64	0.14	**0.93**	5.42	0.35	0.81	8.61	0.18	**0.91**
	EPR	26.56	0.33	0.82	12.80	0.16	**0.93**	5.42	0.35	0.82	8.49	0.18	**0.93**

Moreover, scatter plots of downscaled versus observed Prec., Tmax and Tmin data during the validation period are presented to assess the model performance more directly. All the output data from validation period are plotted and a comparison line which represents the perfect model is also shown on the plot. Figure 6 shows the logarithmic scale plots of downscaled Prec. versus observed Prec. using SDSM, TLFN, and EPR respectively. It can be seen that all the spots from TLFN and EPR are distributed more closely around the perfect model line than those of SDSM. Scatter plots for Tmax and Tmin can be seen in Figures 7 and 8. All the three methods demonstrated good performance in downscaling Tmax and Tmin, but TLFN and EPR perform similarly and significantly better than SDSM.

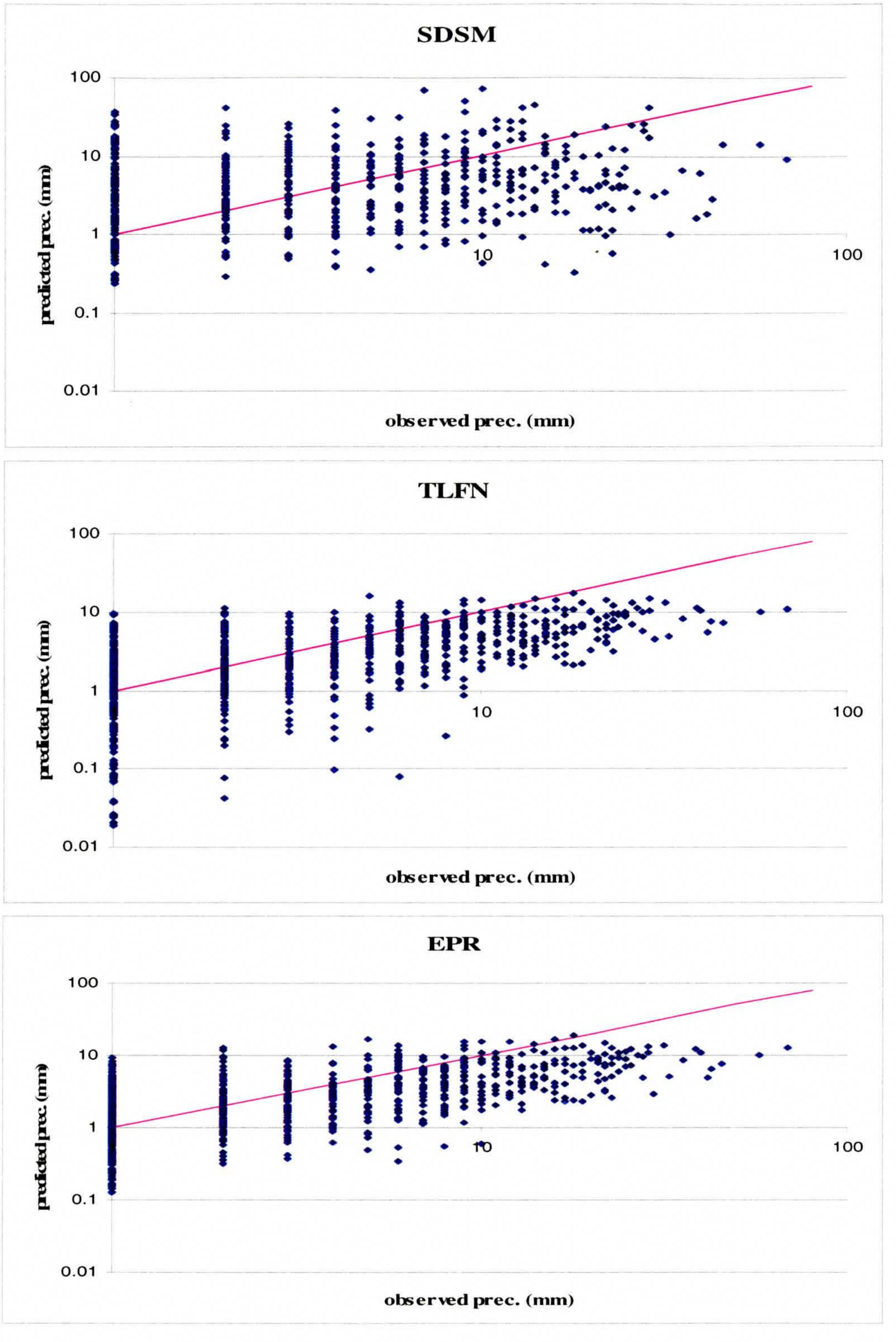

Figure 6: Scatter plots of observed vs downscaled Prec. at CDD Station using SDSM, TLFN, and EPR

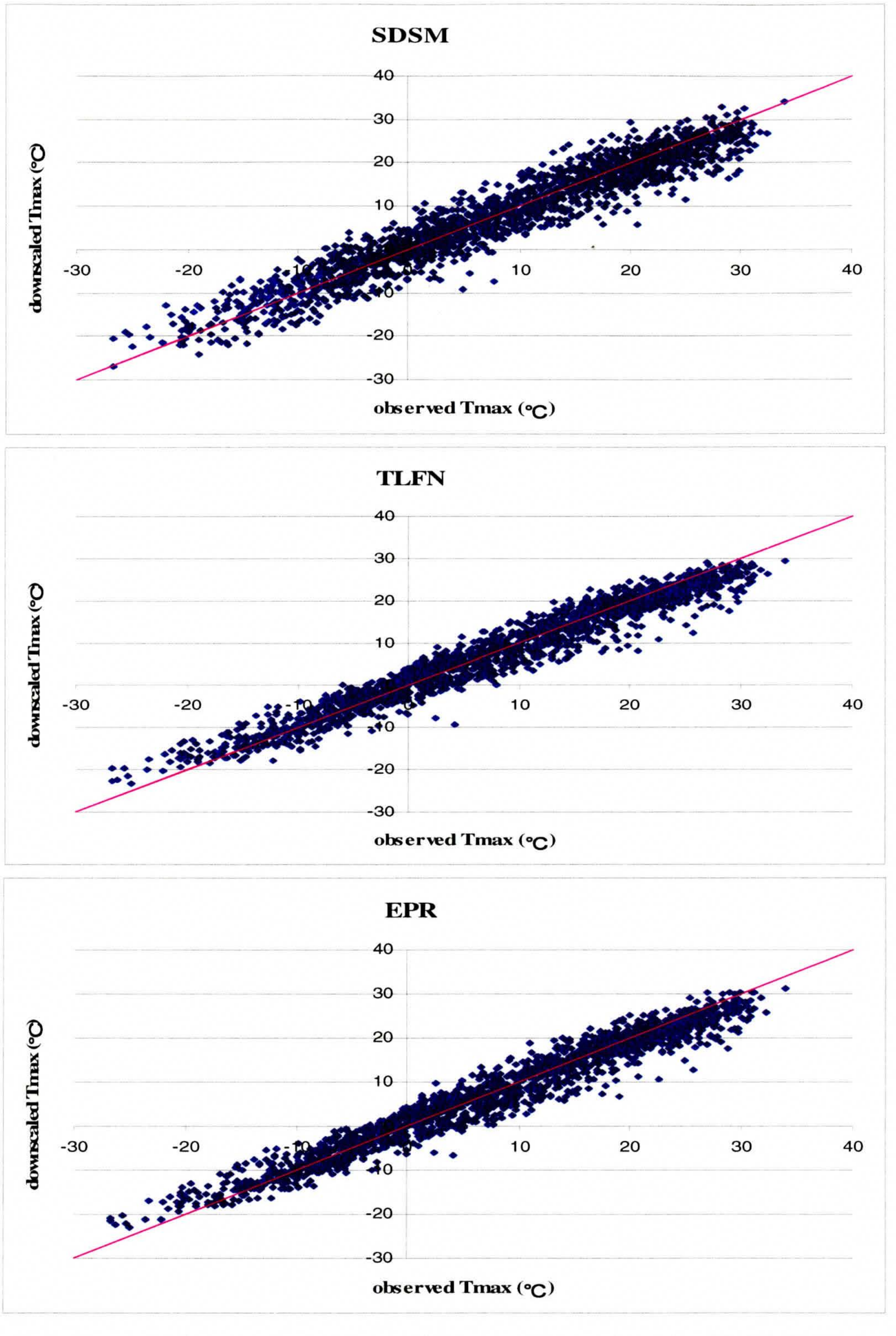

Figure 7: Scatter plots of observed vs downscaled Tmax at CDD station using SDSM, TLFN, and EPR

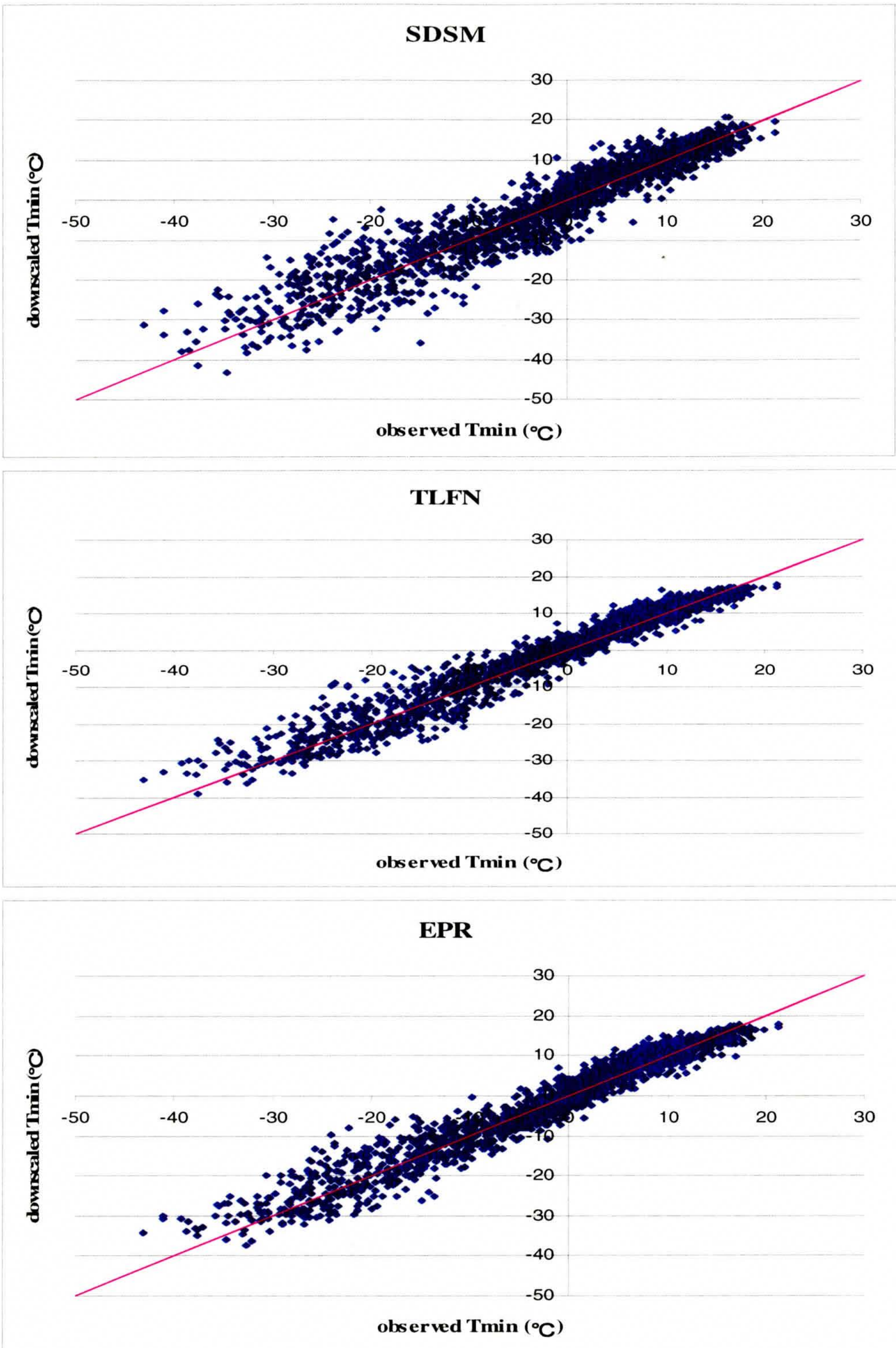

Figure 8: Scatter plots of observed vs downscaled Tmin at CDD station using SDSM, TLFN, and EPR

4.2.2 Downscaling Results at CDP station

Just as the downscaling results at CDD station are shown above, the validation statistics from the three models in downscaling Prec., Tmax, and Tmin at the CDP station are shown in Table 9. Judging by the statistics, all the three models perform quite well in downscaling temperature; the correlations from all the three models are above 0.95, and the NMSE are under 0.1. In downscaling Prec., all the three models perform less well than temperature, as all the correlations are no more than 0.61. Still, the TLFN and EPR perform better than SDSM, considering their MSE is approximately 20 compared to approximately 40 for SDSM model.

Table 9: Downscaling results for Prec., Tmax, Tmin at CDP Station

Predictands	Downscaling Methods	Statistics		
		MSE	NMSE	r
Prec.	SDSM	**38.76**	1.30	0.29
	TLFN	**20.48**	0.69	0.56
	EPR	**18.81**	0.63	0.61
Tmax	SDSM	9.94	0.06	**0.97**
	TLFN	5.67	0.03	**0.98**
	EPR	6.18	0.04	**0.98**
Tmin	SDSM	17.25	0.10	**0.95**
	TLFN	9.82	0.06	**0.97**
	EPR	10.48	0.06	**0.97**

The seasonal downscaling results at the CDP station are shown in Table 10. It shows that in downscaling Prec., all the models best perform in Winter, and worst in Summer. Especially when judged by the MSE, the MSE of TLFN and EPR are less than 10 in Winter, while more than 35 in Summer. For SDSM, the MSE is 20 in Winter while nearly 60 in Summer. All the three models have better performance in downscaling Prec. in Spring and Autumn than in Summer. Just like the entire year results, TLFN and EPR perform better than SDSM in every season.

In downscaling temperature, all the models perform well, and the correlations are all above 0.80. The models perform better in Spring and Autumn than the other two seasons, especially for SDSM. In almost all the seasons, TLFN and EPR have better performance in downscaling temperature than SDSM.

The model performance can be observed more directly through scatter plots of downscaled versus observed Prec., Tmax and Tmin data at CDP station during the whole validation period. Figure 9 shows the logarithmic scale plots of downscaled Prec. versus observed Prec. using SDSM, TLFN, and EPR. It can be seen that all the spots from TLFN and EPR are distributed more closely around the perfect model line than those of SDSM, and the distribution of the spots from TLFN and EPR are quite close. Scatter plots for Tmax and Tmin can be seen in Figures 10 and 11. All three methods demonstrated good performance in downscaling Tmax and Tmin, all the data points are distributed closely around the perfect model line. Judging by the scatter plots, TLFN out performs than EPR and SDSM in downscaling Tmin.

Table 10: Seasonal downscaling results for Prec., Tmax, Tmin at CDP Station

Predictands	**Models**	**Seasons**											
		Winter			**Spring**			**Summer**			**Autumn**		
		MSE	NMSE	r	MSE	NMSE	r	MSE	NMSE	r	MSE	NMSE	r
prec.	SDSM	**20.21**	1.82	0.34	28.60	1.33	0.28	**58.11**	1.17	0.21	47.86	1.48	0.34
	TLFN	**8.46**	0.76	0.61	14.48	0.68	0.57	**37.95**	0.76	0.50	20.73	0.64	0.61
	EPR	**6.92**	0.62	0.62	12.90	0.60	0.65	**36.44**	0.73	0.53	18.75	0.58	0.67
Tmax	SDSM	12.06	0.25	0.87	12.39	0.15	**0.93**	8.09	0.39	0.80	7.23	0.11	**0.94**
	TLFN	7.10	0.15	0.93	6.45	0.08	**0.97**	4.46	0.22	0.89	4.70	0.07	**0.96**
	EPR	7.09	0.15	0.93	8.10	0.10	**0.96**	4.38	0.21	0.89	5.17	0.08	**0.96**
Tmin	SDSM	26.69	0.36	0.82	20.31	0.25	**0.88**	9.63	0.59	0.70	12.51	0.25	**0.88**
	TLFN	15.61	0.21	0.90	11.26	0.14	**0.93**	5.29	0.32	0.83	7.20	0.14	**0.93**
	EPR	17.75	0.24	0.89	11.89	0.14	**0.93**	5.32	0.32	0.82	7.08	0.14	**0.93**

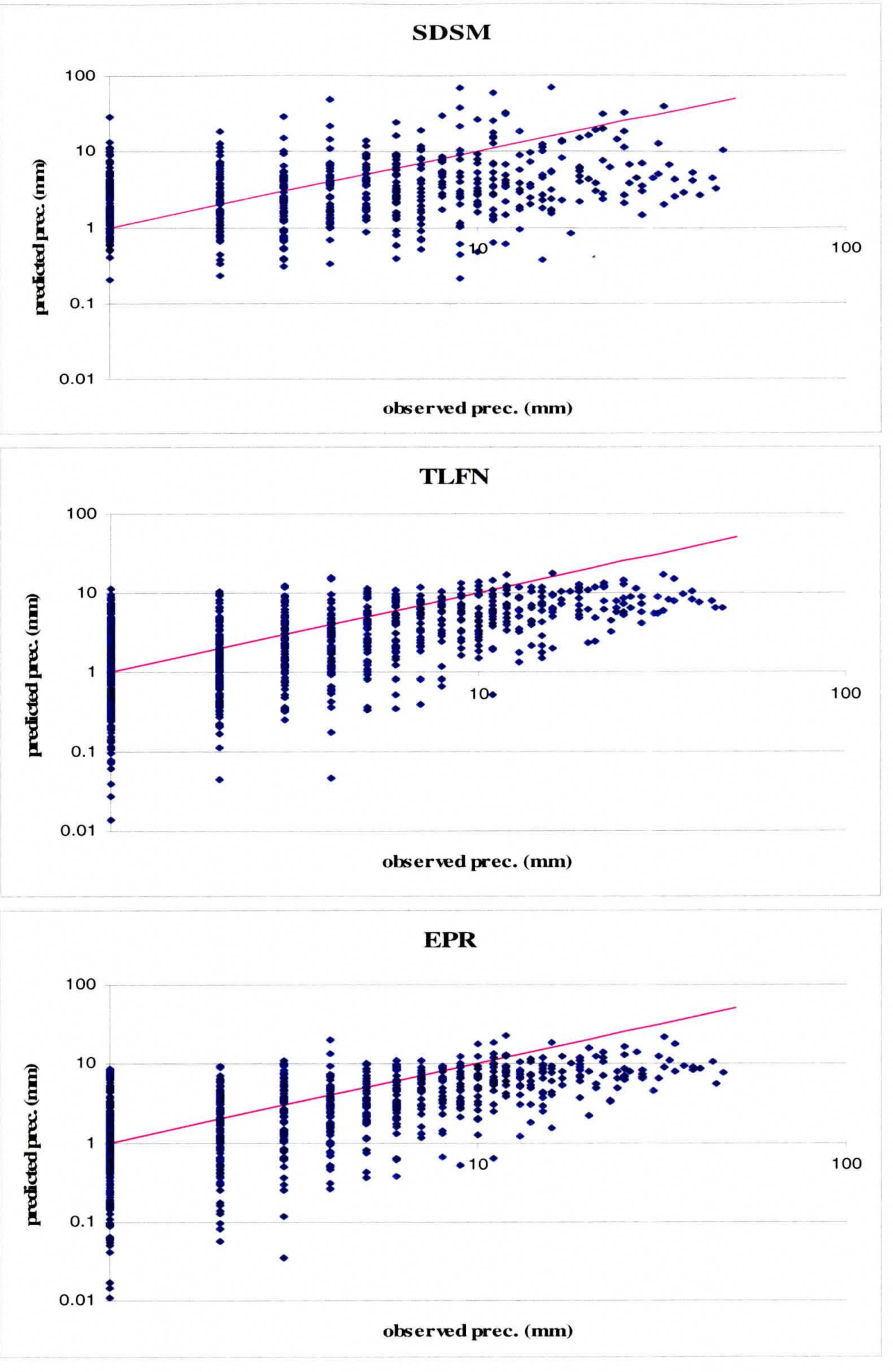

Figure 9: Scatter plots of observed vs downscaled Prec. at CDP station using SDSM, TLFN, and EPR

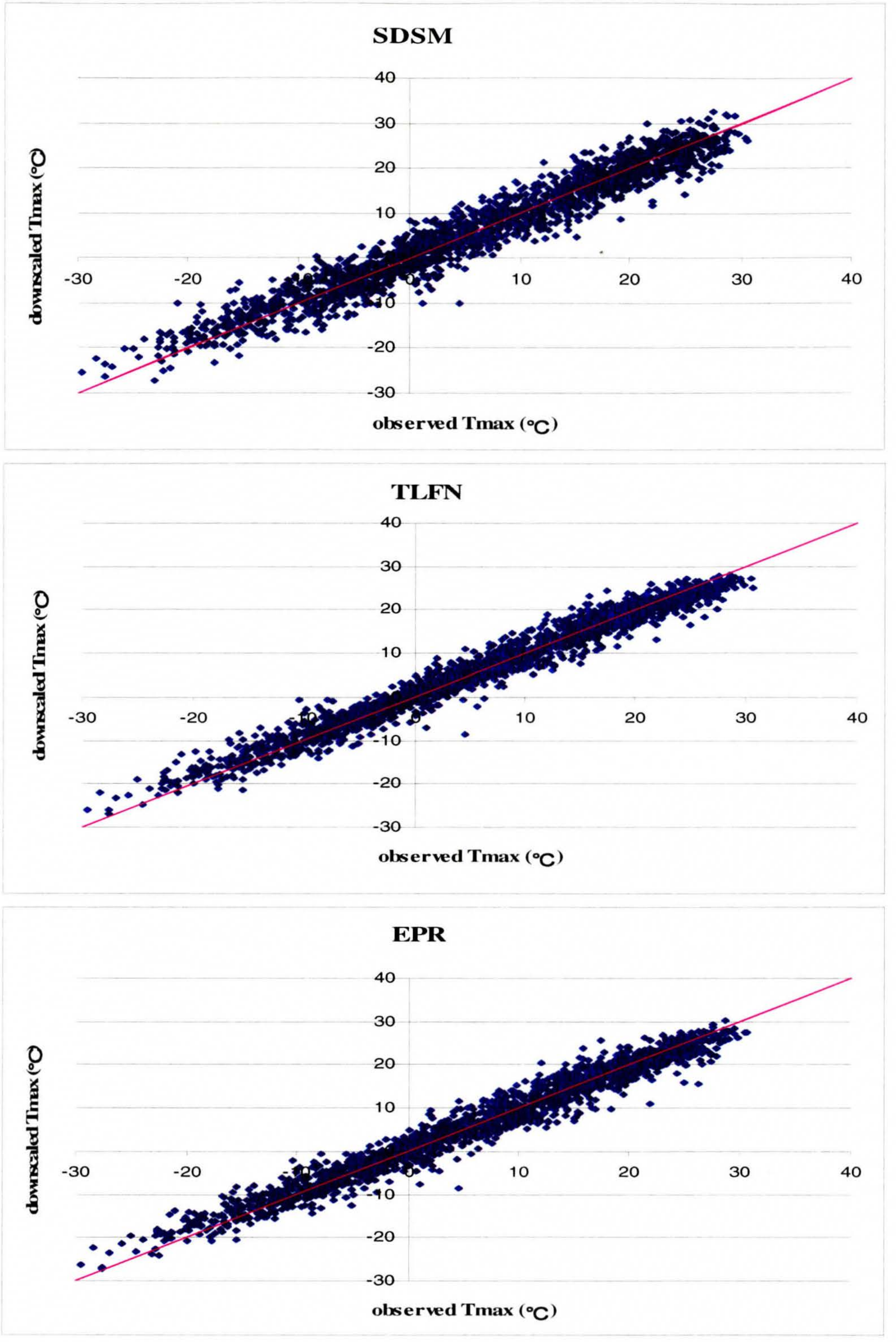

Figure 10: Scatter plots of observed vs downscaled Tmax at CDP station using SDSM, TLFN, and EPR

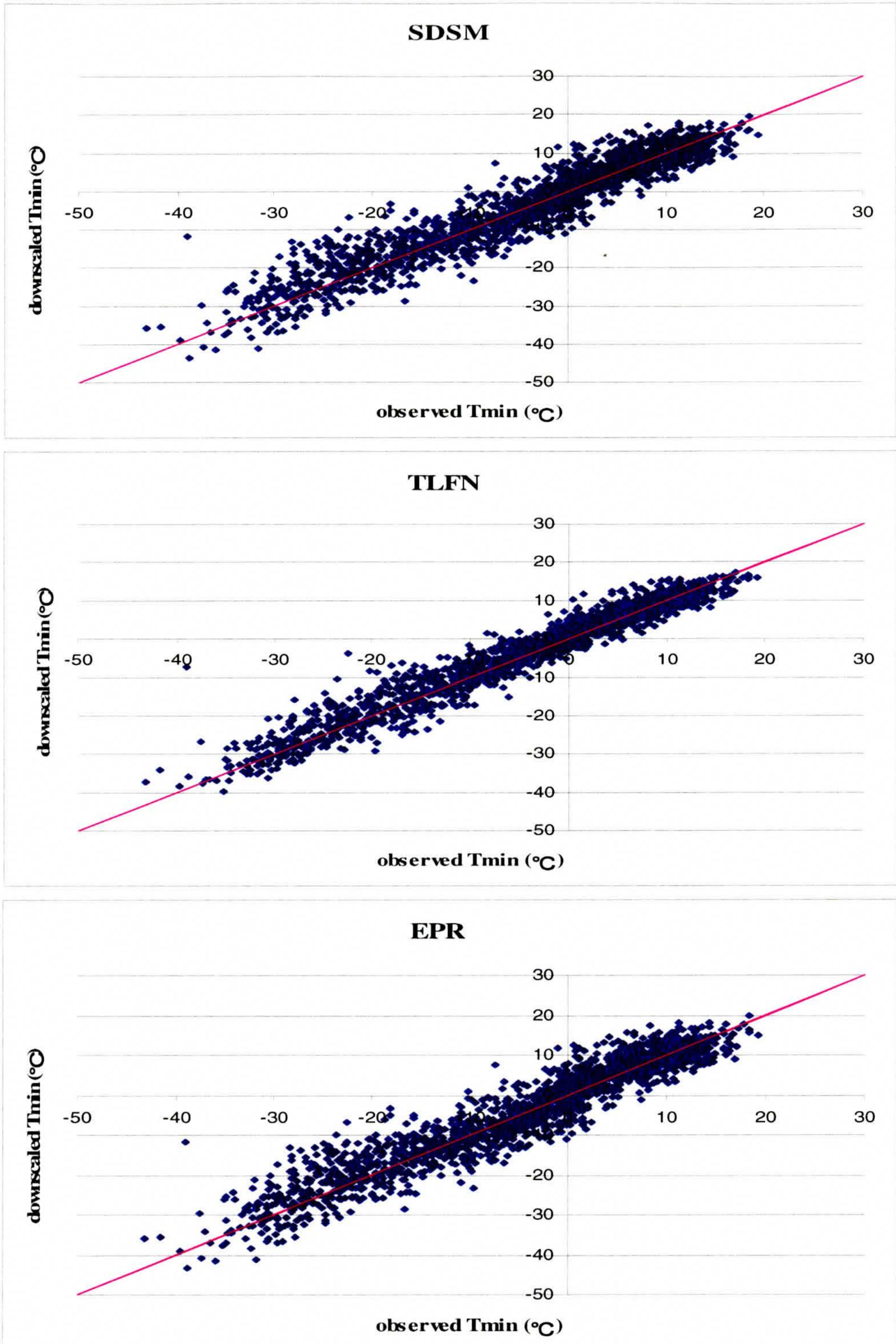

Figure 11: Scatter plots of observed versus downscaled Tmin at CDP station using SDSM, TLFN, and EPR

4.2.3 Discussion of Downscaling Results

Through analysis of the downscaling results of precipitation and temperature at the two meteorological stations using SDSM, TLFN, and EPR methods, the following conclusions can be drawn.

At both stations, all the three models have good performance in downscaling temperature (Tmax and Tmin). TLFN and EPR models perform slighly better than SDSM for both entire year results and seasonal results. TLFN and EPR models have quite similar performance in most cases, while TLFN performs slightly better than EPR in downscaling Tmin at CDP station.

In downscaling precipitation, the performance of all the three models is not as good as in downscaling temperature. TLFN and EPR models perform quite similarly, and much better than SDSM. This may be because SDSM method trains the models based on monthly mean statistics, and when the method is used to predict daily data, the model does not perform as well. Another possible reason is that SDSM is a linear model, while TLFN and EPR are non-linear models. However, SDSM consistently uses a much smaller number of parameters whatever the predictand of concern. In general, the comparative results suggest that TLFN and EPR have a good potential for downscaling MRF ensemble weather forecasts. However, further improvement is needed for the downscaling of precipitation time series.

In the following chapter, the downscaled daily precipitation and temperature data from SDSM and TLFN are used as input to the hydrologic models to improve the short term reservoir inflow and river flow forecasting. Although in most cases, TLFN and EPR have very close performance, the TLFN model results are selected because the model outperforms EPR in downscaling Tmin, and is well understood by the author. SDSM model results are also applied as a comparison because it is a widely used downscaling model.

Chapter 5: Hydrologic Forecasts using BNN and HBV with Downscaled Data

5.1 Hydrologic Forecasting Models

5.1.1 Hydrologic Model Introduction

Hydrological models are mathematical formulations which determine the runoff that leaves a watershed basin from the rainfall received by this basin. They provide a means of quantitative prediction of watershed runoff that may be required for efficient management of water resources systems, such as flood control and management, reservoir operation and management, and the design of various hydraulic structures. In the past several decades, various models have been studied and constructed for the modeling of rainfall–runoff processes. These models can be divided into three major categories: spatially distributed physically based models, semi-distributed conceptual models, and data-driven models.

Distributed physically based models, such as MIKE SHE (Refsgaard and Storm, 1995; Moretti and Montanari, 2007), SHETRAN (Ewen et al., 2000), and CASC2D (Moretti and Montanari, 2007), are designed based on the physical characteristics of the watershed. In order to reliably model the physical processes taking place in the watershed, these kinds of models require vast amounts of high quality and fine resolution data, which may prevent the wide application of these models (Beven, 1989; Moretti and Montanari, 2007).

Conceptual models are alternative approaches to the rainfall-runoff model. Conceptual models represent physical processes with far less detail, but still give a spatially distributed representation of the watershed. These models were developed to simplify the simulations of practical case studies without including a detailed representation of the processes involved in the catchment. They are distributed models where some (or all) of the hydrological processes are modeled using conceptual schemes (Moretti and Montanari, 2007).

There have many kinds of conceptual models designed and applied in late years. The SLURP (Simple LUmped Reservoir Parametric) model subdivides the catchment into sub-units according to different landuses of the catchment. It has been primarily designed in order to make use of remotely sensed data, and applied in climate change studies (Kite, 1978). Another conceptual model, TACD (Uhlenbrook and Sieber, 2005), is an example of a raster-based conceptual model. The core of the model is a process-oriented runoff generation routine based on experimental findings, including tracer studies (Uhlenbrook et al., 2002). TOPMODEL (Beven and Kirkby, 1979) is designed to predict the dynamics of the contributing areas based on the pattern of the soil topographic index. It has been applied in many practical hydrological studies such as estimation of flood frequency distribution, by continuous simulation, in ungauged catchments (Blazkova and Beven, 1997, 2002, 2004; Moretti and Montanari, 2007). The Australian Water Balance Model (AWBM) is a conceptual model that simulates the spatial variability of the saturation overland flow by means of the conceptual basis of the Antecedent Precipitation Index (API) model (Boughton, 2004, 2006; Moretti and Montanari, 2007).

The distributed physically based models and conceptual models described above are designed to simulate the physical mechanism that determine the hydrological cycle. This involves the physical laws of water transfer and the parameters associated with the characteristics of the catchment area. Such models may require sophisticated mathematical tools, a significant amount of calibration data, and some degree of expertise and experience with the model. Because the runoff process in a catchment is a complex and non-linear process affected by many inter-related physical factors (Zhang and Govindaraju, 2000), the use of physical or conceptual models of the rainfall–runoff process are sometimes viewed sceptical (Grayson et al, 1992).

While data-driven models do not need any information on the physics of the hydrologic processes, they are very useful for river flow forecasting where the main concern is accurate predictions of runoff (Nayak et al., 2005). This kind of models are designed to explore solutions through modeling direct relationship between the input and output data without considering the complete physical characteristics of the system. The data-driven models include linear regression statistical models, such as auto-regressive (AR) models, and non-linear models, such as neuro-fuzzy systems, and artificial neural networks (ANNs). ANNs models have been widely used in recent years in many areas such as groundwater modeling (Coulibaly et al., 2001; Daliakopoulos et al., 2005), river flow forecasting (Imrie et al., 2000; Hu et al., 2001; Kumar et al., 2004), and rainfall forecasting (Kuligowski and Barros, 1998; Luk et al., 2001; Rami'rez et al., 2005; Aqil et al, 2007).

The AR type of streamflow forecast models were earliest applied by Thomas and Fiering (1962) and Yevjevich (1963). Carlson et al. (1970) proposed significant developments in the form of auto-regressive moving average (ARMA) hydrologic time series models. McKerchar and Delleur (1974) used the auto-regressive integrated moving average (ARIMA) method to model monthly streamflow of 16 watersheds in Indiana, Illinois and Kentucky (Aqil et al., 2007).

ANNs application in hydrologic modeling is another fascinating area that has emerged in the 1990s. Because ANNs have the ability to recursively learn from data and can result in significant savings in time required for model development, they are particularly suited for modeling nonlinear systems where traditional parameter estimation techniques are not convenient (Singh et al, 2002). Many studies have demonstrated that the ANNs are adequate to model the rainfall-runoff process and can even perform better than the conventional modeling techniques (Valenca and Ludermir, 2000; Chang and Chen, 2001; Xiong et al., 2001; Vernieuwe et al., 2005; Nayak et al., 2004, 2005). Jain et al. compared the ANN models with regression and time series models in making short-term water demand predictions at the Indian Institute of Technology (Jain et al., 2001; Jain and Kumar, 2007). Jain and Ormsbee (2002) used ANN to model the short-term water demand process in Kentucky, USA, and found its performance to be better than theAR type regression and time series models. Jain and Indurthy (2003) used past flow information to model the complex rainfall–runoff process and compared the same with the regression models. (Jain and Indurthy, 2003; Jain and Kumar, 2007) Coulibaly et al. (2001) presented multilayer perceptron (MLP), input delayed neural network (IDNN) and recurrent neural networks with and without input delays for reservoir inflow prediction in the Chute-du-Diable catchment in Canada.

In this study, one data-driven model, Bayesian neural network (BNN), is applied for up to 14 day ahead reservoir inflow and river flow forecasting, and the results are compared with a widely used conceptual model, HBV. These two models are described in the follow sections.

5.1.2 Bayesian Neural Network (BNN)

The Bayesian approach is applied here because of its particular advantage compared with classical models. ANNs have been successfully used in rainfall-runoff modeling for more than a decade. Since its inception, many researchers (Halff et al., 1993; Tokar and Johnson, 1999; Coulibaly et al., 2000; Jain and Srinivasulu, 2004) have demonstrated its capability in complex non-linear rainfall-runoff modeling. The main conclusions of those studies are that artificial neural networks can be considered as a robust modeling alternative to the conceptual and physically based hydrologic models. However, there are major limitations in the conventional neural network approach (Coulibaly et al., 2001a). One of the main limitations is that the network is trained by maximizing a likelihood function of the parameters or equivalently minimizing an error function in order to obtain the best set of parameters starting with an initial random set of parameters. Sometimes a regularization term with an error function is used to prevent overfitting. In this method, a complex model can fit the training data well but it does not necessarily mean that it will provide smaller errors with respect to new data. This happens because of not considering uncertainty about the model parameters or the uncertainty about the relationship between input and output mapped by the network during training. The Bayesian approach overcomes this problem, and provides prediction with uncertainty estimates in the form of confidence intervals.

In the Bayesian approach, the uncertainty about the relationship between input output is represented by a probability density function of the parameters. Before observing data, the parameters are described by a prior probability density function, which is typically very broad to reflect the fact that we have little idea of what values the parameters should be. Once the data are observed, by using Bayesian theory corresponding the posterior probability density function is derived (Khan and Coulibaly, 2006). The posterior distribution may be narrower than the prior distribution because some values of the parameters are more consistent with data than others. Account for uncertainty in parameter estimation enables the network to predict more accurately reducing the problem of overfitting while dealing with new data. Moreover, the posterior distribution over network weights will provide a distribution over the outputs of the network, which is known as predictive distribution for the new data. If a single-valued prediction is needed, one might use the mean of the predictive distribution but the full predictive distribution also tells how uncertain this prediction is. It has been shown in the work of Sarle (1995) that even the crudest Bayesian computation (maximizing over both parameters and hyperparamters) is capable of generalizing better than early stopping when learning nonlinear functions.

BNN has been used in various sectors both for regression and classification problems. It has been used to study the effects of air pollution on housing prices in Boston. It was found that the predictive performance of the Bayesian method for forecasting housing prices was substantially better than the methods employed previously. Lampinen and Vehtari (2001) in their work provided a brief review of the Bayesian approach for neural networks and demonstrated the application in three areas such as in a regression problem of predicting the quality of concrete in the concrete manufacturing process; in a classification problem of recognizing tree trunks in forest scenes; and in approximating an inverse mapping in a topographic image reconstruction problem. In these real world problems the advantages of the BNN models were demonstrated as compared to the standard neural network methods and other statistical models.

Furthermore, the overfitting problem can be solved by using Bayesian methods to control model complexity. In the Bayesian approach, cross-validation is not required because Bayesian methods allow the values of regularization coefficients to be selected using only the training data (Khan and Coulibaly, 2006). Because of these advantages, BNN models are applied here in short term hydrologic forecasting to provide reliable forecasts that can be used for decision-making. A detailed description of the BNN as used herein can be found in Khan and Coulibaly (2006).

5.1.3 HBV Models

The HBV model was developed to cover the most important runoff generating processes by using the most simple and robust structure possible, and it belongs to the class of semi-distributed conceptual models. The HBV model was developed at the Swedish Meteorological and Hydrological Institute (Bergström, 1976; Lindström et al., 1996; Khan and Coulibaly, 2006). The HBV-model is named after the abbreviation of Hydrologiska Byråns Vattenbalansavdelning (Hydrological Bureau Water balance-section).

The HBV model has been applied to a wide range of applications including the analysis of extreme floods, effects of land-use change and effects of climate change (Arheimer and Brandt, 1998; Brandt, 1990; Lidén and Harlin, 2000; Dibike and Coulibaly, 2005). It has a routine for snow-accumulation and snowmelt based on a degree-day relation with an altitude correction of temperature. Input data required for this model are observed precipitation, air temperature, and estimates of potential evapotranspiration. The time step is usually one day, but it is possible to use shorter time steps. The evaporation values used are usually monthly averages, but daily values can also be used. Air temperature data are used for calculations of snow accumulation and melt. Air temperature can also be used to calculate potential evapotranspiration, or to adjust potential evapotranspiration when the temperature deviates from normal values. In the case where elevations in a basin vary with a considerable range, then the basin can be subdivided into elevation zones for the snow and soil moisture routines. Each elevation zone can further be divided into different vegetation zones (forested and non-forested areas). The model can be run independently for several sub-basins and their contributions are combined into a full basin output. The model has recently been applied for simulating the hydrologic impact of climate change in the Saguenay watershed (Dibike and Coulibaly, 2005) in northern Quebec.

The model parameters are determined through a calibration process, where the parameters are adjusted until simulated and observed runoff shows a good agreement. The calibrated model can then be used as a simulation tool in numerous applications. In this study, the HBV models are used for up to 14 day ahead hydrological forecasting as a good reference model for comparing the performance of the BNN.

5.2 Selection of Predictors

As described in the first chapter, the second part of this study aims to improve short term reservoir inflow and river flow forecasting by including downscaled meteorological data. In this chapter, up to 14 day ahead reservoir inflow and river flow are forecasted based on the following three cases of different input data:

- case 1: observed meteorological data without downscaled data
- case 2: observed meteorological data and TLFN downscaled data
- case 3: observed meteorological data and SDSM downscaled data

Both HBV and BNN models are applied based on these three different cases to perform short term reservoir inflow and river flow forecasting, and their performance are compared. The forecasting results are compared in the following section.

In the case of without downscaled data, predictors used here are the same as those selected by Khan and Coulibaly (2006) in a previous study in the same area. Because Khan and Coulibaly (2006) carefully select optimum predictors for one day ahead reservoir inflow and river flow forecasting at this location, here the same predictors are applied in the case of without downscaled data. To simulate the Serpent river flow at time t+1 to t+14, the following predictors are used: (a) total daily precipitation of last 12 days starting from t to t-11 has been considered as 12 separate inputs; (b) the moving sum of the last four weeks snowfall as another input; (c) the mean daily temperature at t; (d) moving average of last two weeks mean daily temperature; (e) flow at time t and (g) months as logical inputs to account for seasonal variability. Altogether 28 input vectors have been used to simulate the river flow. The above input variables have been found optimal in producing network outputs closer to the observed data, and by providing the minimum root-mean-square error, the highest correlation coefficient, and the largest Nash and Sutcliffe model efficiency statistics. Moreover, the goodness-of-fit of predicted and observed flows has also been checked in choosing the optimum combination of the input variables. The common trial-and-error approach is used in this input selection. Precipitation has been used up to past 12 days to consider the influence of antecedent rainfall to flow generation at the outlet of the basin. As snow accumulation and its subsequent melting is a process of several weeks or even months, in modeling that process a moving sum over the last 4 weeks snow and average temperature over last 2 weeks have been found as potential inputs. Temperature inputs can also be considered as "indirect" inputs of evapotranspiration. The flow of immediate past day has been considered as an input because of a significant lag-1 autocorrelation of the daily flow. Months have been considered as logical inputs using 0 and 1 for considering time and/or seasonal effects on the outputs of the system. In representing months as logical inputs, 12 input columns have been included for 12 months, for example, if the computation is in January then the logical input will be 1 for that month, and 0 for the other 11 months. Subsequently, if the computation is in February, then the logical input will be 1 for that month and 0 for the other 11 months, and so on (Khan and Coulibaly, 2006). Although this approach introduces a discontinuity at monthly boundaries because of considering January 31 the same as January 1, similarly February 1 to be the same as Feb 28, and so on, it effectively accounts for seasonal effects that are particularly important in cold and snowy region (Khan and Coulibaly, 2006).

Similarly, for daily reservoir inflow predictions from time t+1 to t+14 the following input variables have been considered: (a) total daily precipitation of last seven days starting from t to t –6 has been considered as seven separate inputs; (b) the moving sum of last ten weeks snow as another input; (c) the mean daily temperature at t-1; (d) the moving average of last nine weeks of mean daily temperature; (e) the flow at time $t-1$ and, (g) the month as a logical input.

For the Serpent river flow prediction, out of 11 years (1991-2001) of daily data (flow, temperature and precipitation), 8 years (1991-1998) of data were used for model calibration and the remaining 3 years (1999-2001) of data were used for model validation. For the reservoir inflow prediction, out of a total of 23 years of daily data (1979-2001), 18 years (1979-1996) of data were used for model calibration and the remaining 5 years (1997-2001) of data were used for model validation.

For the cases of including downscaled precipitation and temperature data in the model input, when HBV model is applied for t+n reservoir inflow or river flow forecasting, the downscaled precipitation and temperature for t+n are included in the input data. When the BNN model is applied for t+n reservoir inflow or river flow forecasting, the downscaled precipitation and temperature from t+1 to t+n are included in the input data.

5.3 Short-term Reservoir Inflow Forecasting using HBV and BNN

5.3.1 Short-term Reservoir Inflow Forecasting for Entire year

In this section, up to 14 day ahead reservoir inflows are forecasted based on three different cases of input data, namely, observed meteorological data without downscaled data (case 1), observed meteorological data with TLFN downscaled data (case 2), and observed meteorological data and SDSM downscaled data (case 3). The forecasting is performed based on each case of the input data using HBV and BNN respectively, and the results are presented in Table 11s and 12 respectively. The model performance is evaluated by the three statistics, root mean square error (RMSE), correlation coefficient (r), and Nash and Sutcliffe model efficiency statistic (R^2).

From Table 11, we can see that the HBV models have good performance in forecasting up to 5 day ahead inflows, where the r values are all above 0.85 and the R^2 are around or more than 0.7, while the models performances deteriorate in forecasting more than 6 day ahead inflows. When TLFN downscaled data are included in the forecasting models, from 6 day to 14 day ahead forecasting compared with model without downscaled data, the RMSE decreases by 12% to 21%, which means there is obvious improvement. In the 14 day ahead forecasting, the r increase from 0.66 to 0.80, and R^2 increase from 0.39 to 0.61, which shows potential for improvement. However, there is no obvious improvement of model performance in forecasting one day to five day ahead inflows, and in two day ahead forecasting, the model even performs worse than the model without downscaled data. When SDSM downscaled data are included in the forecasting models, there is some improvement from 6 to 14 day ahead forecasting, the RMSE decreases about 10%; however, in 1 to 5 day ahead forecasting, the models perform worse, and the RMSE increased by 10% to 20%. This may be caused by the poor performance of the SDSM models in downscaling precipitation data.

Table 12 shows the BNN models results in forecasting up to 14 day ahead reservoir inflows. Judging by the RMSE and R^2, it can be seen that the BNN models have good performance up to 8 days ahead forecasting, the R^2 values are all around or more than 0.70. When TLFN downscaled data are included, the models do not show obvious improvement, as the decrease in RMSE is very slight. When SDSM downscaled data are included, the models perform a little bit worse, RMSE increased about 5%. It can be concluded from these results that the BNN models have no obvious improvements in the short term reservoir inflow forecasting when downscaled meteorological data are included. This may suggest that BNN are not able to capture the relevant information from the downscaled weather forecasts that the HBV model can.

In order to better evaluate the HBV and BNN model performances in short term reservoir inflow forecasting, the observed and simulated 1, 8, and 14 day ahead inflows from the two hydrological models are plotted in Figures 12 and 13 respectively. From the two figures, we can see that both HBV and BNN give very good simulated inflow series in one day ahead forecasting. In the 8 and 14 day ahead forecasting, the HBV models show obvious improvement in simulating peak flows when downscaled data are included, and both TLFN and SDSM downscaled data are helpful in simulating peak flows. When including SDSM downscaled data, the models have no obvious improvement in simulating low flows, but improve in simulating peak flows. The BNN models simulate almost perfect low flows in one day ahead reservoir inflow forecasting, but there is an underestimation of the peak flows of May, 1999 of more than 300 m^3/s. For 8 and 14 day ahead forecasting, BNN models obviously underestimate the peak flows. When TLFN and SDSM downscaled data are included in the BNN models, there is a slight improvement in simulating peak flows, but not much.

Table 11: Up to 14 day ahead reservoir inflow forecasts for entire year using HBV annual model

Forecasting lags	**without downscaled data**			**including downscaled data (TLFN)**				**including downscaled data (SDSM)**			
	RMSE	r	R2	RMSE	r	R2	Decrease in RMSE	RMSE	r	R2	Decrease in RMSE
Flows forecasting 1-day-ahead	74.56	0.94	**0.87**	74.69	0.93	**0.87**	0%	94.02	0.92	0.79	-26%
Flows forecasting 2-day-ahead	83.25	0.93	**0.83**	99.46	0.90	**0.76**	-19%	94.50	0.91	0.79	-14%
Flows forecasting 3-day-ahead	97.70	0.90	**0.77**	101.93	0.89	**0.75**	-4%	112.96	0.88	0.69	-16%
Flows forecasting 4-day-ahead	105.62	0.86	**0.73**	107.36	0.88	**0.72**	-2%	116.80	0.87	0.67	-11%
Flows forecasting 5-day-ahead	113.71	0.85	0.69	110.15	0.87	**0.71**	3%	122.38	0.86	0.64	-8%
Flows forecasting 6-day-ahead	126.55	0.80	0.62	109.77	0.86	**0.71**	13%	117.82	0.86	0.67	7%
Flows forecasting 7-day-ahead	131.71	0.78	0.58	115.56	0.85	0.68	**12%**	122.97	0.84	0.64	**7%**
Flows forecasting 8-day-ahead	146.30	0.74	0.55	121.05	0.84	0.65	**17%**	120.32	0.85	0.65	**18%**
Flows forecasting 9-day-ahead	134.39	0.77	0.57	115.01	0.85	0.68	**14%**	125.48	0.84	0.62	**7%**
Flows forecasting 10-day-ahead	142.32	0.73	0.51	118.85	0.84	0.66	**16%**	131.21	0.82	0.59	**8%**
Flows forecasting 11-day-ahead	148.24	0.71	0.47	118.27	0.84	0.66	**20%**	126.52	0.82	0.61	**15%**
Flows forecasting 12-day-ahead	150.57	0.70	0.46	119.86	0.83	0.65	**20%**	130.14	0.81	0.59	**14%**
Flows forecasting 13-day-ahead	154.77	0.67	0.42	121.73	0.82	0.64	**21%**	134.88	0.80	0.56	**13%**
Flows forecasting 14-day-ahead	159.34	0.66	0.39	128.06	0.80	0.61	**20%**	137.51	0.79	0.55	**14%**

Table 12: Up to 14 day ahead reservoir inflow forecasts for entire year using BNN annual model

Forecasting lags	**without downscaled data**			**including downscaled data (TLFN)**				**including downscaled data (SDSM)**			
	RMSE	r	R2	RMSE	r	R2	Decrease in RMSE	RMSE	r	R2	Decrease in RMSE
Flows forecasting 1-day-ahead	40.70	0.98	**0.96**	43.60	0.98	**0.95**	-7%	38.90	0.98	**0.96**	4%
Flows forecasting 2-day-ahead	54.80	0.96	**0.93**	50.60	0.97	**0.94**	8%	51.60	0.97	**0.94**	6%
Flows forecasting 3-day-ahead	68.80	0.94	**0.89**	63.90	0.95	**0.90**	7%	71.60	0.94	**0.88**	-4%
Flows forecasting 4-day-ahead	83.30	0.92	**0.83**	78.30	0.92	**0.85**	6%	84.50	0.91	**0.83**	-1%
Flows forecasting 5-day-ahead	96.50	0.89	**0.78**	89.80	0.90	**0.81**	7%	103.20	0.87	**0.75**	-7%
Flows forecasting 6-day-ahead	104.80	0.87	**0.74**	100.10	0.87	**0.76**	4%	108.40	0.85	**0.72**	-3%
Flows forecasting 7-day-ahead	109.70	0.85	**0.71**	101.30	0.87	**0.75**	**8%**	116.50	0.83	0.67	**-6%**
Flows forecasting 8-day-ahead	114.20	0.84	0.69	108.30	0.85	**0.72**	**5%**	122.20	0.81	0.64	**-7%**
Flows forecasting 9-day-ahead	116.40	0.83	0.68	116.60	0.82	0.67	**0%**	122.10	0.81	0.64	**-5%**
Flows forecasting 10-day-ahead	117.20	0.83	0.67	118.50	0.82	0.66	**-1%**	126.10	0.79	0.62	**-8%**
Flows forecasting 11-day-ahead	119.20	0.83	0.66	122.10	0.81	0.64	**-2%**	129.00	0.79	0.60	**-8%**
Flows forecasting 12-day-ahead	122.70	0.81	0.64	120.80	0.81	0.65	**2%**	132.30	0.77	0.58	**-8%**
Flows forecasting 13-day-ahead	125.40	0.81	0.63	123.70	0.80	0.63	**1%**	133.70	0.77	0.57	**-7%**
Flows forecasting 14-day-ahead	129.80	0.79	0.60	123.50	0.80	0.63	**5%**	133.40	0.77	0.58	**-3%**

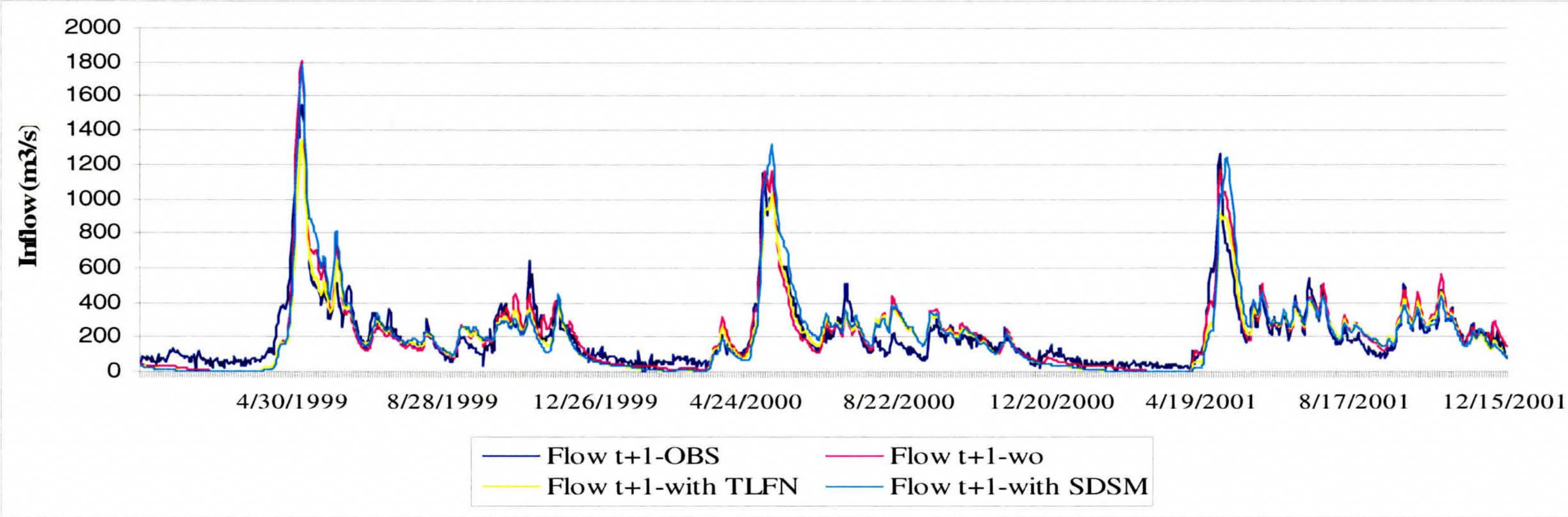

Figure 12 (a): One day ahead reservoir inflow forecasts (HBV annual model) for entire year

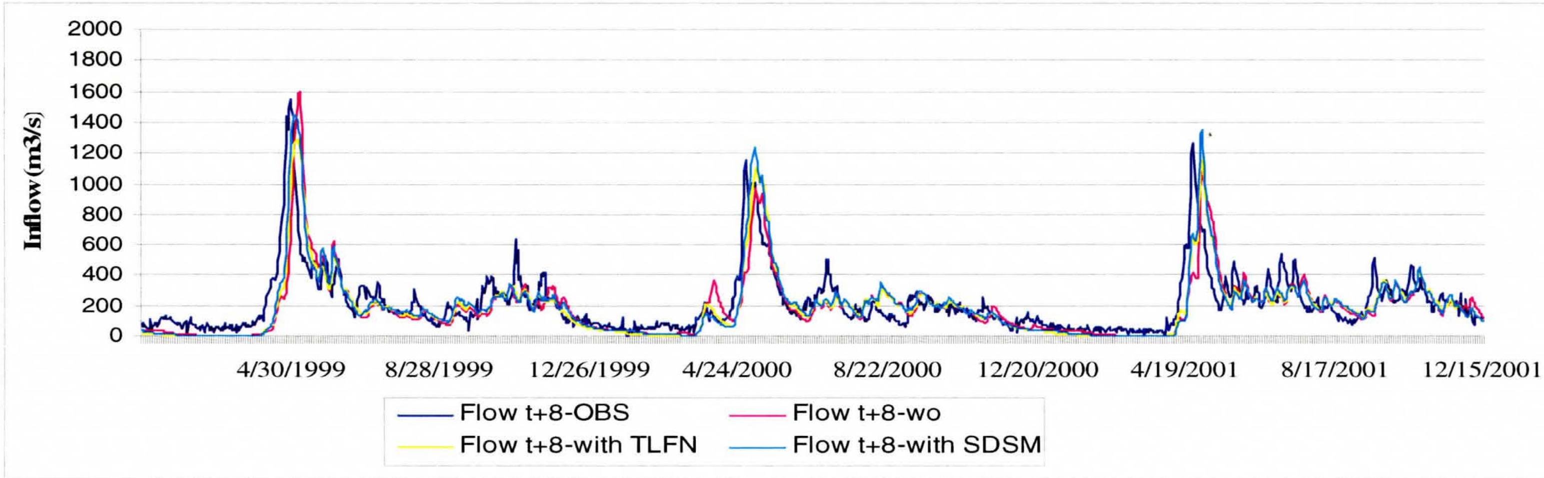

Figure 12 (b): Eight day ahead reservoir inflow forecasts (HBV annual model) for entire year

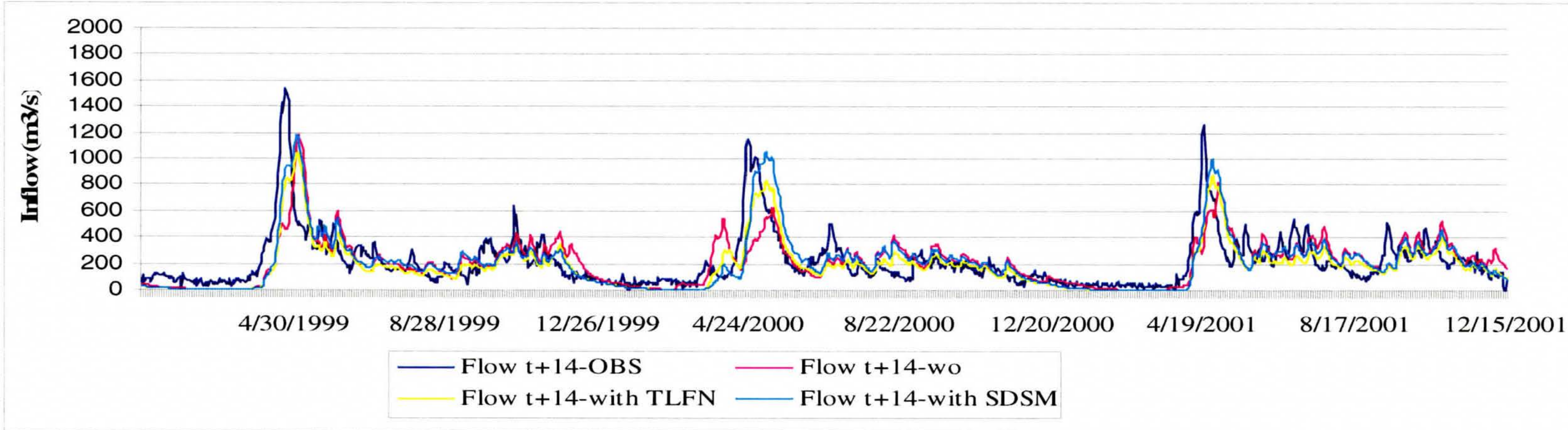

Figure 12 (c): Fourteen day ahead reservoir inflow forecasts (HBV annual model) for entire year

Figure 12: Comparison of short term reservoir inflow forecasts (HBV annual model) for entire year with and without downscaled data

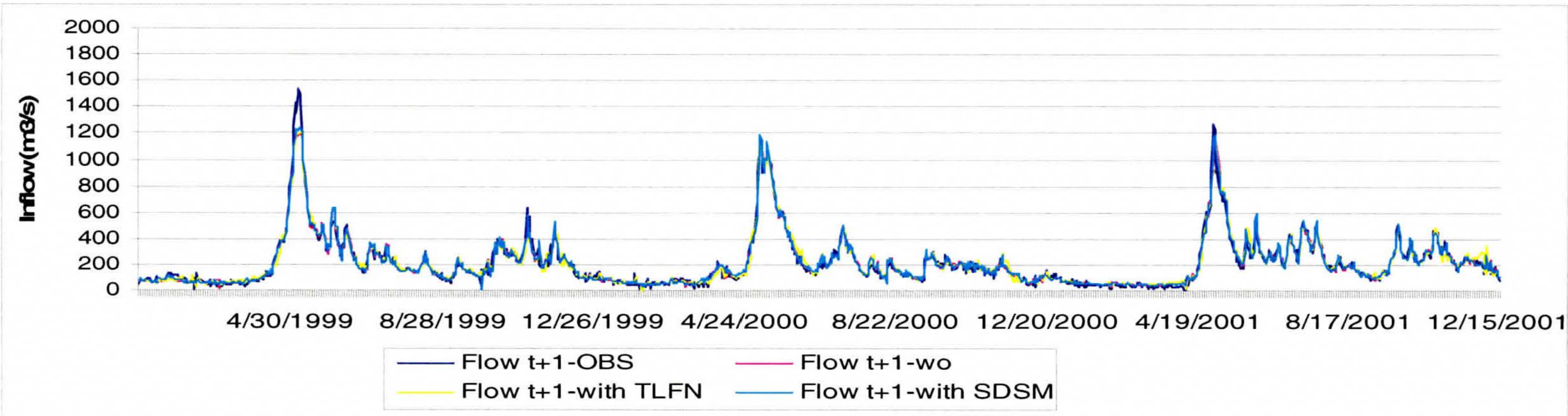

Figure 13 (a): One day ahead reservoir inflow forecasts (BNN annual model) for entire year

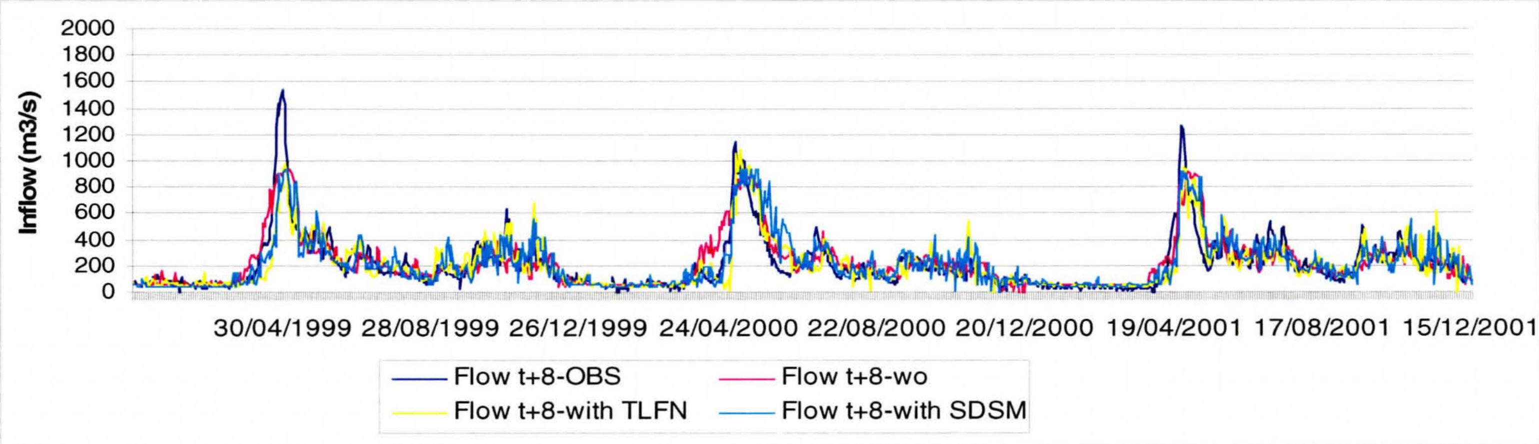

Figure 13 (b): Eight day ahead reservoir inflow forecasts (BNN annual model) for entire year

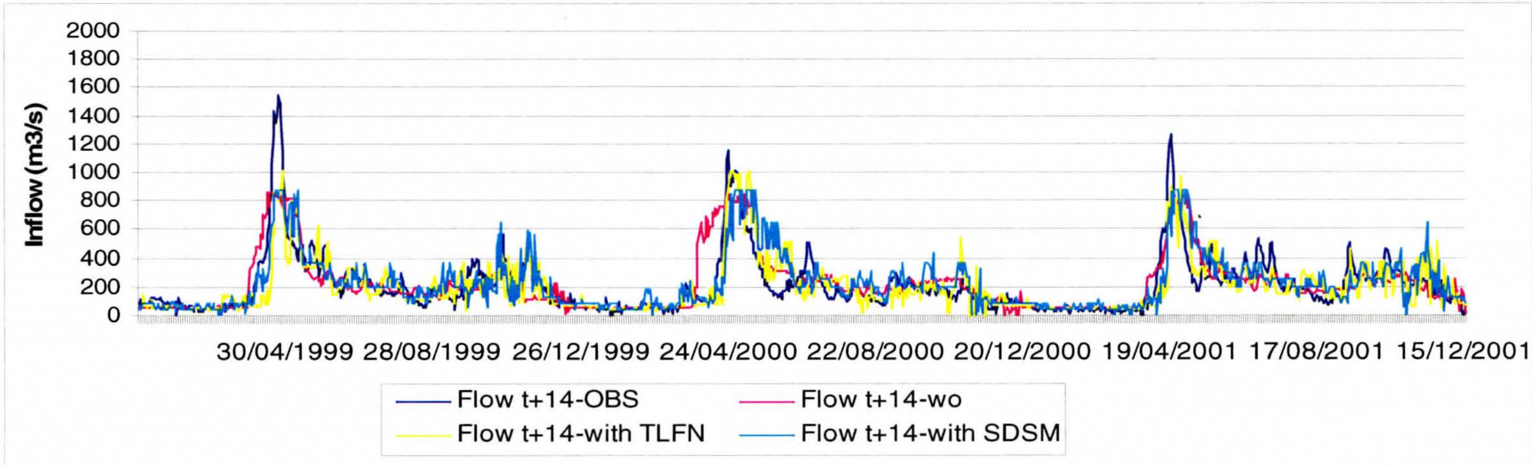

Figure 13 (c): Fourteen day ahead reservoir inflow forecasts (BNN annual model) for entire year

Figure 13: Comparison of short term reservoir inflow forecasts (BNN annual model) for entire year with and without downscaled data

5.3.2 Short-term Reservoir Inflow Forecasting for Spring Season using Annual Models

The hydrologic models' forecast results are more thoroughly explored by dividing the entire year inflow series into seasonal inflows, and the models' performance based on seasonal data are calculated. Statistics of all the four seasons are calculated. Because inflows in Spring are particularly important for reservoir operation, only Spring inflows forecasts are analyzed and explained, as shown in Table 13 and Table 14. The models results for other seasons can be found in Appendix A.

From Table 13, we can see the HBV models' forecast results for Spring are similar with the results for the entire year, which are shown in Table 11. The models have good performance up to 5 day ahead forecasting, and there are improvements from 6 to 14 day ahead inflows forecasting when downscaled data are included. The only difference lies in that the improvements are more obvious for Spring season, the RMSE decrease by more than 20% in almost all the forecasts from 7 to 14 day with TLFN downscaled data, and more than 15% with SDSM downscaled data. However, the models perform less well in the first 5 lags forecasting when downscaled data included, this may be caused by the use of less accurate downscaled precipitation data.

Table 14 shows the BNN models' performance in forecasting up to 14 day ahead Spring inflows. It can be seen that when there is no downscaled data included, the models give good results in up to 9 day ahead forecasting, better than that of HBV models. When TLFN downscaled data are included, there is a slight improvement in the models' performance, but not significant. With SDSM downscaled data, the model performs even worse, and can give good forecasting results up to only 8 day ahead.

The observed and simulated reservoir inflow series for spring season from HBV and BNN models are plotted in Figures 14 and 15. Figure 14 shows the HBV annual models' simulation results in 1, 8, and 14 day ahead spring inflows. For 1 day ahead forecasting, the model performs well with all the three dataset, especially with TLFN downscaled data. For 8 and 14 day ahead forecasting, the model underestimates the peak flows in most cases. When downscaled data are included, there is an obvious improvement in simulating peak flows, especially for 14 day ahead forecasting.

From Figure 15 we can see the BNN model performance in short term reservoir inflow forecasting for Spring. Just like the forecasting results for the entire year, the BNN model has good results for 1 day ahead forecasting, and in 8 and 14 days forecasting, the model underestimates the peak flows obviously. When downscaled data are included, there is no significant improvement, and the model still underestimates the peak flows.

Table 13: Up to 14 day ahead reservoir inflow forecasts for Spring season using HBV annual model

Forecasting lags	without downscaled data			including downscaled data (TLFN)				including downscaled data (SDSM)			
	RMSE	r	R^2	RMSE	r	R^2	Decrease in RMSE	RMSE	r	R^2	Decrease in RMSE
Flows forecasting 1-day-ahead	89.57	0.97	0.93	97.86	0.97	0.92	-9%	143.57	0.94	0.82	-60%
Flows forecasting 2-day-ahead	109.01	0.96	0.89	154.89	0.91	0.79	-42%	140.26	0.93	0.83	-29%
Flows forecasting 3-day-ahead	139.11	0.92	0.83	157.87	0.90	0.78	-13%	177.15	0.89	0.72	-27%
Flows forecasting 4-day-ahead	160.94	0.89	0.77	169.09	0.89	0.74	-5%	185.88	0.89	0.69	-15%
Flows forecasting 5-day-ahead	172.21	0.87	0.73	175.74	0.88	0.72	-2%	193.68	0.88	0.66	-12%
Flows forecasting 6-day-ahead	207.15	0.81	0.61	171.90	0.88	0.73	17%	187.09	0.87	0.68	10%
Flows forecasting 7-day-ahead	217.87	0.78	0.57	185.39	0.86	0.69	**15%**	203.15	0.85	0.62	**7%**
Flows forecasting 8-day-ahead	253.12	0.72	0.41	198.40	0.84	0.64	**22%**	196.68	0.86	0.65	**22%**
Flows forecasting 9-day-ahead	222.19	0.77	0.54	183.04	0.85	0.69	**18%**	207.38	0.84	0.60	**7%**
Flows forecasting 10-day-ahead	240.92	0.72	0.46	191.26	0.84	0.66	**21%**	211.82	0.82	0.58	**12%**
Flows forecasting 11-day-ahead	252.26	0.68	0.40	189.27	0.84	0.66	**25%**	206.44	0.82	0.60	**18%**
Flows forecasting 12-day-ahead	256.52	0.67	0.38	191.37	0.83	0.65	**25%**	213.39	0.81	0.57	**17%**
Flows forecasting 13-day-ahead	262.34	0.65	0.34	192.13	0.83	0.65	**27%**	224.30	0.79	0.52	**15%**
Flows forecasting 14-day-ahead	260.80	0.64	0.35	205.52	0.80	0.59	**21%**	224.52	0.78	0.52	**14%**

Table 14: Up to 14 day ahead reservoir inflow forecasts for Spring season using BNN annual model

Forecasting lags	**without downscaled data**			**including downscaled data (TLFN)**				**including downscaled data (SDSM)**			
	RMSE	r	R^2	RMSE	r	R^2	Decrease in RMSE	RMSE	r	R^2	Decrease in RMSE
Flows forecasting 1-day-ahead	53.02	0.99	0.98	56.05	0.99	0.97	-6%	48.73	0.99	0.98	8%
Flows forecasting 2-day-ahead	76.33	0.97	0.95	73.84	0.98	0.95	3%	72.20	0.98	0.95	5%
Flows forecasting 3-day-ahead	98.29	0.96	0.91	94.49	0.96	0.92	4%	104.40	0.95	0.90	-6%
Flows forecasting 4-day-ahead	123.52	0.93	0.86	116.73	0.94	0.88	6%	123.15	0.93	0.86	0%
Flows forecasting 5-day-ahead	149.06	0.90	0.80	134.70	0.91	0.84	10%	155.29	0.89	0.78	-4%
Flows forecasting 6-day-ahead	162.26	0.89	0.76	157.65	0.88	0.78	3%	164.02	0.87	0.76	-1%
Flows forecasting 7-day-ahead	173.12	0.86	0.73	153.79	0.89	0.78	**11%**	179.74	0.84	0.71	**-4%**
Flows forecasting 8-day-ahead	183.10	0.85	0.69	166.19	0.87	0.75	**9%**	184.86	0.83	0.69	**-1%**
Flows forecasting 9-day-ahead	183.43	0.85	0.69	176.86	0.85	0.71	**4%**	191.75	0.82	0.66	**-5%**
Flows forecasting 10-day-ahead	187.61	0.84	0.67	184.48	0.83	0.68	**2%**	196.23	0.81	0.64	**-5%**
Flows forecasting 11-day-ahead	192.27	0.83	0.65	187.81	0.82	0.67	**2%**	201.95	0.79	0.62	**-5%**
Flows forecasting 12-day-ahead	196.13	0.82	0.64	182.13	0.84	0.69	**7%**	205.82	0.78	0.60	**-5%**
Flows forecasting 13-day-ahead	202.60	0.81	0.61	188.35	0.82	0.66	**7%**	207.75	0.78	0.59	**-3%**
Flows forecasting 14-day-ahead	214.23	0.78	0.56	185.80	0.82	0.67	**13%**	207.12	0.77	0.59	**3%**

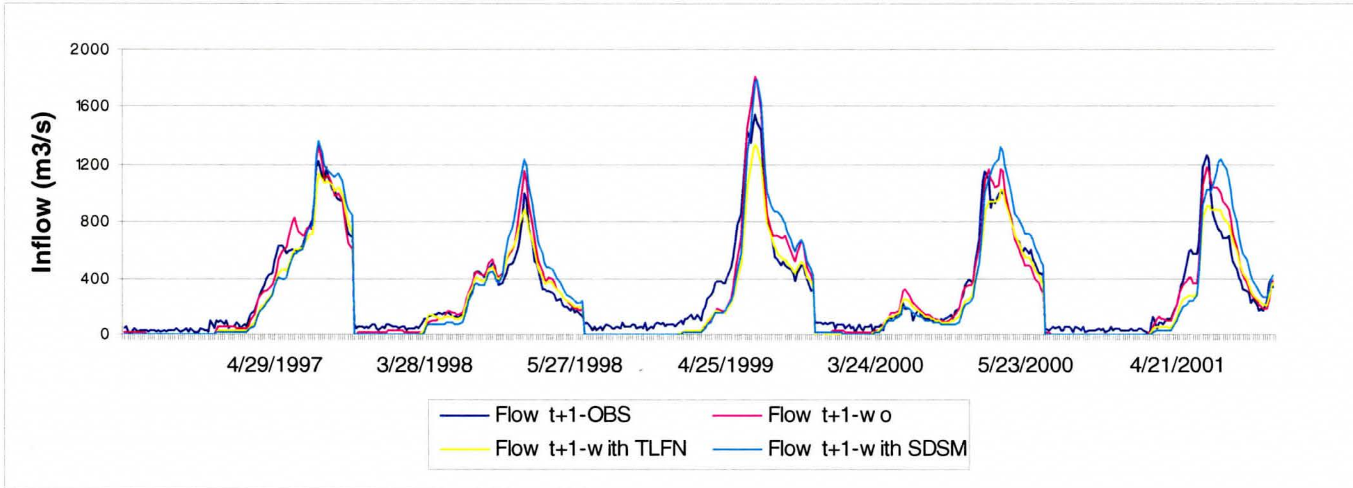

Figure 14 (a): One day ahead reservoir inflow forecasts (HBV annual model) for Spring season

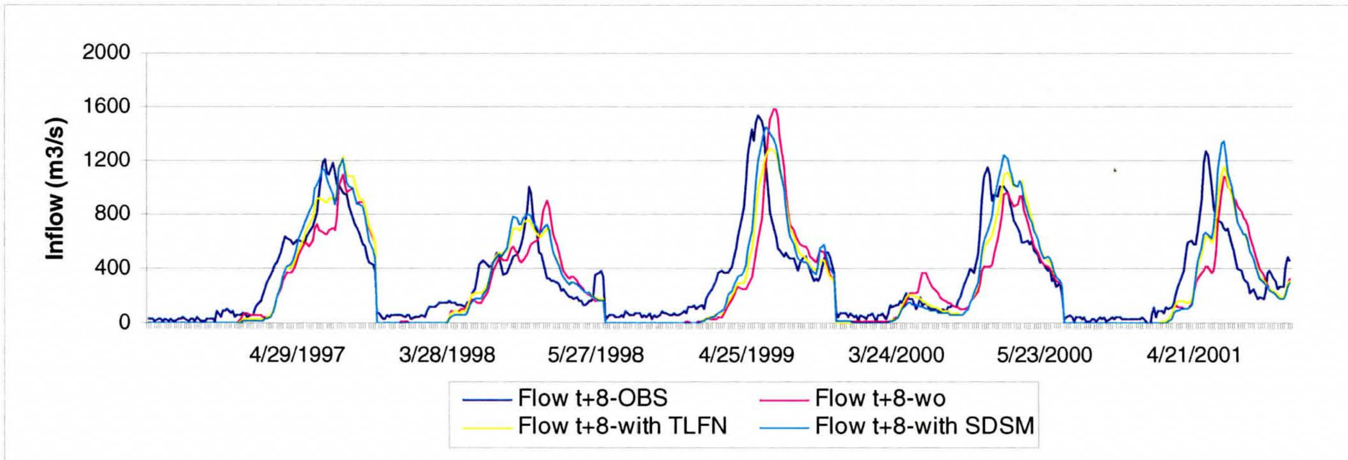

Figure 14 (b): Eight day ahead reservoir inflow forecasts (HBV annual model) for Spring season

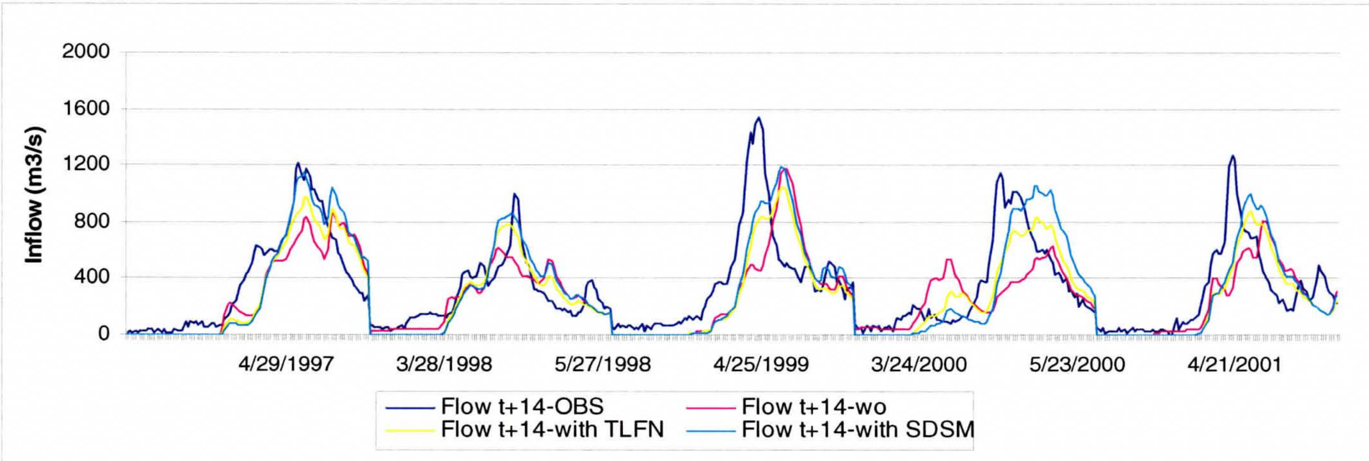

Figure 14 (c): Fourteen day ahead reservoir inflow forecasts (HBV annual model) for Spring season

Figure 14: Comparison of short term reservoir inflow forecasts (HBV annual model) for Spring season with and without downscaled data

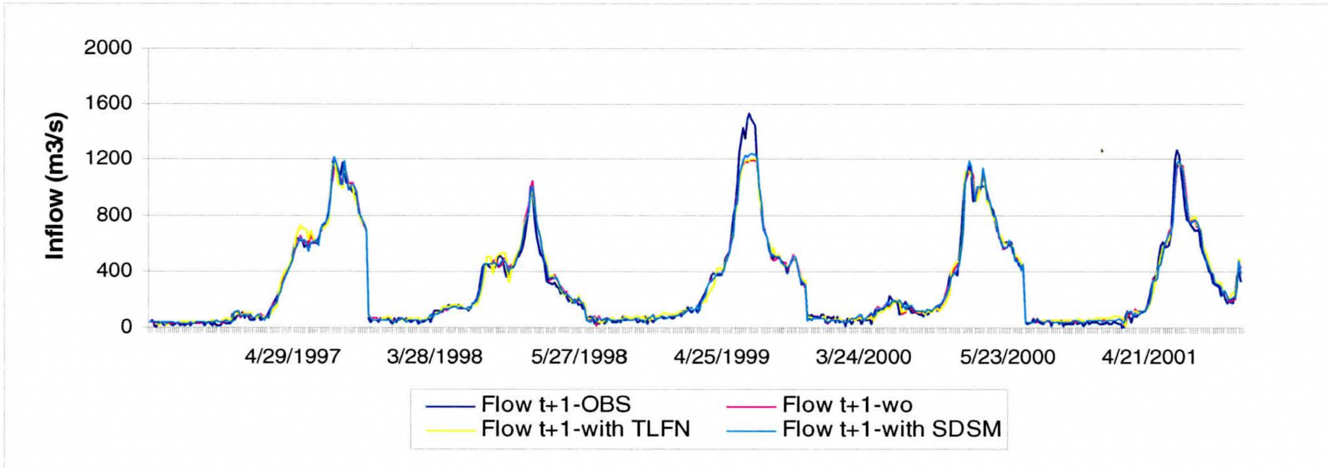

Figure 15 (a): One day ahead reservoir inflow forecasts (BNN annual model) for Spring season

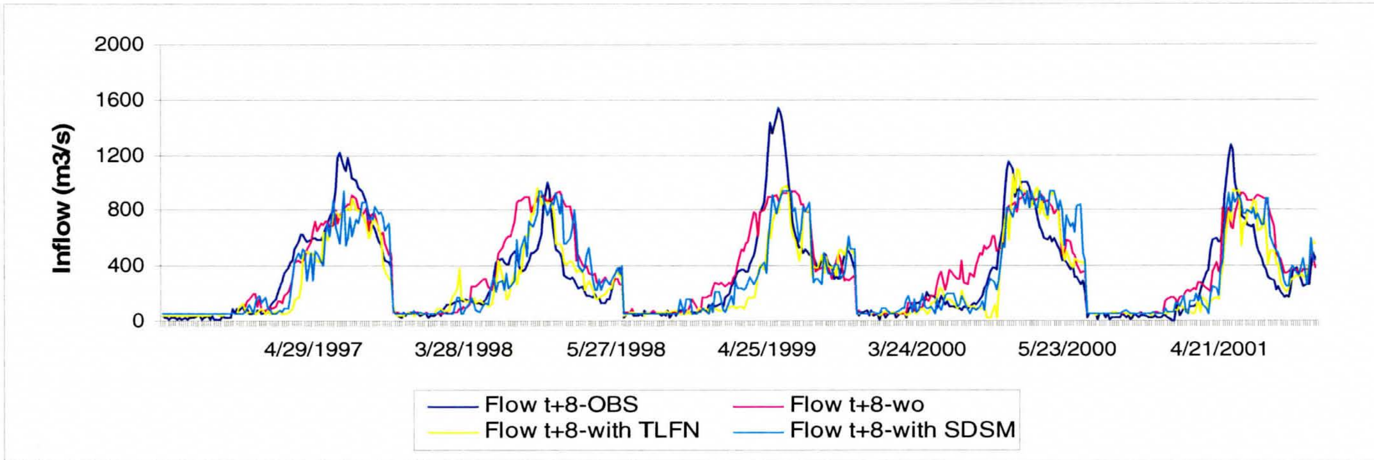

Figure 15 (b): Eight day ahead reservoir inflow forecasts (BNN annual model) for Spring season

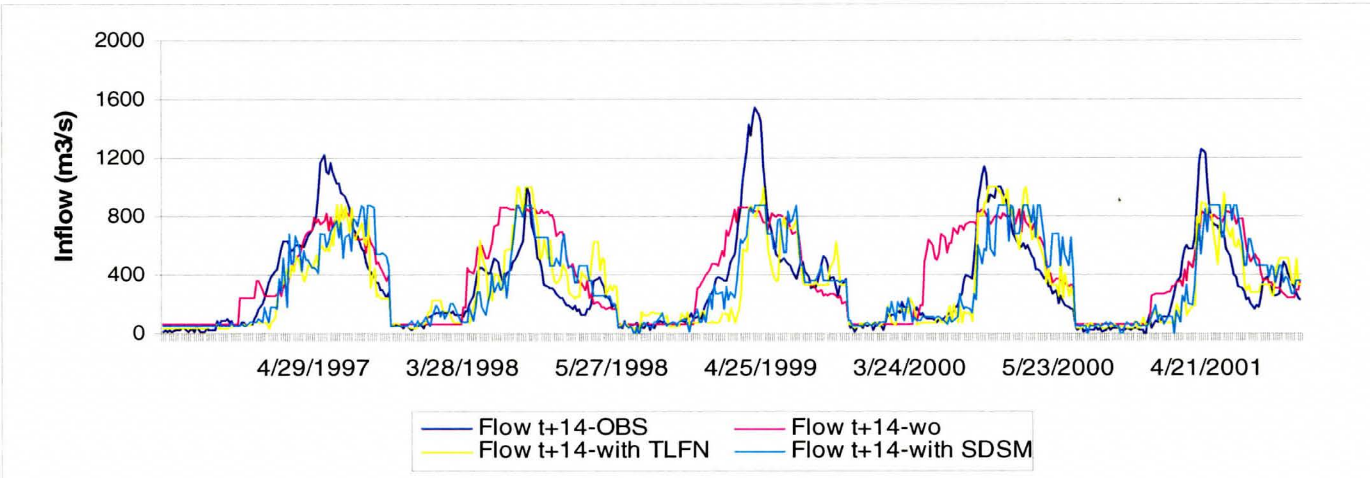

Figure 15 (c): Fourteen day ahead reservoir inflow forecasts (BNN annual model) for Spring season

Figure 15: Comparison of short term reservoir inflow forecasts (BNN annual model) for Spring season with and without downscaled data

5.3.3 Short-term Reservoir Inflow Forecasting for Spring using Seasonal Models

In order to simulate the Spring inflow properly, HBV and BNN seasonal models are constructed and trained to forecast short term reservoir inflows. This time only TLFN downscaled data is included in the hydrologic models and the results are compared with the models without including downscaled data. Table 15 show the results of up to 14 day ahead reservoir inflow forecasts for Spring using HBV seasonal models. We can see that the models perform similar to the annual models when there are no downscaled data included, and have very good results for up to 5 day ahead forecasting (R^2 more than 0.7), and the performance deteriorates in the following lags. When TLFN downscaled data are included, the models are improved for up to 12 day ahead forecasting, and the RMSE decrease by more than 25% in for 7 to 14 day ahead forecasting.

Forecasting results of BNN seasonal models for Spring season are presented in Table 16. Judged by the R^2, the results are very close to the results from annual models. The BNN models have good forecasting results up to 9 day ahead in both case of input data. There is a slight decrease in the RMSE when the TLFN data are included, suggesting that BNN seasonal models are similar to annual models.

Table 15: Up to 14 day ahead reservoir inflow forecasts for Spring using HBV seasonal models

Forecasting lags	**without downscaled data**			**including downscaled data (TLFN)**			
	RMSE	r	R2	RMSE	r	R2	**Decrease in RMSE**
Flows forecasting 1-day-ahead	93.05	0.97	**0.92**	105.07	0.97	**0.90**	-13%
Flows forecasting 2-day-ahead	103.39	0.96	**0.90**	111.50	0.95	**0.89**	-8%
Flows forecasting 3-day-ahead	151.43	0.90	**0.80**	139.14	0.92	**0.83**	8%
Flows forecasting 4-day-ahead	160.94	0.89	**0.73**	173.91	0.87	**0.79**	-8%
Flows forecasting 5-day-ahead	179.29	0.86	**0.71**	161.07	0.89	**0.78**	10%
Flows forecasting 6-day-ahead	203.56	0.82	0.62	166.26	0.89	**0.75**	18%
Flows forecasting 7-day-ahead	236.37	0.75	0.49	178.42	0.87	**0.71**	**25%**
Flows forecasting 8-day-ahead	229.44	0.76	0.52	179.95	0.87	**0.70**	**22%**
Flows forecasting 9-day-ahead	241.97	0.73	0.46	174.90	0.86	**0.72**	**28%**
Flows forecasting 10-day-ahead	243.81	0.71	0.45	179.41	0.85	**0.70**	**26%**
Flows forecasting 11-day-ahead	243.31	0.70	0.44	178.91	0.85	**0.70**	**26%**
Flows forecasting 12-day-ahead	256.52	0.67	0.38	192.41	0.83	0.65	**25%**
Flows forecasting 13-day-ahead	264.93	0.64	0.33	184.06	0.84	0.68	**31%**
Flows forecasting 14-day-ahead	259.17	0.65	0.36	203.55	0.81	0.60	**21%**

Table 16: Up to 14 day ahead reservoir inflow forecasts for Spring using BNN seasonal model

Forecasting lags	**without downscaled data**			**including downscaled data (TLFN)**			
	RMSE	r	R2	RMSE	r	R2	**Decrease in RMSE**
Flows forecasting 1-day-ahead	52.70	0.99	**0.98**	52.50	0.99	**0.98**	0%
Flows forecasting 2-day-ahead	84.70	0.97	**0.94**	76.70	0.97	**0.95**	9%
Flows forecasting 3-day-ahead	104.90	0.95	**0.91**	99.89	0.95	**0.91**	5%
Flows forecasting 4-day-ahead	118.70	0.94	**0.88**	122.90	0.93	**0.86**	-4%
Flows forecasting 5-day-ahead	142.90	0.91	**0.83**	142.90	0.90	**0.82**	0%
Flows forecasting 6-day-ahead	156.40	0.89	**0.79**	151.60	0.89	**0.79**	3%
Flows forecasting 7-day-ahead	171.40	0.86	**0.74**	165.10	0.87	**0.75**	**4%**
Flows forecasting 8-day-ahead	182.50	0.85	**0.71**	167.60	0.86	**0.74**	**8%**
Flows forecasting 9-day-ahead	189.10	0.84	**0.70**	182.40	0.84	**0.70**	**4%**
Flows forecasting 10-day-ahead	198.70	0.82	0.66	186.10	0.83	0.69	**6%**
Flows forecasting 11-day-ahead	205.10	0.79	0.62	189.50	0.82	0.67	**8%**
Flows forecasting 12-day-ahead	203.00	0.81	0.64	196.80	0.80	0.64	**3%**
Flows forecasting 13-day-ahead	205.70	0.80	0.62	189.70	0.82	0.66	**8%**
Flows forecasting 14-day-ahead	207.50	0.78	0.60	190.60	0.81	0.66	**8%**

As shown in the results of downscaling MRF data, the TLFN models do not perform well in downscaling precipitation. In order to find out if the downscaling precipitation or temperature help improving spring reservoir inflow forecasting or not, only downscaled temperature data from TLFN models are included in HBV models for short term inflows forecasting. The forecasting results are compared with the results of the case where there is no downscaled data included, and when there are both precipitation and temperature data included. Table 17 shows the comparison of up to 14 day ahead reservoir inflow forecasts for Spring using HBV seasonal model including only downscaled temperature data. It can be seen that the models performance improves obviously in forecasting from 7 to 14 day ahead reservoir inflows when only downscaled temperature are included, and the improvement is a little less than that of the case when both downscaled temperature and precipitation are included. This means the downscaled temperature plays an important role in improving the spring short term reservoir inflow forecasts, and the precipitation also helps, but not as much as the temperature. Those results (Table 17) also suggest that the accuracy of downscaled data may be particularly important. Temperature is very well downscaled by the TLFN and therefore makes a large contribution in improving spring inflow forecasts.

Table 17: Comparison of up to 14 day ahead reservoir inflow forecasts for Spring using HBV seasonal model including only downscaled temperature data

Forecasting lags	**without downscaled data**			**including downscaled Tmean (TLFN)**				**including downscaled P and T (TLFN)**			
	RMSE	r	R2	RMSE	r	R2	Decrease in RMSE	RMSE	r	R2	Decrease in RMSE
Flows forecasting 1-day-ahead	93.05	0.97	0.92	95.13	0.96	0.92	-2%	105.07	0.97	0.90	-13%
Flows forecasting 2-day-ahead	103.39	0.96	0.90	137.17	0.93	0.83	-33%	111.50	0.95	0.89	-8%
Flows forecasting 3-day-ahead	151.43	0.90	0.80	150.80	0.91	0.80	0%	139.14	0.92	0.83	8%
Flows forecasting 4-day-ahead	160.94	0.89	0.73	167.11	0.89	0.75	-4%	173.91	0.87	0.79	-8%
Flows forecasting 5-day-ahead	179.29	0.86	0.71	168.04	0.89	0.75	6%	161.07	0.89	0.78	10%
Flows forecasting 6-day-ahead	203.56	0.82	0.62	187.91	0.86	0.68	8%	166.26	0.89	0.75	18%
Flows forecasting 7-day-ahead	236.37	0.75	0.49	185.92	0.86	0.69	**21%**	178.42	0.87	0.71	**25%**
Flows forecasting 8-day-ahead	229.44	0.76	0.52	174.53	0.87	0.72	**24%**	179.95	0.87	0.70	**22%**
Flows forecasting 9-day-ahead	241.97	0.73	0.46	198.92	0.83	0.63	**18%**	174.90	0.86	0.72	**28%**
Flows forecasting 10-day-ahead	243.81	0.71	0.45	205.40	0.81	0.61	**16%**	179.41	0.85	0.70	**26%**
Flows forecasting 11-day-ahead	243.31	0.70	0.44	184.21	0.85	0.68	**24%**	178.91	0.85	0.70	**26%**
Flows forecasting 12-day-ahead	256.52	0.67	0.38	204.38	0.81	0.61	**20%**	192.41	0.83	0.65	**25%**
Flows forecasting 13-day-ahead	264.93	0.64	0.33	203.68	0.81	0.60	**23%**	184.06	0.84	0.68	**31%**
Flows forecasting 14-day-ahead	259.17	0.65	0.36	205.87	0.80	0.59	**21%**	203.55	0.81	0.60	**21%**

5.3.4 Comparison of HBV and BNN Performance in Short-term Reservoir Inflow Forecasting

In this section, the performance of HBV and BNN annual models in the optimal case (with TLFN downscaled data) of short-term reservoir inflow forecasting are compared. The forecasting results from both HBV and BNN methods are plotted and compared with the observed inflow. Figure 16 shows the scatter plots of 1,8, and 14 day ahead forecasting versus observed reservoir inflows using HBV models, and Figure 17 shows the scatter plots of 1,8, and 14 day ahead forecasting versus observed reservoir inflows using BNN models. From these two figures we can see that both HBV and BNN models perform quite well in one day ahead forecasting, and the BNN model performs much better than HBV in low flow forecasting, but it obviously underestimates peak flows. For 8 and 14 day ahead forecasting, the BNN model performs better than the HBV model in low flow forecasting and worse in peak flow forecasting, but both models underestimate the peak flows.

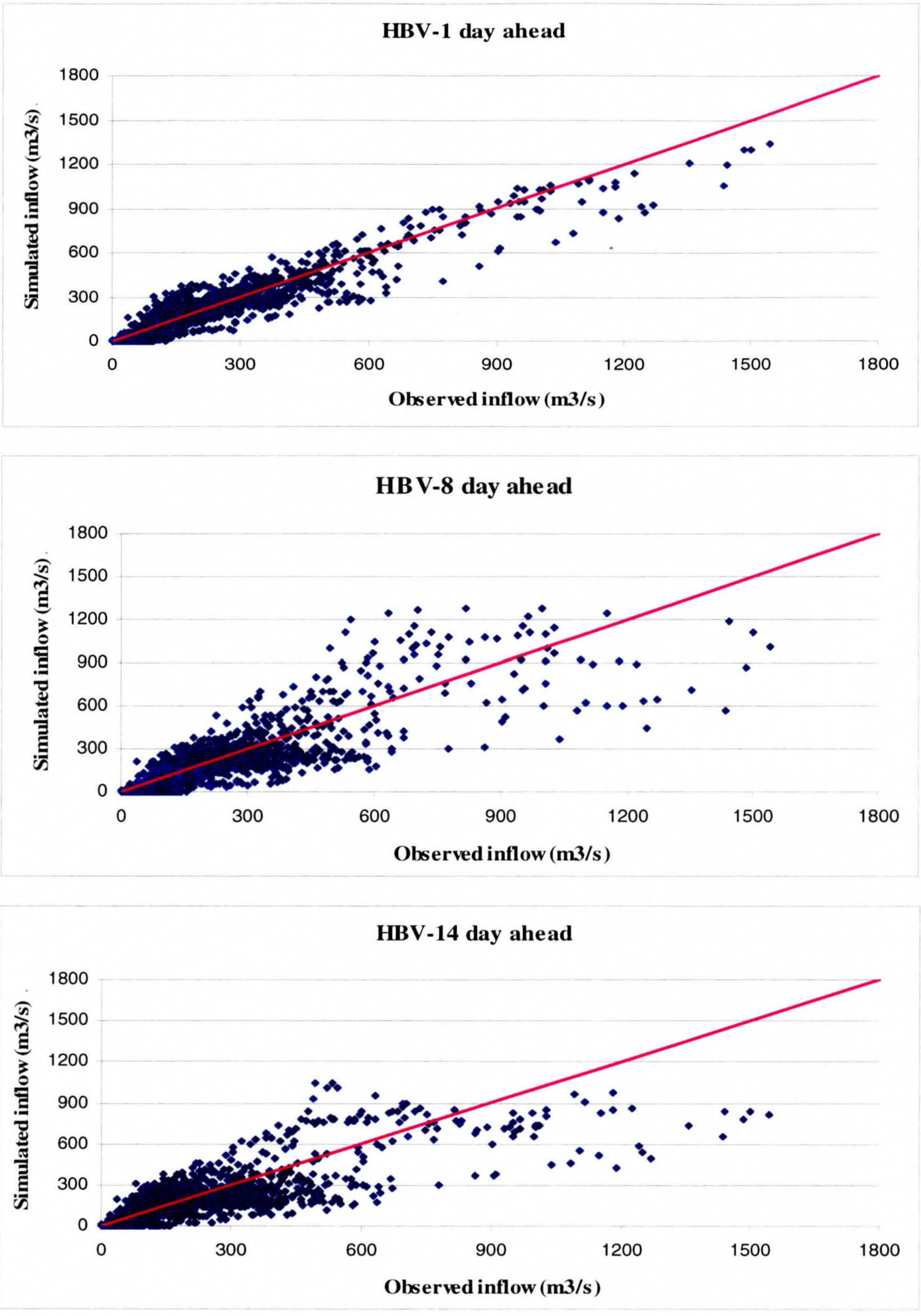

Figure 16: Scatter plots of observed vs simulated short term reservoir inflow forecasts using HBV model with TLFN downscaled data

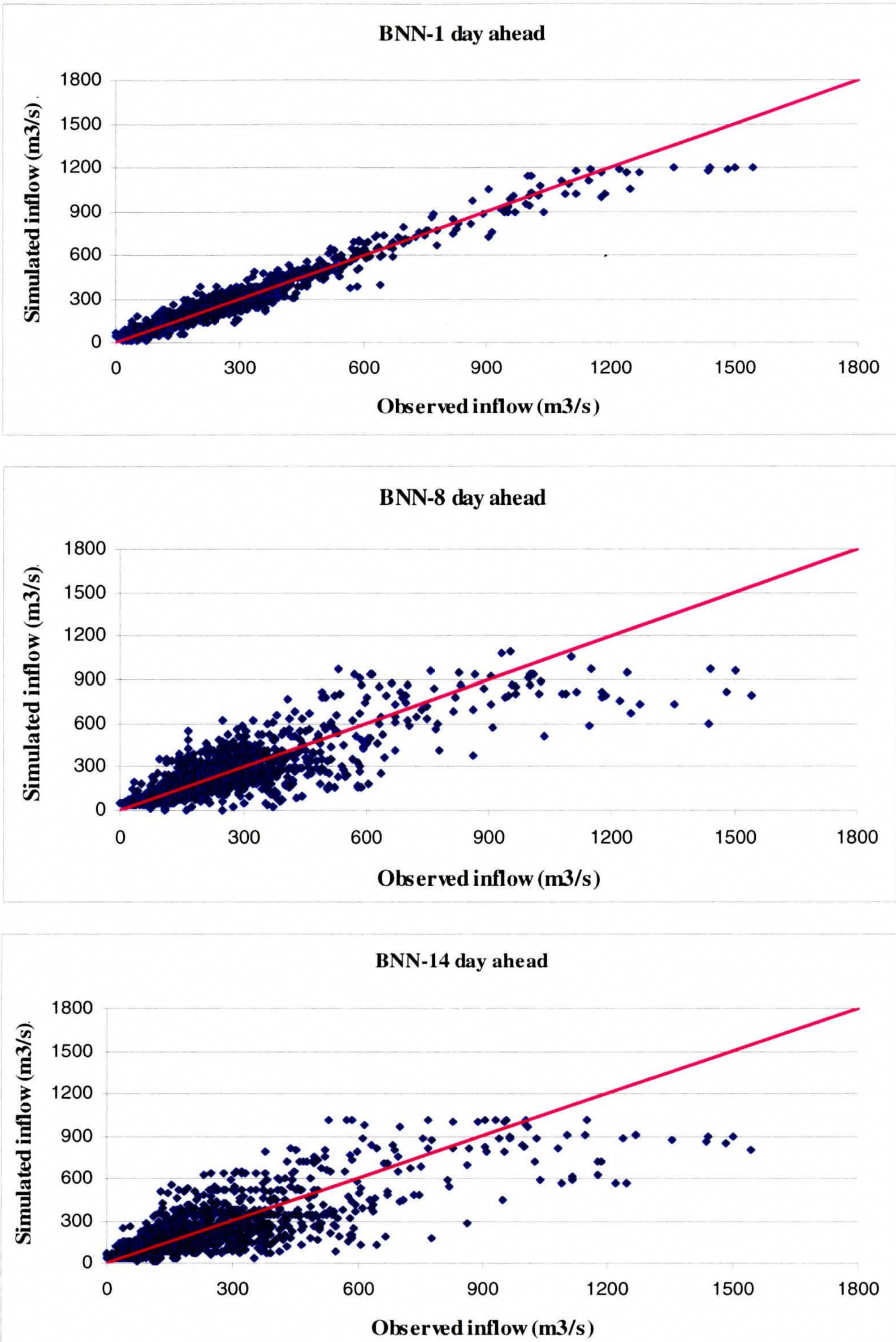

Figure 17: Scatter plots of observed versus simulated short term reservoir inflow forecasts using BNN model with TLFN downscaled data

5.4 Short-term Serpent River Flow Forecasting using HBV and BNN

5.4.1 Short-term Serpent River Flow Forecasting for Entire Year

Similar to the reservoir inflow forecasting, in this section, up to 14 day ahead Serpent river flows are forecasted based on the three different cases of input data, namely, observed meteorological data without downscaled data (case 1), observed meteorological data and TLFN downscaled data (case 2), and observed meteorological data and SDSM downscaled data (case 3). The forecasting results using HBV and BNN are presented in Tables 18 and 19 respectively.

From Table 18, we can see that the HBV model performs well in forecasting up to 3 day ahead inflows, the r values are above 0.85 and the R^2 are more than 0.70, and the models' performance deteriorates in forecasting more than 3 day ahead inflows. When TLFN downscaled data are included in the forecasting models, the model performs well in up to 5 day ahead forecasting. From 7 day to 14 day ahead forecasting, compared to the model run without downscaled data, the RMSE decreases more than 15% on average. In the 14 day ahead forecasting scenario, the r increase from 0.63 to 0.81, and R^2 increase from 0.30 to 0.56, which shows a potential for improvement. When SDSM downscaled data are included in the forecasting models, there are also improvements from 7 to 14 day ahead forecasting, the RMSE decreases about 15% on average.

Table 19 shows the BNN model results in forecasting up to 14 day ahead river flows. It can be found from the table that the BNN model performs well for up to 5 day ahead forecasting, the R^2 values are about or more than 0.70. When TLFN or SDSM downscaled data are included, the models do not show any improvement. In forecasting from 8 to 14 day ahead, the models even perform slightly worse, and the RMSE increases slightly. It can be concluded that the downscaled meteorological data does not help improve short term Serpent river flow predictions using BNN models.

The observed and simulated 1, 8, and 14 day ahead river flow forecasts from the two models are plotted in Figures 18 and 19 respectively to describe the models performance more clearly. From the two figures, it can be seen that both the HBV and

BNN models give very good flow forecasts for one day ahead forecasting. In the 8 and 14 day ahead forecasting, the HBV model shows obvious improvement in simulating peak flows when including TLFN and SDSM downscaled data. The same situation as that in forecasting reservoir inflows, the BNN model simulates almost perfect low flows in one day ahead river flow forecasting, but there is obvious underestimation in the peak flows. For 8 and 14 day ahead forecasting, BNN models obviously underestimate the peak flows. When TLFN and SDSM downscaled data are included in the BNN model, it does not show any improvement.

Table 18: Up to 14 day ahead Serpent river flow forecasts for entire year using HBV annual model

Forecasting lags	without downscaled-Testing			including TLFN-testing				including SDSM-testing			
	RMSE	r	R2	RMSE	r	R2	Decrease in RMSE	RMSE	r	R2	Decrease in RMSE
Flows forecasting 1-day-ahead	18.69	0.93	**0.83**	19.86	0.93	**0.82**	-6%	19.70	0.92	**0.81**	-5%
Flows forecasting 2-day-ahead	20.73	0.91	**0.76**	19.97	0.93	**0.81**	4%	21.41	0.92	**0.78**	-3%
Flows forecasting 3-day-ahead	24.32	0.89	**0.72**	22.55	0.92	**0.76**	7%	24.05	0.91	**0.72**	1%
Flows forecasting 4-day-ahead	26.67	0.86	0.66	25.13	0.90	**0.70**	6%	25.20	0.89	**0.70**	5%
Flows forecasting 5-day-ahead	29.08	0.81	0.60	25.43	0.88	**0.69**	13%	26.31	0.86	0.67	10%
Flows forecasting 6-day-ahead	32.37	0.75	0.50	27.64	0.88	0.63	15%	26.59	0.88	0.66	18%
Flows forecasting 7-day-ahead	32.28	0.76	0.50	28.53	0.85	0.61	**12%**	30.18	0.84	0.56	**7%**
Flows forecasting 8-day-ahead	33.98	0.73	0.45	28.54	0.86	0.61	**16%**	28.55	0.84	0.61	**16%**
Flows forecasting 9-day-ahead	35.47	0.69	0.40	29.33	0.84	0.59	**17%**	28.81	0.84	0.60	**19%**
Flows forecasting 10-day-ahead	35.38	0.70	0.40	30.62	0.82	0.55	**13%**	31.76	0.80	0.52	**10%**
Flows forecasting 11-day-ahead	35.88	0.69	0.38	30.07	0.83	0.57	**16%**	27.96	0.85	0.63	**22%**
Flows forecasting 12-day-ahead	36.11	0.69	0.38	27.89	0.85	0.63	**23%**	30.65	0.82	0.55	**15%**
Flows forecasting 13-day-ahead	37.80	0.65	0.32	29.74	0.84	0.58	**21%**	31.70	0.81	0.52	**16%**
Flows forecasting 14-day-ahead	38.15	0.63	0.30	30.48	0.81	0.56	**20%**	32.33	0.79	0.50	**15%**

Table 19: Up to 14 day ahead Serpent river flow forecasts for entire year using BNN annual model

Forecasting lags	without downscaled-Testing			including TLFN-testing				including SDSM-testing			
	RMSE	r	R^2	RMSE	r	R^2	Decrease in RMSE	RMSE	r	R^2	Decrease in RMSE
Flows forecasting 1-day-ahead	8.35	0.98	0.97	8.01	0.98	0.97	4%	8.78	0.98	0.96	-5%
Flows forecasting 2-day-ahead	15.40	0.94	0.89	14.49	0.95	0.90	6%	14.27	0.95	0.90	7%
Flows forecasting 3-day-ahead	20.66	0.89	0.80	20.39	0.90	0.80	1%	20.22	0.90	0.81	2%
Flows forecasting 4-day-ahead	22.46	0.87	0.76	21.39	0.89	0.79	5%	23.82	0.86	0.73	-6%
Flows forecasting 5-day-ahead	25.33	0.83	0.69	26.55	0.82	0.66	-5%	25.51	0.84	0.69	-1%
Flows forecasting 6-day-ahead	28.59	0.79	0.61	27.99	0.80	0.63	2%	28.60	0.79	0.61	0%
Flows forecasting 7-day-ahead	29.97	0.76	0.57	29.54	0.77	0.58	1%	28.92	0.78	0.60	4%
Flows forecasting 8-day-ahead	30.97	0.74	0.54	31.90	0.73	0.51	-3%	30.57	0.75	0.56	1%
Flows forecasting 9-day-ahead	31.48	0.73	0.53	32.94	0.70	0.48	-5%	32.14	0.72	0.51	-2%
Flows forecasting 10-day-ahead	32.41	0.71	0.50	35.61	0.67	0.43	-10%	32.86	0.70	0.49	-1%
Flows forecasting 11-day-ahead	32.03	0.72	0.52	33.74	0.68	0.46	-5%	33.36	0.69	0.47	-4%
Flows forecasting 12-day-ahead	33.34	0.70	0.48	35.69	0.65	0.40	-7%	34.07	0.68	0.45	-2%
Flows forecasting 13-day-ahead	33.04	0.70	0.48	35.82	0.64	0.39	-8%	34.89	0.65	0.43	-6%
Flows forecasting 14-day-ahead	33.31	0.69	0.48	35.83	0.63	0.40	-8%	34.71	0.66	0.43	-4%

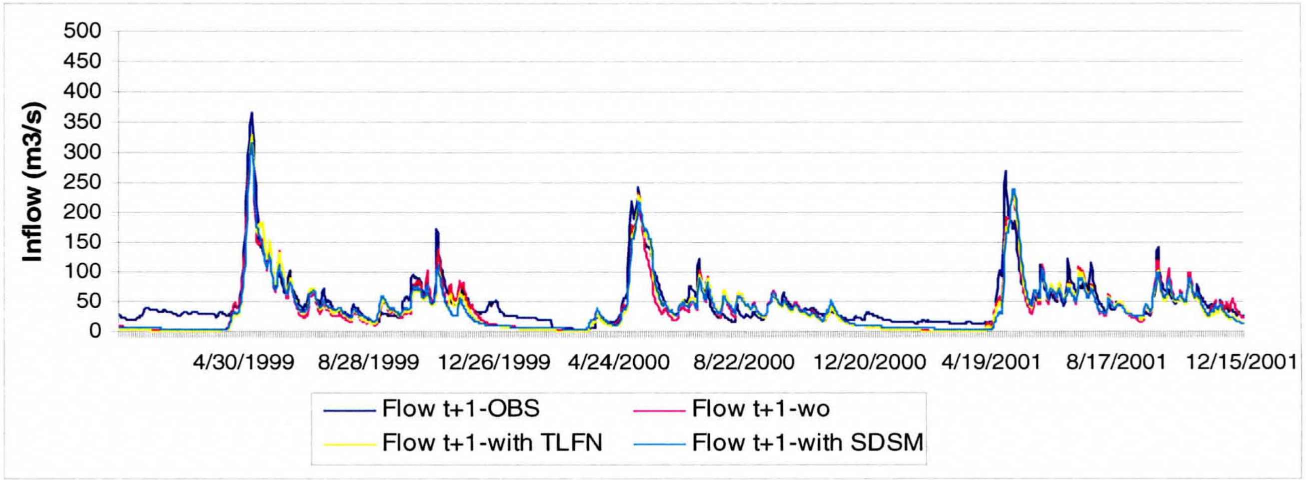

Figure 18 (a): One day ahead Serpent river flow forecasts (HBV annual model) for entire year

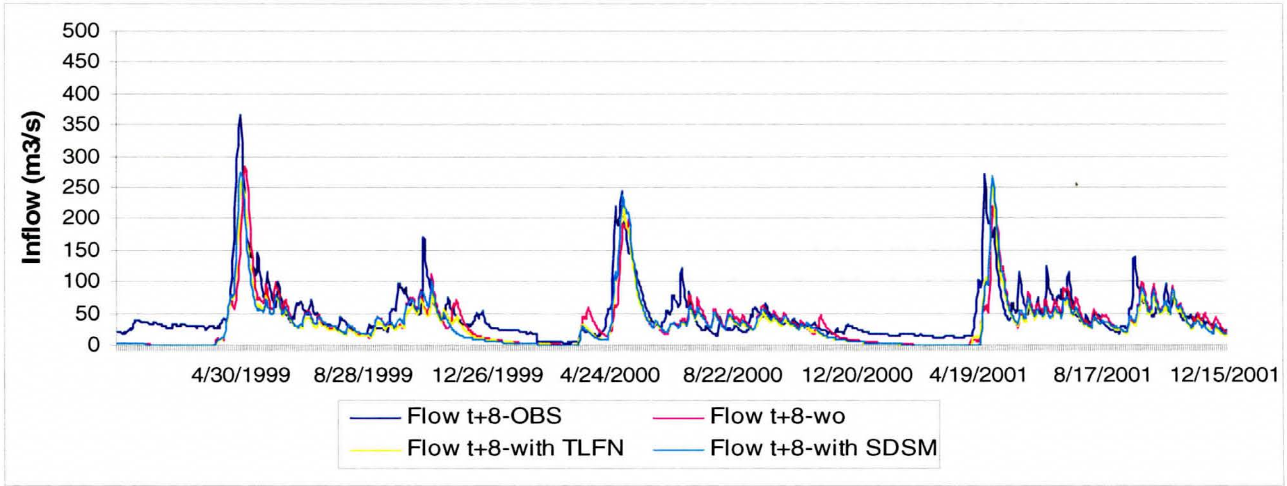

Figure 18 (b): Eight day ahead Serpent river flow forecasts (HBV annual model) for entire year

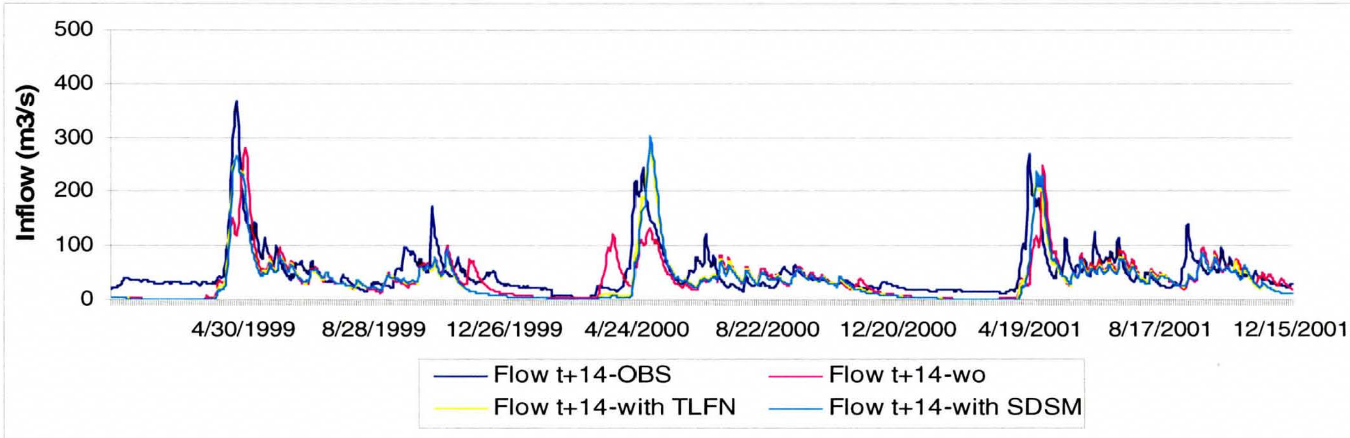

Figure 18 (c): Fourteen day ahead Serpent river flow forecasts (HBV annual model) for entire year

Figure 18: Comparison of short term Serpent river flow forecasts (HBV annual model) for entire year with and without downscaled data

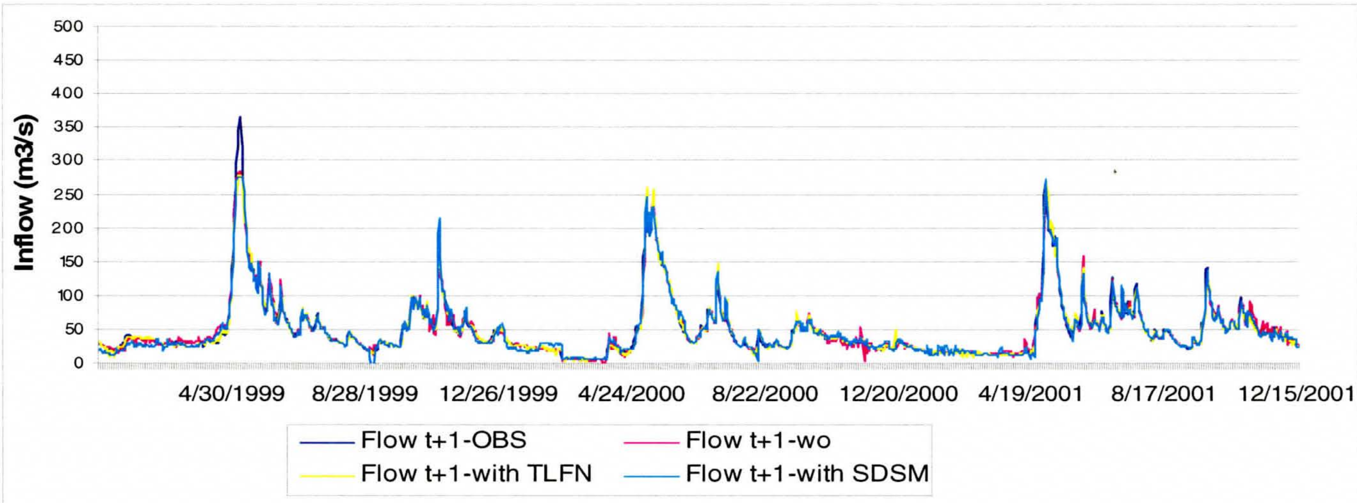

Figure 19 (a): One day ahead Serpent river flow forecasts (BNN annual model) for entire year

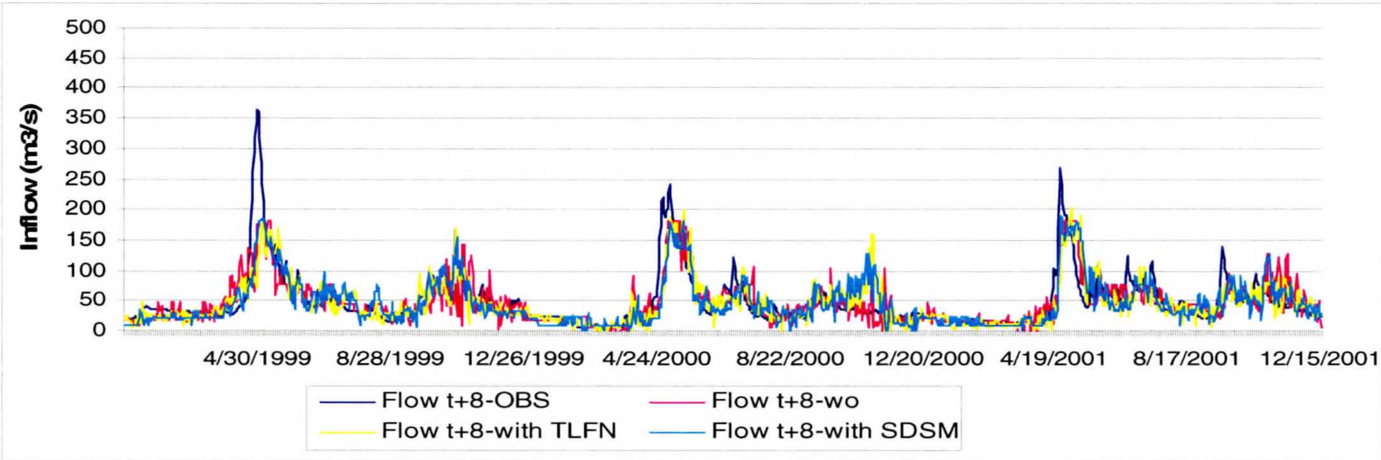

Figure 19 (b): Eight day ahead Serpent river flow forecasts (BNN annual model) for entire year

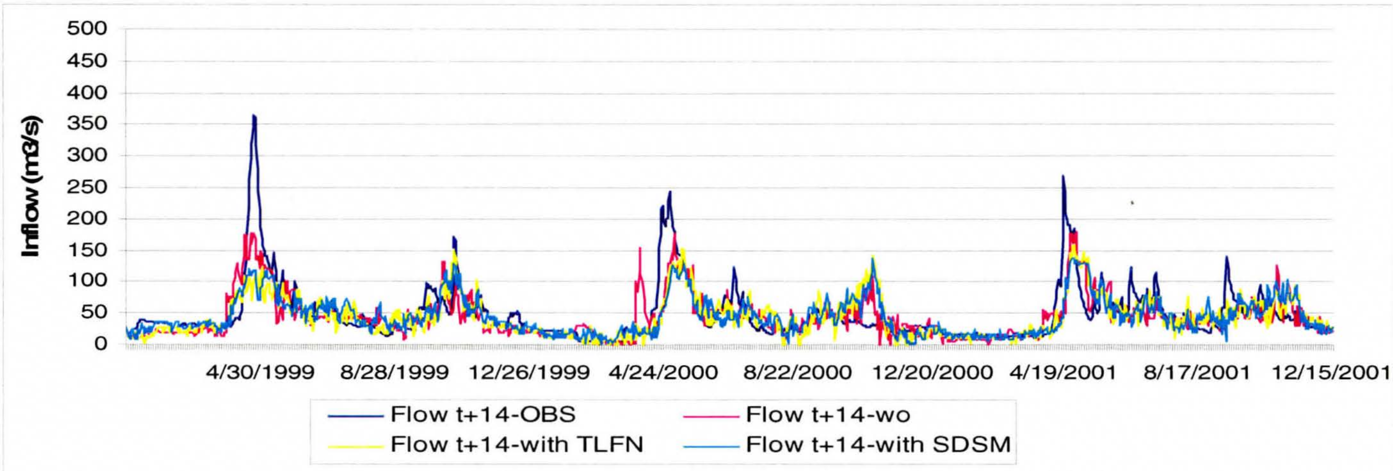

Figure 19 (c): Fourteen day ahead Serpent river flow forecasts (BNN annual model) for entire year

Figure 19: Comparison of short term Serpent river flow forecasts (BNN annual model) for entire year with and without downscaled data

5.4.2 Short-term Serpent River Flow Forecasting for Spring Season

The hydrologic models results in forecasting river flows are also more thoroughly explored by dividing the entire year of inflow series into seasonal inflows. Statistics of all the four seasons are calculated. In the following, Spring flows forecasts by HBV and BNN models are analyzed and presented in Tables 20 and 21. The models performance statistics for all the other seasons forecasting can be found in Appendix A2.

From Table 20, it can be seen that the HBV model provides good forecasts for Spring flows up to 4 day ahead with only observed meteorological data. When TLFN downscaled data are included, the model performs well up to 8 day ahead forecasting, and the R^2 values are all above 0.70. The RMSE also decreases by 25% to 30% for 6 to 14 day ahead forecasting when TLFN downscaled data are included. For the models including SDSM downscaled data, good forecasting for up to 6 day ahead can be obtained, and the RMSE decreases by 20% on average. But the models slightly deteriorate in one day ahead forecasting when downscaled data are included; this maybe caused by use of the inaccurate downscaled precipitation.

Table 21 shows the BNN model performance in forecasting up to 14 day ahead Spring river flows. It can be seen that when downscaled data are not included, the models give good results for up to 5 day ahead forecasting, which is better than that of the HBV model. When downscaled data are included, the models perform worse in most of the flow forecasting lags.

The observed and simulated river flow series for spring season from HBV and BNN models are plotted in Figures 20 and 21. Figure 20 shows the HBV annual model simulation results in 1, 8, and 14 day ahead Spring river flow forecasting. For 1 to 7 day ahead forecasting, the model performs well with all the three datasets. For 8 and 14 day ahead forecasting, the model underestimates the peak flow in some cases. When downscaled data are included, there is significant improvement in the flow forecasting skill.

From Figure 21, the BNN model's performance for short term river flow forecasting for Spring can be found. Just like the forecasting results for the entire year, the BNN model generated good results for 1 day ahead forecasting except for the underestimation of the peak flow in May, 1999. For 8 and 14 days forecasts, the model underestimates the peak flows, and there is no improvement when downscaled data are included, and the model performs worse for 14 day ahead forecasts.

Table 20: Up to 14 day ahead Serpent river flow forecasts for Spring season using HBV annual model

Forecasting lags	**without downscaled-Testing**			**including TLFN-testing**				**including SDSM-testing**			
	RMSE	r	R^2	RMSE	r	R^2	Decrease in RMSE	RMSE	r	R^2	Decrease in RMSE
Flows forecasting 1-day-ahead	24.27	0.97	0.90	26.59	0.96	0.88	-10%	28.14	0.95	0.87	-16%
Flows forecasting 2-day-ahead	27.18	0.95	0.88	24.90	0.97	0.90	8%	29.39	0.95	0.86	-8%
Flows forecasting 3-day-ahead	34.15	0.91	0.81	28.13	0.95	0.87	18%	33.00	0.93	0.82	3%
Flows forecasting 4-day-ahead	38.85	0.89	0.75	32.23	0.93	0.83	17%	34.49	0.92	0.80	11%
Flows forecasting 5-day-ahead	45.25	0.84	0.66	35.62	0.91	0.79	21%	38.93	0.90	0.75	14%
Flows forecasting 6-day-ahead	52.31	0.79	0.54	36.35	0.92	0.78	31%	36.37	0.91	0.78	30%
Flows forecasting 7-day-ahead	51.64	0.79	0.55	41.14	0.89	0.71	**20%**	45.91	0.86	0.64	**11%**
Flows forecasting 8-day-ahead	56.01	0.75	0.47	41.98	0.89	0.70	**25%**	43.39	0.87	0.68	**23%**
Flows forecasting 9-day-ahead	59.71	0.71	0.39	43.95	0.88	0.67	**26%**	43.87	0.87	0.67	**27%**
Flows forecasting 10-day-ahead	58.96	0.72	0.40	47.33	0.84	0.62	**20%**	50.57	0.82	0.56	**14%**
Flows forecasting 11-day-ahead	59.82	0.70	0.38	45.14	0.86	0.65	**25%**	40.85	0.89	0.71	**32%**
Flows forecasting 12-day-ahead	59.82	0.69	0.38	39.32	0.89	0.73	**34%**	46.55	0.85	0.62	**22%**
Flows forecasting 13-day-ahead	63.36	0.64	0.30	42.51	0.87	0.68	**33%**	47.69	0.84	0.60	**25%**
Flows forecasting 14-day-ahead	63.58	0.63	0.29	45.31	0.85	0.64	**29%**	50.39	0.82	0.55	**21%**

Table 21: Up to 14 day ahead Serpent river flow forecasts for Spring season using BNN annual model

Forecasting lags	without downscaled-Testing			including TLFN-testing				including SDSM-testing			
	RMSE	r	R^2	RMSE	r	R^2	Decrease in RMSE	RMSE	r	R^2	Decrease in RMSE
Flows forecasting 1-day-ahead	12.98	0.99	0.97	13.37	0.99	0.97	-3%	12.91	0.99	0.97	1%
Flows forecasting 2-day-ahead	20.61	0.97	0.93	21.80	0.96	0.92	-6%	21.08	0.97	0.93	-2%
Flows forecasting 3-day-ahead	29.16	0.93	0.86	29.28	0.93	0.86	0%	29.94	0.93	0.85	-3%
Flows forecasting 4-day-ahead	33.06	0.91	0.82	34.74	0.90	0.80	-5%	32.57	0.91	0.82	1%
Flows forecasting 5-day-ahead	38.29	0.87	0.75	41.19	0.85	0.72	-8%	37.02	0.88	0.77	3%
Flows forecasting 6-day-ahead	44.34	0.82	0.67	44.53	0.83	0.67	0%	41.24	0.85	0.71	7%
Flows forecasting 7-day-ahead	46.07	0.80	0.64	48.00	0.79	0.61	**-4%**	43.52	0.84	0.68	**6%**
Flows forecasting 8-day-ahead	48.16	0.78	0.61	52.72	0.74	0.53	**-9%**	47.03	0.80	0.62	**2%**
Flows forecasting 9-day-ahead	50.82	0.76	0.56	53.14	0.74	0.52	**-5%**	51.15	0.76	0.55	**-1%**
Flows forecasting 10-day-ahead	51.57	0.75	0.54	58.76	0.66	0.41	**-14%**	52.80	0.75	0.52	**-2%**
Flows forecasting 11-day-ahead	51.24	0.75	0.55	53.66	0.74	0.50	**-5%**	53.86	0.74	0.50	**-5%**
Flows forecasting 12-day-ahead	53.21	0.73	0.51	58.31	0.67	0.41	**-10%**	54.51	0.72	0.48	**-2%**
Flows forecasting 13-day-ahead	51.16	0.75	0.54	57.28	0.69	0.43	**-12%**	55.18	0.73	0.47	**-8%**
Flows forecasting 14-day-ahead	55.10	0.69	0.47	59.20	0.68	0.38	**-7%**	59.06	0.70	0.39	**-7%**

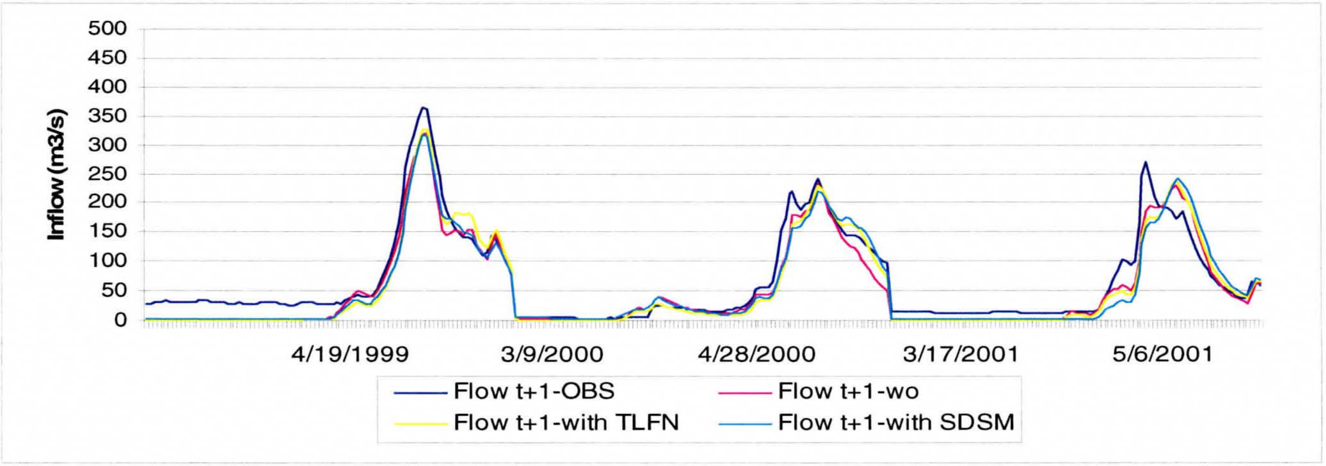

Figure 20 (a): One day ahead Serpent river flow forecasts (HBV annual model) for Spring season

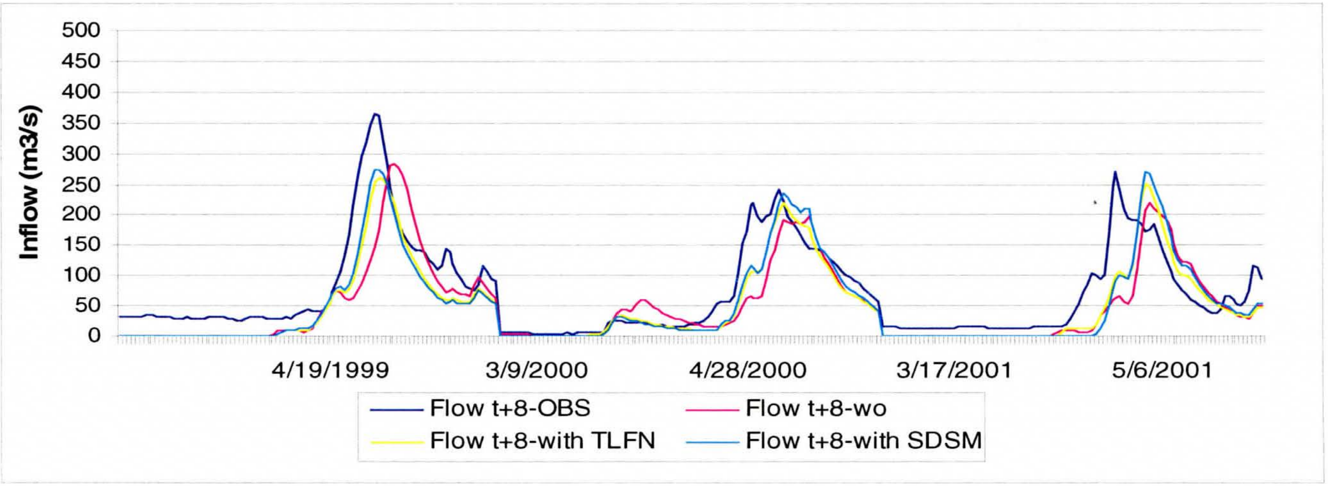

Figure 20 (b): Eight day ahead Serpent river flow forecasts (HBV annual model) for Spring season

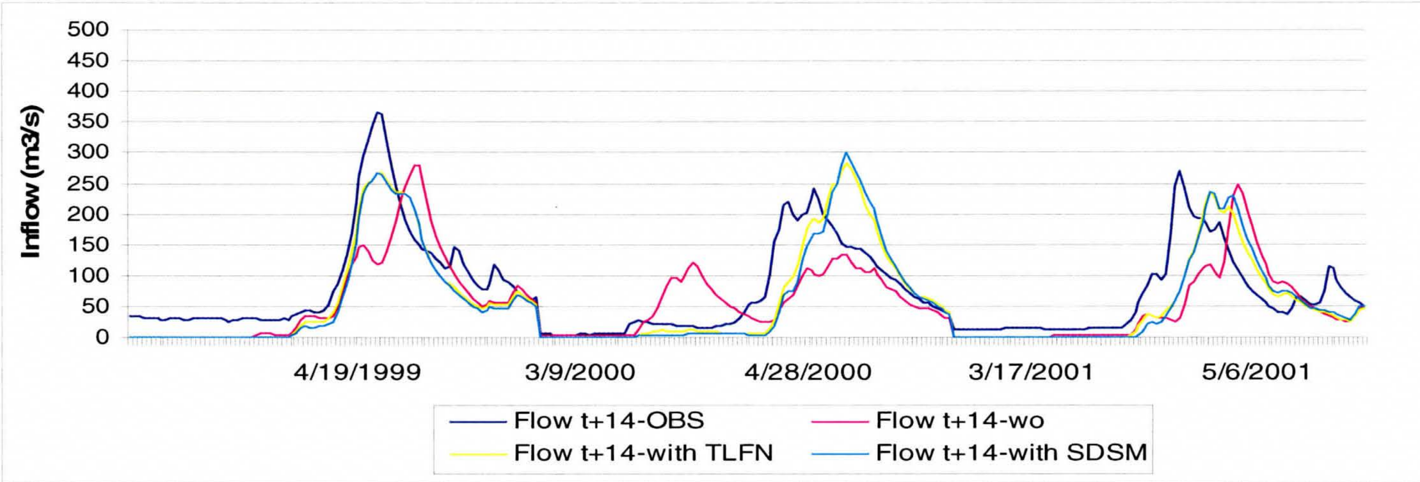

Figure 20 (c): Fourteen day ahead Serpent river flow forecasts (HBV annual model) for Spring season

Figure 20: Comparison of short term Serpent river flow forecasts (HBV annual model) for Spring season with and without downscaled data

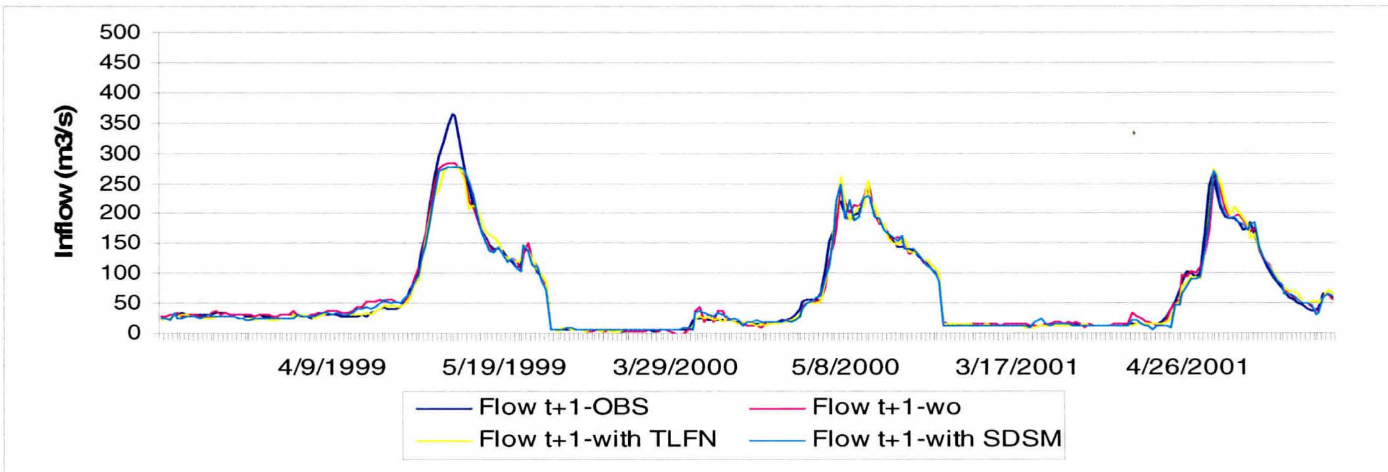

Figure 21 (a): One day ahead Serpent river flow forecasts (BNN annual model) for Spring season

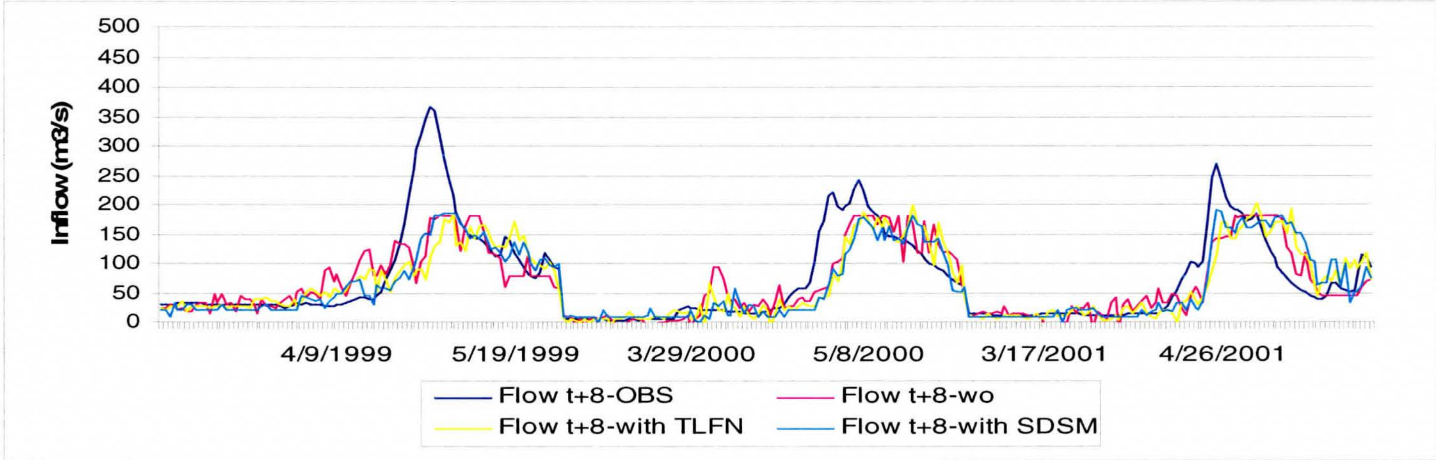

Figure 21 (b): Eight day ahead Serpent river flow forecasts (BNN annual model) for Spring season

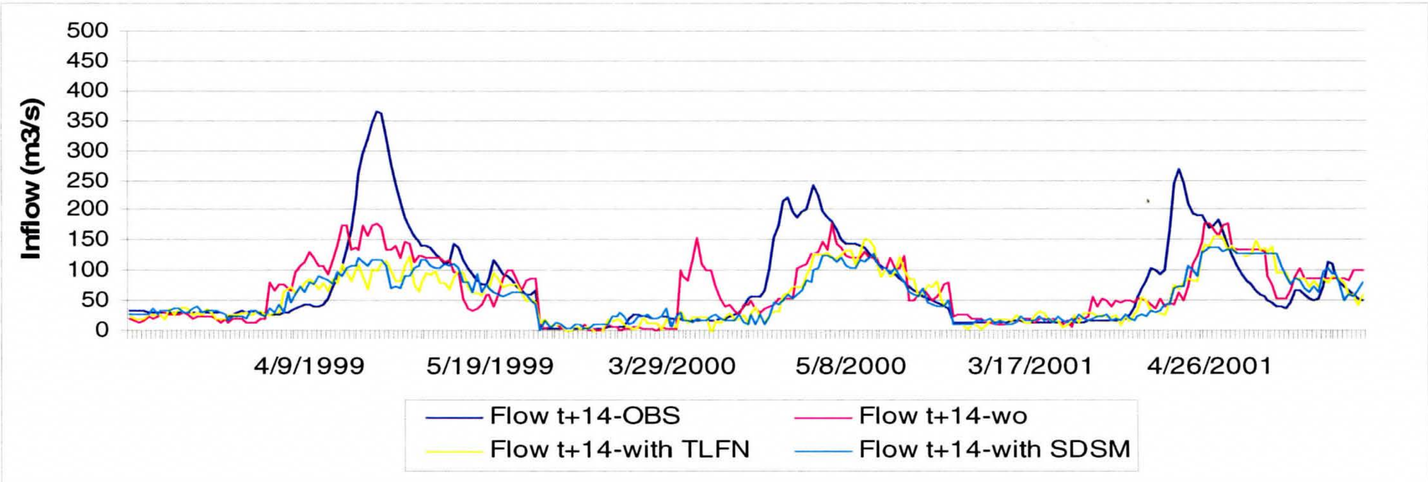

Figure 21 (c): Fourteen day ahead Serpent river flow forecasts (BNN annual model) for Spring season

Figure 21: Comparison of short term Serpent river flow forecasts (BNN annual model) for Spring season with and without downscaled data

Chapter 6: Conclusions

Through above analysis of downscaling results and hydrological forecasting results, conclusions can be drawn according to the two part results respectively.

In downscaling MRF ensemble predictions to derive local daily precipitation and temperature, all the three methods of TLFN, EPR, and SDSM have quite close performance at CDD station and CDP station. At both stations, all the three models have good performance in downscaling temperature. For Tmax and Tmin, the correlations between downscaled and observed data are above 0.95 for entire year results and also for most seasonal results. TLFN and EPR models perform better than SDSM, especially in some seasons. TLFN and EPR models have quite similar performance in most cases.

When downscaling precipitation, the three models do not perform as well as in downscaling temperature. The correlations are no more than 0.62, and the MSE are usually more than 20mm. While TLFN and EPR models have better performance in Winter than the other three seasons, the MSE are less than 10 and the r values are more than 0.70, and NMSE are about 0.5. TLFN and EPR models still perform quite similarly, and better than SDSM. Judged by NMSE, MSE and r, SDSM models perform poorly in the entire year and also in all the seasons, the NMSE are more than 2 times compared with the NMSE of TLFN and EPR.

In general, the comparative results suggest TLFN and EPR have a good potential for downscaling MRF ensemble weather forecasts. Because TLFN models are more thoroughly explored and the results are slightly better than EPR in some cases, the downscaled data from TLFN models are included as predictors in the hydrological models and compared with the situations where SDSM downscaled data are included and when there are no downscaled data included.

In the up to 14 day ahead reservoir inflow forecasting using HBV models, the forecasting results from the three different input datasets are compared. When there are no downscaled precipitation and temperature data included (case 1), the models give good results for up to 5 day ahead forecasting (R^2 more than 0.7). When TLFN downscaled data are included, there is no significant improvement for 1 to 5 day ahead forecasting, but there is significant improvement for 6 to 14 day ahead forecasting, the RMSE decrease by 20% in average. When SDSM downscaled data are included, there is also some improvement for 6 to 14 day ahead forecasting, the RMSE decreases by 10% in average.

When the entire year HBV models are used for reservoir inflow forecasting in Spring, the models also have good performance in up to 5 day ahead forecasting, and there are improvements for 6 to 14 day ahead inflow forecasting when downscaled data is included. The RMSE decrease more than 20% in almost all the forecasts from 7 to 14 day with TLFN downscaled data, and more than 15% with SDSM downscaled data. The HBV seasonal models perform similarly to the annual models when there is no downscaled data included, and give good results for up to 5 day ahead forecasting, and the performance deteriorates in the following lags. When TLFN downscaled data are included, the models can give good results for up to 11 day ahead forecasting, and the RMSE decrease more than 25% for 7 to 14 day ahead forecasting. It can be concluded that downscaled meteorological data can help to improve 7 to 14 day ahead forecasting in HBV models.

When only downscaled temperature data from TLFN models are included in HBV Spring models for short term inflows forecasting, the results show that the models performance improves significantly in forecasting from 7 to 14 day ahead reservoir inflows, but the improvement is a little less than that of the case when both downscaled temperature and precipitation are included. This means the downscaled temperature plays an important role in improving the short term Spring inflows forecasting, and the precipitation also helps, but is less important than temperature in this case. This may be mostly due to the poor quality of the downscaled precipitation data.

When BNN models are applied for up to 14 day ahead reservoir inflow forecasting, the same input data are used. When there is no downscaled data included, the models have good performance in up to 8 days ahead forecasting, the R^2 values are all around or more than 0.70. When TLFN downscaled data are included, the models do not show obvious improvement, the decreases in RMSE are very slight. When SDSM downscaled data are included, the models even perform a little bit worse, RMSE increase around 5%. The entire year models and seasonal BNN models are also used for reservoir inflow forecasting in Spring season respectively. The forecasting results are quite close to the entire year inflow forecasting results. When there is no downscaled data included, the models have good performance in up to 8 days ahead forecasting. When downscaled data are included, there is no decrease in RMSE compared with the case when no downscaled data included. It can be concluded from these results that the BNN models have no obvious improvement in the short term reservoir inflow forecasting when downscaled meteorological data are included.

From the scatter plots and the plots of the observed and forecasted inflows from the HBV and BNN models respectively, it can be found that the BNN models have better performance than HBV models in low flows forecasting, while worse in peak flow forecasting. When downscaled precipitation and temperature data is included, there is significant improvement when HBV models are applied. But BNN models do not show any improvement when including downscaled meteorological data.

The HBV and BNN models performance in river flows forecasting is quite close to that of reservoir inflow forecasting. HBV models give good forecasting results for up to 3 day ahead forecasting, while BNN models have good performance for up to 5 day ahead forecasting when there is no downscaled data included. When downscaled data is included, HBV models give improved forecasting in entire year flows and also Spring flows, especially in peak flows forecasting, while there is no significant improvement in BNN models forecasting results.

Through above analysis and conclusions, some recommendations can be given. In downscaling precipitation, the models do not have good enough performance, and the correlation between the observed and downscaled precipitation are no more than 0.62. There is a need to further improve the accuracy of the downscaled precipitation. In the hydrological forecasting part, both HBV and BNN models do not perform well in peak flows forecasting. Although HBV models show improvement for 6 to 14 day ahead forecasting when including TLFN downscaled data, the results are still not good enough for application in operational forecasting. There is still a large room for improvement.

Reference

Aqil, M., Kita, I., Yano, A., Nishiyama, S., 2007. A comparative study of artificial neural networks and neuro-fuzzy in continuous modeling of the daily and hourly behaviour of runoff, Journal of Hydrology, 337, 22– 34.

Arheimer, B., Brandt, M., 1998. Modelling nitrogen transport and retention in the catchments of southern Sweden, Ambio, 27, 471-480.

Bergström, S., Carlsson, B., Gardelin, M., Lindstroem, G., Pettersson, A., Rummukainen, M., 2001. Climate change impacts on runoff in Sweden — assessments by global climate models, dynamical downscaling and hydrological modeling, Climate Research, 16, 101–112.

Bergström, S., 1976. Development and application of a conceptual runoff model for Scandinavian catchments, SMHI Rep. 7, Norrköping, Sweden.

Beven, K.J., 1989. Changing ideas in hydrology: the case of physically-based models, Journal of Hydrology, 105, 157-172.

Beven, K.J., Kirkby, M.J., 1979. A physically based, variable contributing area model of basin hydrology, Hydrological Science Bulletin ,24 (1), 43-69.

Blazkova, S., Beven, K.J., 1997. Flood frequency prediction for data limited catchments in the Czech Republic using a stochastic rainfall model and TOP-MODEL, Journal of Hydrology, 195, 256-278.

Blazkova, S., Beven, K.J., 2002. Flood frequency estimation by continuous simulation for a catchment treated as ungauged (with uncertainty), Water Resources Research, 38 (8).

Blazkova, S., Beven, K.J., 2004. Flood frequency estimation by continuous simulation of subcatchment rainfalls and discharges with the aim of improving dam safety assessment in a large basin in the Czech Republic, Journal of Hydrology, 292, 153-172.

Boughton, W., 2004. The Australian water balance model, Environmental Modelling & Software, 19 (10), 943-956.

Boughton, W., 2006. Calibrations of a daily rainfallerunoff model with poor quality data, Environmental Modelling & Software, 21 (8), 1114-1128.

Brandt, M., 1990. Simulation of runoff and nitrate transport from mixed basins in Sweden, Nord. Hydrology, 21, 13-34.

Burger.G, Chen.Y, 2005. Regression-based downscaling of spatial variability for hydrologic applications, Journal of Hydrology, 299-317.

Cannon, A.J., and Whitfield P.H., 2002. Downscaling recent streamflow conditions in British Columbia, Canada using ensemble neural network models, Journal of Hydrology, 259, 136-151.

Carlson R.F., MacCormick A.J.A., Watts D.G., 1970. Application of linear models to four annual streamflow series, Water Resources Research, 6 (4), 1070–1078.

Chang, F.J., Chen, Y.C., 2001. A counterpropagation fuzzy-neural network modeling approach to real time streamflow prediction, Journal of Hydrology, 245, 153–164.

Conway, D., Wilby, R.L. and Jones. P.D. 1996, Precipitation and air flow indices over the British Isles, Climate Research 7, 169–83.

Coulibaly P., Anctil F., Bobee B., 2001a. Multivariate reservoir inflow forecasting using temporal neural networks, Journal of Hydrologic Engineering, ASCE6 (5), 367–376.

Coulibaly, P., 2004. Downscaling daily extreme temperatures with genetic programming, Geophysical Research Letters, 31, L16203.

Coulibaly, P., Anctil, F., Aravena, R., Bobee, B., 2001b. Artificial neural network modeling of water table depth fluctuations, Water Resources Research, 37, 885–896.

Coulibaly, P., Anctil, F., Bobee, B., 2000. Daily reservoir inflow forecasting using artificial neural networks with stopped training approach, Journal of Hydrology, 230, 244-257.

Coulibaly, P., Dibike, Y.B, Anctil, F., 2005. Downscaling precipitation and temperature with temporal neural networks, Journal of Hydrometeorology, 483-495.

Coulibaly, P., Hache, M., Fortin, V., and Bobee, B., 2005. Improving daily reservoir inflow forecasts with model combination, Journal of Hydrologic Engineering, 2, 91-99.

Crane, R.G., Hewitson. B. C., 1998. Doubled CO_2 precipitation changes for the

Susquehanna Basin: Downscaling from the GENESIS general circulation model, International Journal of Climatology 18, 65–76.

Daliakopoulos, I.N., Coulibalya, P., Tsanis, I.K., 2005. Groundwater level forecasting using artificial neural networks, Journal of Hydrology, 309, 229–240.

Davidson, J.W., Savic, D.A., Walters G.A, 2000. Approximators for the Colebrook-White Formula Obtained through a Hybrid Regression Method, Computational Methods in Water Re-sources, Bentley.

Dibike, Y.B, and Coulibaly, P., 2005. Hydrologic impact of climate change in the Saguenay watershed: comparison of downscaling methods and hydrologic models, Journal of Hydrology, 145-163.

Dibike, Y.B, and Coulibaly, P., 2006. Temporal neural networks for downscaling climate variability and extremes, Neural Networks, 19 (2), 135-144.

Ewen, J., Parkin, G., O'Connell, P.E., SHETRAN, 2000. Distributed river basin flow and transport modeling system. In: Proceedings of the American Society of Civil Engineering, Journal of Hydrologic Engineering 5, 250-258.

Giorgi. F., Mearns, L.O., 1999. Introduction to special section: Regional climate modeling revisited, J. Geophys. Res.-Atmos. 104, 6335–6352.

Giustolisi, O., Savic, D.A., 2003. Evolutionary Polynomial Regression (EPR): Development and Applications, School of Engineering, Computer Science and Mathematics, Centre for Water Systems, University of Exeter.

Giustolisi, O., Savic, D.A., 2005. A Symbolic Data-driven Technique Based on Evolutionary Poly-nomial Regression, Journal of Hydroinformatics, 8 (3), 207-222.

Giustolisi, O., Savic, D.A.: A novel strategy to perform genetic programming: Evolutionary Polynomial Regression, 6th Int. Conf. on Hydroinformatics, Singapore, Liong, Phoon & Babovic (eds), World Scientific Publishing Company, 1, 787-794, 2004.

Goswami, M., and O'Connor, K, 2007. Real-time flow forecasting in the absence of quantitative precipitation forecasts: A multi-model approach, Journal of Hydrology, 334, 125– 140.

Grayson, R.B., Moore I.D., McMahon T.A., 1992. Physically based hydrologic modeling, 2, Is the concept realistic, Water Resour. Res. 28 (10) 2659–2666.

Halff, A.H., H.M.Halff, and M. Azmoodeh, 1993. Predicting runoff from rainfall using neural networks, in Proceedings of Engineering Hydrology, pp. 760-765.

Hamill, T.M., Whitaker, J.S., Wei, X., 2004. Ensemble Reforecasting: Improving Medium-Range Forecast Skill Using Retrospective Forecasts, Monthly Weather Review, 132(6), 1434-1447.

Hay, L. E., Clark, M. P., 2003. Use of statistically and dynamically downscaled atmospheric model output for hydrologic simulations in three mountainous basins in the western United States, Journal of Hydrology, 282, 56-75

Hay, L.E., McCabe, G.J., Wolock, D.M. and Ayers, M.A. 1991. Simulation of precipitation by weather type analysis, Water Resources Research 27, 493–501.

Hay, L.E., Wilby, R.L., Leavesley, G.H., 2000. A comparison of delta change and downscaled GCM scenarios for three mountainous basins in the United States, Journal of the American Water Research Association, 36, 387–397.

Hu, T.S., Lam, K.C., Ng, S.T., 2001. River flow time series prediction with a range-dependent neural network, Hydrol. Sci. J. 46, 729–745.

Imrie, C.E., Durucan, S., Korre, A., 2000. River flow prediction using artificial neural networks: generalisation beyond the calibration range, J. Hydrol. 233, 138–153.

Jain A., Indurthy S.K.V.P., 2003. Comparative analysis of event based rainfall–runoff modeling techniques—deterministic, statistical, and artificial neural networks, J. Hydrol. Eng. ASCE 8 (2), 93–98.

Jain A., Ormsbee L.E., 2002. Evaluation of short-term water demand forecast modeling techniques: conventional v/s artificial intelligence, J. Am.Water Works Assoc. 94 (7), 64–72.

Jain A., Varshney A.K., Joshi U.C., 2001. Short-term water demand forecast modeling at IIT Kanpur using artificial neural networks, Water Resour.Manage., 15 (5), 299–321.

Jain, A., and Kumar, A, M., 2007. Hybrid neural network models for hydrologic time series forecasting, Applied Soft Computing, 7, 585–592.

Jain, A., and S. Srinivasulu, 2004. Development of effective and efficient rainfall-runoff models using integration of deterministic, real-coded genetic algorithms and artificial neural network techniques, Water Resource Research, 40, W04302.

Kalnay, E., Kanamitsu, M., Kistler, R., Collins, W., Deaven, D., Gandin, L., Iredell, M., Saha, S., White, G, Woollen, J., Zhu, Y., Chelliah, M., Ebisuzaki, W., Higgins, W., Janowiak, J., Mo, K.C., Ropelewski, C., Wang , J., Leetmaa, A., Reynolds, R., Jenne, R., Joseph, D., 1996. The NCEP/NCAR reanalysis project, Bulletin of the American Meteorological Society, 77, 437–471.

Karl T.R, Wang WC, Schlesinger ME, Knight RW, Portman D, 1990. A method of relating general circulation model simulated climate to the observed local climate, Part I: seasonal statistics. J Clim, 3, 1053-1079.

Karunasinghe, D., Liong, S., 2006. Chaotic time series prediction with a global model: Artificial neural network, Journal of Hydrology, 323, 92–105.

Katz, R.W. 1996. Use of conditional stochastic models to generate climate change scenarios, Climatic Change, 32, 237–55.

Khan, M.S., Coulibaly, P., 2006. Bayesian neural network for rainfall-runoff modeling, Water Resources Research, 42, W07409.

Kite, G.W., 1978. Development of a hydrologic model for a Canadian watershed, Canadian Journal of Civil Engineering 5 (1), 126-134.

Koza, J.R., 1992. Genetic Programming: On the Programming of Computers by Natural Selection, MIT Press, Cambridge, MA .

Kuligowski, R., Barros, A.P., 1998. Localized precipitation forecasts from a numerical weather prediction model using artificial neural networks, Weather Forecast. 13, 1195–1205.

Kumar, D.N., Raju, K.S., Sathish, T., 2004. River flow forecasting using recurrent neural networks, Water Resources Mangement, 18, 143–161.

Lampinen, J. Vehtari A., 2001. Bayesian approach for neural networks-review and case studies, Neural Networks, 14, 257-274.

Landman.W.A., Mason.S.J, et al, 2001. Statistical downscaling of GCM simulations to streamflow, J.Hydrol, 22-236.

Leung, L.R., Hamlet, A.F., Lettenmaier, D.P., Kumar A., 1999. Simulations of the ENSO hydroclimate signals in the Pacific Northwest Columbia River basin, Bulletin of the American Meteorological Society, 80, 2313–2329.

Lidén R., and Harlin, J., 2000. Analysis of conceptual rainfall-runoff modeling performance in different climates, Journal of Hydrology, 238, 231-247.

Lindström, G., Gardelin, M., Johansson, B, Persson, M., Bergström, S, 1996. HBV-96-En areellt fordelad model for vattenkrafthydrologin, Rep. RH 12, Swed. Meteorol. And Hydrol. Inst., Norrköping.

Luk, K.C., Ball, J.E., Sharma, A., 2001. An application of artificial neural networks for rainfall forecasting, Math. Computer Modell. 33, 683–693.

Moretti, G., and Montanari, A., 2007. A spatially distributed grid based rainfallerunoff model for continuous time simulations of river discharge, Environmental Modelling & Software, 22, 823-836

Nayak, P.C., Sudheer, K.P., Rangan, D.M., Ramasastri, K.S., 2004. A neuro-fuzzy computing technique for modeling hydrological time series, J. Hydrol. 291, 52–66.

Nayak, P.C., Sudheer, K.P., Rangan, D.M., Ramasastri, K.S., 2005. Short-term flood forecasting with a neurofuzzy model, Water Resour. Res. 41, 2517–2530.

Olsson.J, Uvo.C.B. et al. 2004. Neural networks for rainfall forecasting by atmospheric downscaling, J Hydrol. Enginee. ASCE, 1-12.

Principe, J. C., Euliano, N. R., Lefebvre, W. C., 2000. Neural and adaptive systems: Fundamentals through simulations, New York.

Rami'rez, M.C.P., Velho, H.F.C., Ferreira, N.J., 2005. Artificial neural network technique for rainfall forecasting applied to the Sao˜ Paulo region, J. Hydrol. 301, 146–162.

Refsgaard, J.C., Storm, B., 1995. Computer Models of Watershed Hydrology, Water Resource Publications, Highlands Ranch, CO.

Sarle, W.S., 1995. Stopped training and other remedies for overfitting, paper presented at the 27th Symposium on the Interface for Computing Science and Statistics, Carneigie Mellon University, Pittsburgh, Pa.

Schubert.S, Henderson.S.A, 1997. A statistical model to downscale local daily temperature extremes from synoptic-scale atmospheric circulation patterns in the Australian region, Climate Dynamics, 13, 223-234.

Singh, V.P., ASCE, F., and Woolhiser D.A., 2002. Mathematical Modeling of Watershed Hydrology, Journal of Hydrologic Engineering, 7 (4), 270-292.

Sivakumar, B, Jayawardena, A., Fernando, T., 2002. River flow forecasting: use of phase-space reconstruction and artificial neural networks approaches, Journal of Hydrology, 265, 225–245.

Thomas H.A., Fiering M.B., 1962. Mathematical synthesis of stream flow sequences for the analysis of river basin by simulation, in: A. Mass, et al. (Eds.), Design of Water Resources Systems, Harvard University Press, Cambridge, MA, 459–493.

Tokar, A.S., and P.A. Johnson, 1999. Rainfall-runoff modeling using artificial neural networks, Journal of Hydrologic Engineering, 4, 232-239.

Uhlenbrook, S., Frey, M., Leibundgut, C., Maloszewski, P., 2002. Hydrograph separations in a mesoscale mountainous basin at event and seasonal time scales, Water Resources Research 38 (6), 1-14.

Uhlenbrook, S., Sieber, A., 2005. On the value of experimental data to reduce the prediction uncertainty of a process-oriented catchment model, Environmental Modelling & Software 20 (1), 19-32.

Valenca, M., Ludermir, T., 2000. Monthly streamflow forecasting using a neural fuzzy network model, Proceedings of the Sixth Brazilian Symposium on Neural Networks, 6, 117–119.

Vernieuwe, H., Georgieva, O., Baets, B.D., Pauwels, V.R.N., Verhoest, N.E.C., Troch, P.D., 2005. Comparison of data-driven Takagi–Sugeno models of rainfall-discharge dynamics, Journal of Hydrology, 302, 173–186.

Wigley TML, Jones PD, Bri¤a KR, Smith G, 1990. Obtaining sub-grid-scale information from coarse resolution general circulation model output, J Geophys Res 95(D1): 1943-1953.

Wilby, R. L., Hay, L, E., Gutowski, Jr, W. J., Arritt, R. W., Takle, E. S., Pan, Z., Leavesley, G, H. and Clark, M. P., 1999. Hydrological responses to dynamically and statistically downscaled climate model output, Geophysical Research Letters, 27, 1199-1202.

Wilby, R.L. 1995. Simulation of precipitation by weather pattern and frontal analysis, Journal of Hydrology, 173, 91–109.

Wilby, R.L. and Wigley, T.M.L. 1997. Downscaling general circulation model output: a review of methods and limitation, Progress in Physical Geography, 21, 530–48.

Wilby, R.L., Dawson, C.W., Barrow, E.M., 2002. SDSM--a decision support tool for the assessment of regional climate change impacts, Environmental Modelling and Software 17, 147–159.

Yevjevich V., 1963. Fluctuations of Wet and Dry Years. Part-I. Research Data Assembly and Mathematical Models, Hydrology Paper 1, Colorado State University, Fort Collins, CO.

Zhang.B, Govindaraju. S, 2000. Prediction of watershed runoff using Bayesian concepts and modular neural networks, Water Resources Research, 36 (3) 753–762.

Appendix

Appendix A

Table A1: 14 day ahead reservoir inflow forecasts for Summer season using HBV annual model

Forecasting lags	without downscaled data			including downscaled data (TLFN)				including downscaled data (SDSM)			
	RMSE	r	R^2	RMSE	r	R^2	RMSE	RMSE	r	R^2	in RMSE
Flows forecasting 1-day-ahead	78.99	0.73	0.51	75.18	0.76	0.56	5%	85.36	0.75	0.43	-8%
Flows forecasting 2-day-ahead	85.57	0.68	0.41	83.52	0.71	0.44	2%	83.94	0.71	0.43	2%
Flows forecasting 3-day-ahead	95.44	0.60	0.25	89.24	0.65	0.35	7%	95.58	0.64	0.25	0%
Flows forecasting 4-day-ahead	98.04	0.52	0.20	94.90	0.58	0.25	3%	103.66	0.59	0.10	-6%
Flows forecasting 5-day-ahead	104.77	0.46	0.06	93.64	0.54	0.25	11%	107.62	0.54	0.01	-3%
Flows forecasting 6-day-ahead	101.81	0.45	0.09	95.38	0.50	0.20	6%	98.64	0.50	0.15	3%
Flows forecasting 7-day-ahead	102.22	0.42	0.06	95.38	0.47	0.18	**7%**	95.12	0.48	0.19	**7%**
Flows forecasting 8-day-ahead	100.36	0.44	0.08	94.80	0.47	0.18	**6%**	94.24	0.47	0.19	**6%**
Flows forecasting 9-day-ahead	101.86	0.39	0.05	94.00	0.47	0.19	**8%**	94.57	0.47	0.18	**7%**
Flows forecasting 10-day-ahead	100.86	0.41	0.07	94.79	0.46	0.18	**6%**	102.32	0.45	0.04	**-1%**
Flows forecasting 11-day-ahead	103.89	0.38	0.02	96.09	0.43	0.16	**8%**	99.28	0.43	0.10	**4%**
Flows forecasting 12-day-ahead	105.97	0.33	-0.02	98.59	0.39	0.12	**7%**	100.05	0.39	0.09	**6%**
Flows forecasting 13-day-ahead	111.03	0.26	-0.12	102.62	0.32	0.05	**8%**	101.55	0.35	0.07	**9%**
Flows forecasting 14-day-ahead	122.09	0.19	-0.35	106.13	0.27	-0.02	**13%**	109.01	0.30	-0.07	**11%**

Table A2: 14 day ahead reservoir inflow forecasts for Summer season using BNN annual model

Forecasting lags	**without downscaled data**			**including downscaled data (TLFN)**				**including downscaled data (SDSM)**			
	RMSE	r	R^2	RMSE	r	R^2	Decrease in RMSE	RMSE	r	R^2	Decrease in RMSE
Flows forecasting 1-day-ahead	38.40	0.94	0.88	40.69	0.94	0.87	-6%	36.45	0.95	0.90	5%
Flows forecasting 2-day-ahead	56.03	0.88	0.75	44.86	0.92	0.84	20%	49.77	0.90	0.80	11%
Flows forecasting 3-day-ahead	72.21	0.79	0.57	64.10	0.83	0.66	11%	69.83	0.81	0.60	3%
Flows forecasting 4-day-ahead	80.74	0.71	0.45	73.08	0.77	0.55	9%	86.94	0.73	0.37	-8%
Flows forecasting 5-day-ahead	93.07	0.62	0.26	84.79	0.67	0.38	9%	101.25	0.61	0.12	-9%
Flows forecasting 6-day-ahead	92.81	0.57	0.25	89.82	0.62	0.29	3%	96.85	0.59	0.18	-4%
Flows forecasting 7-day-ahead	94.59	0.53	0.20	92.93	0.59	0.22	**2%**	102.32	0.53	0.06	**-8%**
Flows forecasting 8-day-ahead	92.54	0.53	0.22	99.77	0.52	0.09	**-8%**	108.42	0.53	-0.07	**-17%**
Flows forecasting 9-day-ahead	94.72	0.49	0.18	103.69	0.49	0.01	**-9%**	105.69	0.49	-0.03	**-12%**
Flows forecasting 10-day-ahead	92.54	0.50	0.21	102.84	0.49	0.03	**-11%**	108.72	0.46	-0.08	**-17%**
Flows forecasting 11-day-ahead	91.67	0.50	0.23	107.95	0.45	-0.06	**-18%**	111.67	0.41	-0.14	**-22%**
Flows forecasting 12-day-ahead	93.08	0.48	0.21	109.45	0.45	-0.09	**-18%**	118.66	0.35	-0.28	**-27%**
Flows forecasting 13-day-ahead	101.72	0.35	0.06	113.84	0.39	-0.17	**-12%**	121.20	0.34	-0.33	**-19%**
Flows forecasting 14-day-ahead	96.79	0.41	0.15	117.52	0.39	-0.25	**-21%**	115.68	0.33	-0.21	**-20%**

Table A3: 14 day ahead reservoir inflow forecasts for Autumn season using HBV annual model

Forecasting lags	**without downscaled data**			**including downscaled data (TLFN)**				**including downscaled data (SDSM)**			
	RMSE	r	R^2	RMSE	r	R^2	Decrease in RMSE	RMSE	r	R^2	Decrease in RMSE
Flows forecasting 1-day-ahead	76.05	0.82	0.39	61.86	0.81	0.60	19%	62.92	0.78	0.58	17%
Flows forecasting 2-day-ahead	79.12	0.80	0.34	67.12	0.79	0.53	15%	70.03	0.79	0.49	11%
Flows forecasting 3-day-ahead	85.86	0.76	0.22	70.05	0.76	0.48	18%	81.34	0.75	0.30	5%
Flows forecasting 4-day-ahead	81.84	0.71	0.29	75.04	0.68	0.41	8%	78.82	0.68	0.35	4%
Flows forecasting 5-day-ahead	92.27	0.67	0.10	75.14	0.67	0.40	19%	86.64	0.66	0.21	6%
Flows forecasting 6-day-ahead	88.75	0.62	0.17	79.10	0.65	0.34	11%	84.74	0.63	0.24	5%
Flows forecasting 7-day-ahead	92.38	0.58	0.10	80.50	0.63	0.32	**13%**	81.69	0.61	0.30	**12%**
Flows forecasting 8-day-ahead	90.97	0.55	0.13	82.54	0.61	0.28	**9%**	85.13	0.58	0.24	**6%**
Flows forecasting 9-day-ahead	94.40	0.54	0.07	83.99	0.59	0.26	**11%**	86.54	0.57	0.22	**8%**
Flows forecasting 10-day-ahead	95.93	0.51	0.04	86.05	0.58	0.23	**10%**	99.67	0.54	-0.04	**-4%**
Flows forecasting 11-day-ahead	97.94	0.50	0.00	87.02	0.55	0.21	**11%**	91.04	0.51	0.14	**7%**
Flows forecasting 12-day-ahead	98.88	0.47	-0.01	88.11	0.54	0.20	**11%**	93.12	0.50	0.10	**6%**
Flows forecasting 13-day-ahead	102.98	0.46	-0.09	91.99	0.52	0.13	**11%**	93.48	0.48	0.10	**9%**
Flows forecasting 14-day-ahead	117.13	0.44	-0.41	94.09	0.49	0.09	**20%**	100.27	0.46	-0.03	**14%**

Table A4: 14 day ahead reservoir inflow forecasts for Autumn season using BNN annual model

Forecasting lags	**without downscaled data**			**including downscaled data (TLFN)**				**including downscaled data (SDSM)**			
	RMSE	r	R^2	RMSE	r	R^2	Decrease in RMSE	RMSE	r	R^2	Decrease in RMSE
Flows forecasting 1-day-ahead	39.77	0.91	0.83	43.71	0.90	0.80	-10%	62.92	0.78	0.58	-58%
Flows forecasting 2-day-ahead	46.25	0.89	0.78	44.76	0.89	0.79	3%	70.03	0.79	0.49	-51%
Flows forecasting 3-day-ahead	55.25	0.83	0.68	48.63	0.87	0.75	12%	81.34	0.75	0.30	-47%
Flows forecasting 4-day-ahead	68.86	0.73	0.50	66.33	0.78	0.54	4%	78.82	0.68	0.35	-14%
Flows forecasting 5-day-ahead	71.04	0.69	0.47	73.57	0.74	0.43	-4%	86.64	0.66	0.21	-22%
Flows forecasting 6-day-ahead	82.65	0.59	0.28	75.23	0.72	0.40	9%	84.74	0.63	0.24	-3%
Flows forecasting 7-day-ahead	81.34	0.57	0.30	82.77	0.67	0.28	**-2%**	81.69	0.61	0.30	**0%**
Flows forecasting 8-day-ahead	88.88	0.48	0.17	88.12	0.66	0.18	**1%**	85.13	0.58	0.24	**4%**
Flows forecasting 9-day-ahead	95.32	0.38	0.05	102.10	0.54	-0.09	**-7%**	86.54	0.57	0.22	**9%**
Flows forecasting 10-day-ahead	91.96	0.45	0.12	98.81	0.54	-0.02	**-7%**	99.67	0.54	-0.04	**-8%**
Flows forecasting 11-day-ahead	95.59	0.37	0.05	104.65	0.53	-0.14	**-9%**	91.04	0.51	0.14	**5%**
Flows forecasting 12-day-ahead	98.20	0.37	0.00	107.01	0.49	-0.18	**-9%**	93.12	0.50	0.10	**5%**
Flows forecasting 13-day-ahead	94.64	0.38	0.08	103.36	0.55	-0.10	**-9%**	93.48	0.48	0.10	**1%**
Flows forecasting 14-day-ahead	96.43	0.35	0.05	104.51	0.52	-0.12	**-8%**	100.27	0.46	-0.03	**-4%**

Table A5: 14 day ahead reservoir inflow forecasts for Winter season using HBV annual model

Forecasting lags	without downscaled data			including downscaled data (TLFN)				including downscaled data (SDSM)			
	RMSE	r	R^2	RMSE	r	R^2	Decrease in RMSE	RMSE	r	R^2	Decrease in RMSE
Flows forecasting 1-day-ahead	44.92	0.76	0.21	55.82	0.77	-0.22	-24%	56.24	0.74	-0.24	-25%
Flows forecasting 2-day-ahead	44.77	0.75	0.15	61.11	0.72	-0.59	-36%	61.65	0.71	-0.62	-38%
Flows forecasting 3-day-ahead	44.16	0.74	0.09	57.94	0.77	-0.56	-31%	58.03	0.72	-0.57	-31%
Flows forecasting 4-day-ahead	43.53	0.72	0.05	48.55	0.69	-0.18	-12%	49.15	0.68	-0.21	-13%
Flows forecasting 5-day-ahead	44.48	0.71	-0.06	51.86	0.70	-0.44	-17%	51.09	0.71	-0.40	-15%
Flows forecasting 6-day-ahead	46.13	0.68	-0.23	52.62	0.68	-0.61	-14%	54.75	0.67	-0.74	-19%
Flows forecasting 7-day-ahead	45.63	0.67	-0.39	53.55	0.66	-0.91	**-17%**	52.73	0.65	-0.85	**-16%**
Flows forecasting 8-day-ahead	45.67	0.64	-0.52	52.65	0.64	-1.02	**-15%**	49.09	0.61	-0.76	**-7%**
Flows forecasting 9-day-ahead	52.20	0.62	-1.11	54.19	0.63	-1.27	**-4%**	52.93	0.65	-1.17	**-1%**
Flows forecasting 10-day-ahead	50.99	0.61	-1.16	53.83	0.63	-1.40	**-6%**	52.85	0.62	-1.31	**-4%**
Flows forecasting 11-day-ahead	52.71	0.59	-1.52	51.87	0.60	-1.44	**2%**	50.11	0.62	-1.28	**5%**
Flows forecasting 12-day-ahead	52.37	0.57	-1.54	51.97	0.58	-1.50	**1%**	52.22	0.58	-1.52	**0%**
Flows forecasting 13-day-ahead	53.44	0.52	-1.79	51.87	0.52	-1.63	**3%**	50.19	0.53	-1.46	**6%**
Flows forecasting 14-day-ahead	60.83	0.48	-2.82	49.65	0.51	-1.55	**18%**	48.65	0.53	-1.44	**20%**

Table A6: 14 day ahead reservoir inflow forecasts for Winter season using BNN annual model

Forecasting lags	without downscaled data			including downscaled data (TLFN)				including downscaled data (SDSM)			
	RMSE	r	R^2	RMSE	r	R^2	Decrease in RMSE	RMSE	r	R^2	Decrease in RMSE
Flows forecasting 1-day-ahead	26.72	0.85	0.72	28.96	0.83	0.67	-8%	24.92	0.87	0.76	7%
Flows forecasting 2-day-ahead	27.68	0.82	0.67	26.26	0.85	0.71	5%	27.81	0.83	0.67	0%
Flows forecasting 3-day-ahead	28.61	0.79	0.62	27.29	0.83	0.65	5%	35.13	0.72	0.43	-23%
Flows forecasting 4-day-ahead	30.20	0.75	0.54	29.76	0.78	0.56	1%	31.51	0.73	0.50	-4%
Flows forecasting 5-day-ahead	29.86	0.73	0.52	33.32	0.72	0.41	-12%	35.72	0.71	0.32	-20%
Flows forecasting 6-day-ahead	40.52	0.63	0.05	31.38	0.72	0.43	23%	35.51	0.64	0.27	12%
Flows forecasting 7-day-ahead	45.48	0.54	-0.38	38.25	0.59	0.02	**16%**	32.98	0.64	0.27	**27%**
Flows forecasting 8-day-ahead	39.16	0.55	-0.12	32.25	0.67	0.24	**18%**	40.66	0.50	-0.21	**-4%**
Flows forecasting 9-day-ahead	42.72	0.42	-0.41	35.53	0.60	0.02	**17%**	40.01	0.37	-0.24	**6%**
Flows forecasting 10-day-ahead	45.45	0.43	-0.71	32.60	0.62	0.12	**28%**	36.49	0.47	-0.10	**20%**
Flows forecasting 11-day-ahead	41.10	0.43	-0.53	31.29	0.58	0.11	**24%**	34.35	0.46	-0.07	**16%**
Flows forecasting 12-day-ahead	53.15	0.36	-1.61	32.83	0.46	0.00	**38%**	34.68	0.51	-0.11	**35%**
Flows forecasting 13-day-ahead	42.43	0.44	-0.76	36.43	0.35	-0.30	**14%**	30.45	0.50	0.10	**28%**
Flows forecasting 14-day-ahead	45.27	0.24	-1.12	30.90	0.48	0.01	**32%**	37.27	0.38	-0.43	**18%**

Table A7: 14 day ahead Serpent river flow forecasts for Summer season using HBV annual model

Forecasting lags	without downscaled-Testing			including TLFN-testing				including SDSM-testing			
	RMSE	r	R^2	RMSE	r	R^2	Decrease in RMSE	RMSE	r	R^2	Decrease in RMSE
Flows forecasting 1-day-ahead	16.71	0.76	0.48	14.95	0.78	0.58	11%	14.22	0.79	0.62	15%
Flows forecasting 2-day-ahead	18.64	0.68	0.35	17.00	0.70	0.46	9%	16.82	0.71	0.47	10%
Flows forecasting 3-day-ahead	22.08	0.60	0.09	20.42	0.64	0.22	7%	20.92	0.65	0.19	5%
Flows forecasting 4-day-ahead	22.32	0.54	0.06	21.64	0.60	0.11	3%	21.31	0.60	0.14	5%
Flows forecasting 5-day-ahead	20.72	0.53	0.18	20.12	0.56	0.22	3%	19.78	0.54	0.25	5%
Flows forecasting 6-day-ahead	21.45	0.49	0.09	24.29	0.53	-0.16	-13%	21.88	0.56	0.06	-2%
Flows forecasting 7-day-ahead	21.40	0.48	0.08	22.10	0.54	0.01	**-3%**	22.73	0.55	-0.04	**-6%**
Flows forecasting 8-day-ahead	20.60	0.50	0.14	21.19	0.55	0.09	**-3%**	20.22	0.53	0.17	**2%**
Flows forecasting 9-day-ahead	20.40	0.50	0.15	21.07	0.54	0.10	**-3%**	21.10	0.52	0.10	**-3%**
Flows forecasting 10-day-ahead	21.05	0.47	0.11	19.51	0.54	0.23	**7%**	20.14	0.53	0.18	**4%**
Flows forecasting 11-day-ahead	21.56	0.45	0.07	20.63	0.51	0.15	**4%**	20.60	0.49	0.15	**4%**
Flows forecasting 12-day-ahead	22.43	0.40	0.00	20.67	0.47	0.15	**8%**	21.04	0.47	0.12	**6%**
Flows forecasting 13-day-ahead	23.14	0.37	-0.06	22.15	0.42	0.03	**4%**	22.72	0.41	-0.02	**2%**
Flows forecasting 14-day-ahead	23.64	0.34	-0.11	21.37	0.39	0.09	**10%**	21.46	0.38	0.09	**9%**

Table A8: 14 day ahead Serpent river flow forecasts for Summer season using BNN annual model

Forecasting lags	without downscaled-Testing			including TLFN-testing				including SDSM-testing			
	RMSE	r	R^2	RMSE	r	R^2	Decrease in RMSE	RMSE	r	R^2	Decrease in RMSE
Flows forecasting 1-day-ahead	6.64	0.96	0.92	5.90	0.97	0.94	11%	7.21	0.95	0.90	-9%
Flows forecasting 2-day-ahead	12.46	0.85	0.71	12.51	0.86	0.71	0%	12.16	0.87	0.73	2%
Flows forecasting 3-day-ahead	17.10	0.73	0.46	17.92	0.74	0.40	-5%	16.43	0.74	0.50	4%
Flows forecasting 4-day-ahead	18.72	0.63	0.34	15.28	0.76	0.56	18%	19.11	0.67	0.31	-2%
Flows forecasting 5-day-ahead	19.94	0.58	0.24	18.22	0.66	0.36	9%	18.74	0.65	0.33	6%
Flows forecasting 6-day-ahead	20.42	0.56	0.18	18.93	0.62	0.29	7%	20.31	0.60	0.19	1%
Flows forecasting 7-day-ahead	22.23	0.41	0.00	18.52	0.64	0.31	**17%**	20.28	0.53	0.17	**9%**
Flows forecasting 8-day-ahead	19.58	0.55	0.22	19.87	0.57	0.20	**-2%**	21.29	0.49	0.08	**-9%**
Flows forecasting 9-day-ahead	20.15	0.48	0.18	19.97	0.56	0.19	**1%**	20.85	0.48	0.12	**-3%**
Flows forecasting 10-day-ahead	21.84	0.41	0.04	21.38	0.53	0.08	**2%**	20.90	0.46	0.12	**4%**
Flows forecasting 11-day-ahead	19.70	0.48	0.22	21.35	0.45	0.09	**-8%**	23.09	0.38	-0.07	**-17%**
Flows forecasting 12-day-ahead	20.62	0.42	0.16	23.05	0.43	-0.05	**-12%**	21.39	0.41	0.09	**-4%**
Flows forecasting 13-day-ahead	21.01	0.39	0.13	23.24	0.40	-0.06	**-11%**	23.34	0.29	-0.07	**-11%**
Flows forecasting 14-day-ahead	19.80	0.49	0.22	20.96	0.47	0.13	**-6%**	21.84	0.39	0.05	**-10%**

Table A9: 14 day ahead Serpent river flow forecasts for Autumn season using HBV annual model

Forecasting lags	without downscaled-Testing			including TLFN-testing				including SDSM-testing			
	RMSE	r	R^2	RMSE	r	R^2	Decrease in RMSE	RMSE	r	R^2	Decrease in RMSE
Flows forecasting 1-day-ahead	12.51	0.87	0.76	14.06	0.87	0.69	-12%	13.68	0.86	0.71	-9%
Flows forecasting 2-day-ahead	15.34	0.80	0.63	14.97	0.83	0.65	2%	14.41	0.85	0.68	6%
Flows forecasting 3-day-ahead	18.32	0.74	0.47	19.46	0.77	0.41	-6%	18.42	0.79	0.47	-1%
Flows forecasting 4-day-ahead	20.30	0.66	0.35	23.04	0.71	0.16	-13%	20.21	0.74	0.36	0%
Flows forecasting 5-day-ahead	21.94	0.58	0.24	21.11	0.64	0.29	4%	19.22	0.67	0.41	12%
Flows forecasting 6-day-ahead	23.39	0.50	0.13	24.96	0.54	0.00	-7%	22.75	0.61	0.17	3%
Flows forecasting 7-day-ahead	24.48	0.46	0.04	24.09	0.53	0.07	**2%**	22.59	0.61	0.18	**8%**
Flows forecasting 8-day-ahead	24.66	0.43	0.01	24.06	0.54	0.06	**2%**	21.67	0.59	0.24	**12%**
Flows forecasting 9-day-ahead	24.93	0.41	-0.02	24.21	0.52	0.04	**3%**	21.84	0.57	0.22	**12%**
Flows forecasting 10-day-ahead	25.15	0.40	-0.05	25.04	0.48	-0.04	**0%**	23.47	0.55	0.09	**7%**
Flows forecasting 11-day-ahead	25.65	0.37	-0.10	25.72	0.45	-0.10	**0%**	23.44	0.51	0.09	**9%**
Flows forecasting 12-day-ahead	26.22	0.34	-0.15	25.67	0.44	-0.10	**2%**	25.21	0.49	-0.06	**4%**
Flows forecasting 13-day-ahead	26.64	0.30	-0.19	26.96	0.43	-0.22	**-1%**	26.41	0.47	-0.17	**1%**
Flows forecasting 14-day-ahead	27.56	0.25	-0.27	26.22	0.40	-0.15	**5%**	25.43	0.45	-0.08	**8%**

Table A10: 14 day ahead Serpent river flow forecasts for Autumn season using BNN annual model

Forecasting lags	without downscaled-Testing			including TLFN-testing				including SDSM-testing			
	RMSE	r	R^2	RMSE	r	R^2	Decrease in RMSE	RMSE	r	R^2	Decrease in RMSE
Flows forecasting 1-day-ahead	7.17	0.96	0.92	5.42	0.98	0.95	24%	6.78	0.97	0.93	6%
Flows forecasting 2-day-ahead	16.12	0.82	0.60	12.60	0.88	0.75	22%	13.47	0.86	0.72	16%
Flows forecasting 3-day-ahead	21.49	0.68	0.28	20.90	0.69	0.32	3%	19.09	0.75	0.43	11%
Flows forecasting 4-day-ahead	22.10	0.62	0.23	15.98	0.78	0.60	28%	26.88	0.67	-0.14	-22%
Flows forecasting 5-day-ahead	24.03	0.52	0.08	26.15	0.58	-0.08	-9%	27.24	0.60	-0.18	-13%
Flows forecasting 6-day-ahead	27.06	0.43	-0.17	25.28	0.58	-0.02	7%	31.77	0.53	-0.61	-17%
Flows forecasting 7-day-ahead	29.02	0.31	-0.36	26.85	0.52	-0.16	**7%**	30.04	0.49	-0.45	**-4%**
Flows forecasting 8-day-ahead	30.92	0.29	-0.55	27.09	0.51	-0.19	**12%**	29.90	0.44	-0.45	**3%**
Flows forecasting 9-day-ahead	29.05	0.25	-0.38	31.20	0.41	-0.60	**-7%**	30.69	0.43	-0.54	**-6%**
Flows forecasting 10-day-ahead	29.71	0.24	-0.46	31.40	0.41	-0.63	**-6%**	30.37	0.41	-0.53	**-2%**
Flows forecasting 11-day-ahead	30.53	0.13	-0.55	32.28	0.34	-0.74	**-6%**	29.33	0.42	-0.43	**4%**
Flows forecasting 12-day-ahead	31.82	0.17	-0.69	31.22	0.40	-0.63	**2%**	32.37	0.36	-0.75	**-2%**
Flows forecasting 13-day-ahead	33.63	0.04	-0.89	33.95	0.37	-0.93	**-1%**	30.06	0.37	-0.51	**11%**
Flows forecasting 14-day-ahead	28.54	0.24	-0.37	31.62	0.31	-0.68	**-11%**	29.72	0.32	-0.48	**-4%**

Table A11: 14 day ahead Serpent river flow forecasts for Winter season using HBV annual model

Forecasting lags	**without downscaled-Testing**			**including TLFN-testing**				**including SDSM-testing**			
	RMSE	r	R^2	RMSE	r	R^2	Decrease in RMSE	RMSE	r	R^2	Decrease in RMSE
Flows forecasting 1-day-ahead	19.32	0.53	-3.09	21.33	0.55	-3.98	-10%	19.26	0.50	-3.07	0%
Flows forecasting 2-day-ahead	19.87	0.50	-3.41	21.59	0.53	-4.21	-9%	21.91	0.53	-4.36	-10%
Flows forecasting 3-day-ahead	18.96	0.48	-3.14	21.05	0.50	-4.10	-11%	20.90	0.49	-4.03	-10%
Flows forecasting 4-day-ahead	19.81	0.46	-3.60	21.69	0.48	-4.52	-10%	21.59	0.48	-4.47	-9%
Flows forecasting 5-day-ahead	19.72	0.45	-3.56	21.21	0.37	-4.27	-8%	21.70	0.48	-4.52	-10%
Flows forecasting 6-day-ahead	20.12	0.39	-3.74	22.39	0.37	-4.87	-11%	22.15	0.38	-4.75	-10%
Flows forecasting 7-day-ahead	20.03	0.38	-3.70	21.68	0.33	-4.51	**-8%**	21.82	0.42	-4.58	**-9%**
Flows forecasting 8-day-ahead	20.01	0.36	-3.66	21.03	0.41	-4.15	**-5%**	21.80	0.33	-4.53	**-9%**
Flows forecasting 9-day-ahead	19.31	0.38	-3.30	21.29	0.40	-4.23	**-10%**	21.14	0.40	-4.16	**-10%**
Flows forecasting 10-day-ahead	20.01	0.34	-3.57	21.80	0.36	-4.42	**-9%**	22.05	0.37	-4.55	**-10%**
Flows forecasting 11-day-ahead	19.81	0.34	-3.42	21.56	0.36	-4.23	**-9%**	21.58	0.37	-4.24	**-9%**
Flows forecasting 12-day-ahead	19.77	0.34	-3.33	21.48	0.35	-4.11	**-9%**	22.04	0.36	-4.38	**-11%**
Flows forecasting 13-day-ahead	19.78	0.35	-3.25	22.13	0.36	-4.33	**-12%**	22.34	0.39	-4.43	**-13%**
Flows forecasting 14-day-ahead	19.70	0.35	-3.15	22.08	0.36	-4.21	**-12%**	22.25	0.37	-4.29	**-13%**

Table A12: 14 day ahead Serpent river flow forecasts for Winter season using BNN annual model

Forecasting lags	without downscaled-Testing			including TLFN-testing				including SDSM-testing			
	RMSE	r	R^2	RMSE	r	R^2	Decrease in RMSE	RMSE	r	R^2	Decrease in RMSE
Flows forecasting 1-day-ahead	3.35	0.94	0.88	3.16	0.95	0.89	6%	6.44	0.79	0.55	-92%
Flows forecasting 2-day-ahead	10.01	0.65	-0.12	6.24	0.80	0.57	38%	5.43	0.84	0.67	46%
Flows forecasting 3-day-ahead	9.00	0.64	0.07	4.91	0.89	0.72	45%	9.27	0.61	0.01	-3%
Flows forecasting 4-day-ahead	7.15	0.74	0.40	10.50	0.69	-0.29	-47%	9.51	0.59	-0.06	-33%
Flows forecasting 5-day-ahead	9.40	0.58	-0.03	8.31	0.67	0.19	12%	10.16	0.55	-0.21	-8%
Flows forecasting 6-day-ahead	10.22	0.51	-0.22	10.53	0.54	-0.30	-3%	10.24	0.52	-0.23	0%
Flows forecasting 7-day-ahead	9.27	0.61	-0.01	8.71	0.60	0.11	**6%**	9.65	0.61	-0.09	**-4%**
Flows forecasting 8-day-ahead	11.21	0.47	-0.46	10.27	0.50	-0.23	**8%**	11.45	0.49	-0.53	**-2%**
Flows forecasting 9-day-ahead	8.70	0.52	0.13	9.10	0.50	0.04	**-5%**	8.93	0.61	0.08	**-3%**
Flows forecasting 10-day-ahead	11.29	0.52	-0.45	10.24	0.57	-0.20	**9%**	10.62	0.41	-0.29	**6%**
Flows forecasting 11-day-ahead	10.11	0.32	-0.15	10.73	0.49	-0.30	**-6%**	9.73	0.55	-0.07	**4%**
Flows forecasting 12-day-ahead	10.78	0.37	-0.29	10.67	0.51	-0.26	**1%**	9.97	0.57	-0.10	**7%**
Flows forecasting 13-day-ahead	10.94	0.39	-0.30	9.23	0.61	0.07	**16%**	10.37	0.58	-0.17	**5%**
Flows forecasting 14-day-ahead	12.34	0.25	-0.63	10.90	0.50	-0.27	**12%**	9.66	0.53	0.00	**22%**

Appendix B

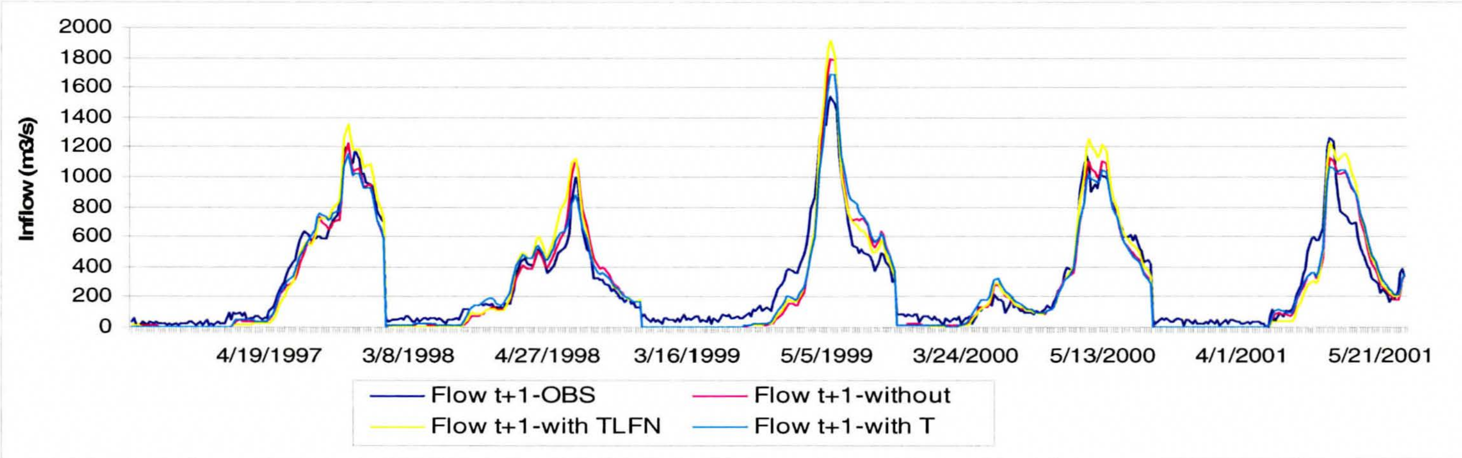

Figure B1 (a): One day ahead reservoir inlfow forecasts (HBV seasonal model) for Spring with and without including downscaled data

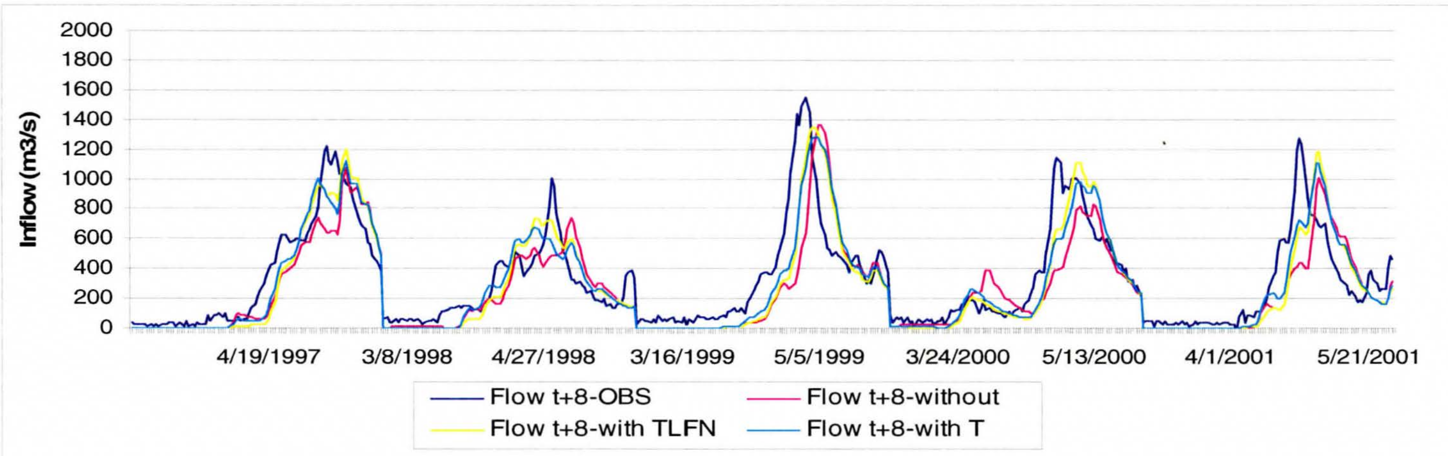

Figure B1 (b): Eight day ahead reservoir inlfow forecasts (HBV seasonal model) for Spring with and without including downscaled data

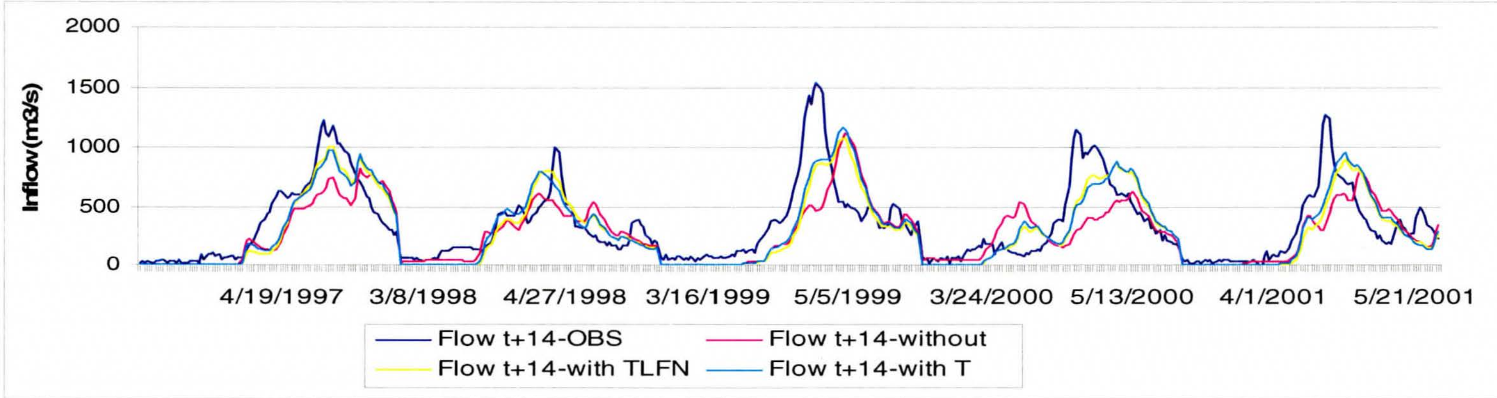

Figure B1 (c): Fourteen day ahead reservoir inlfow forecasts (HBV seasonal model) for Spring with and without including downscaled data

Figure B1: Short term reservoir inlfow forecasts (HBV seasonal model) for Spring with and without including downscaled data

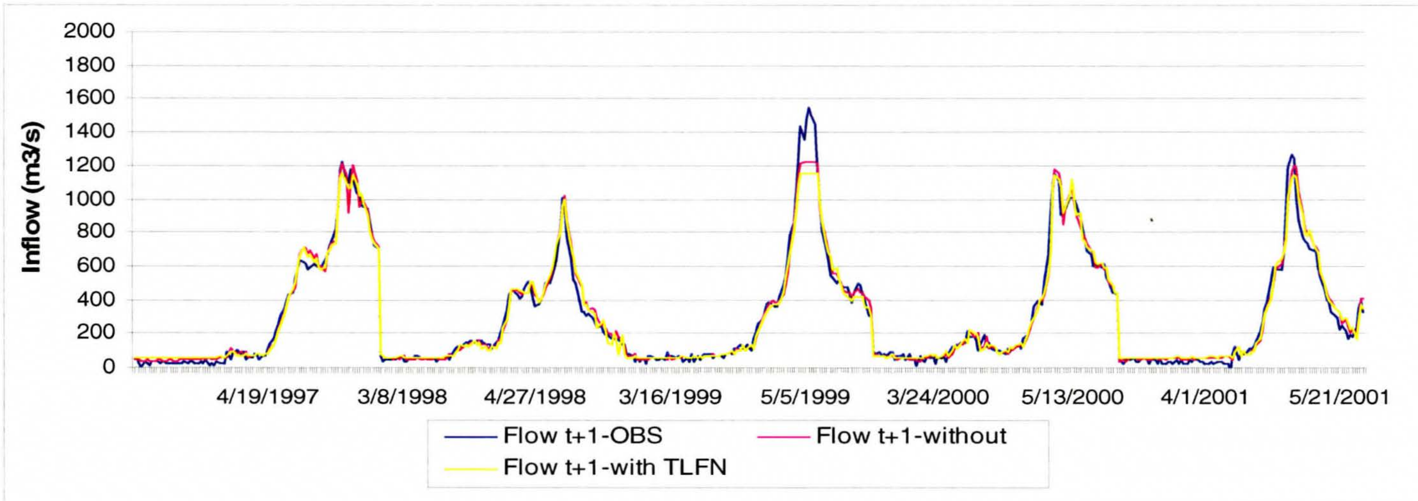

Figure B2 (a): One day ahead reservoir inlfow forecasts (BNN seasonal model) for Spring with and without including downscaled data

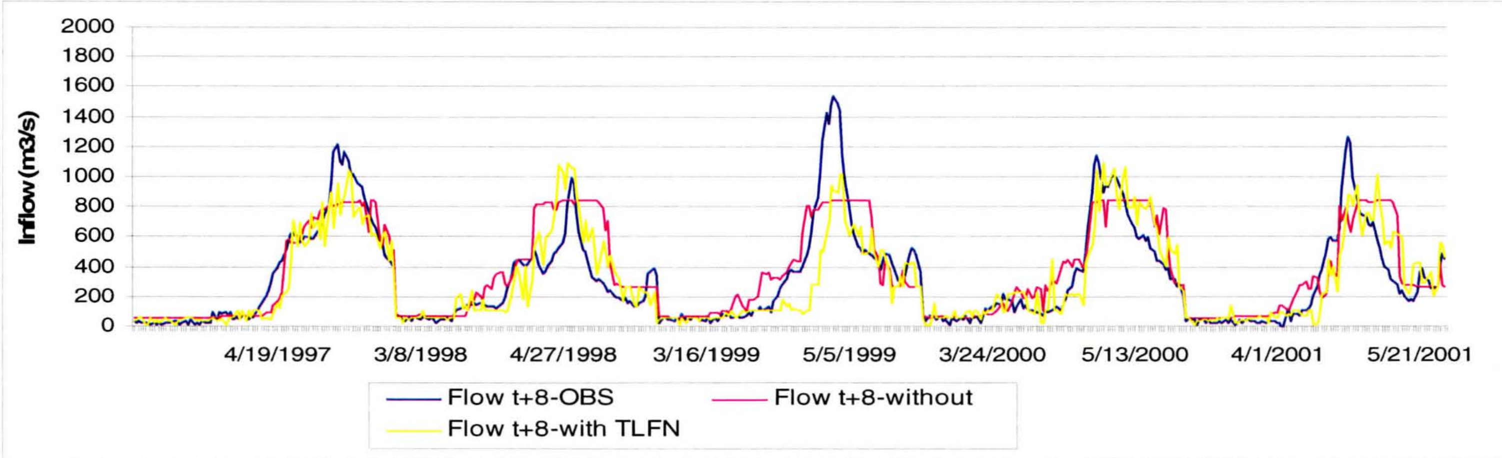

Figure B2 (b): Eight day ahead reservoir inlfow forecasts (BNN seasonal model) for Spring with and without including downscaled data

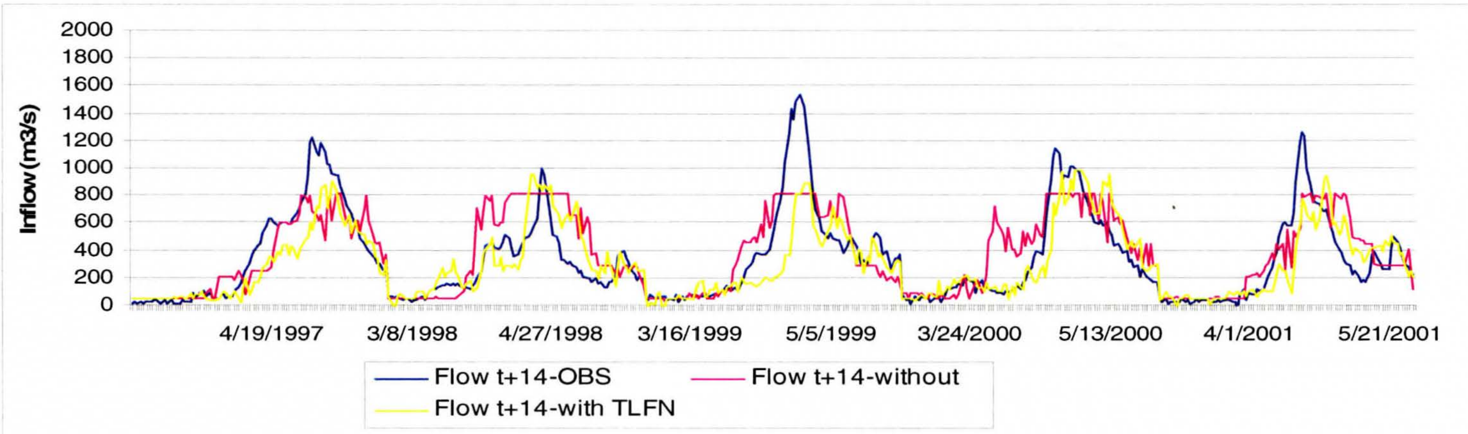

Figure B2 (c): Fourteen day ahead reservoir inlfow forecasts (BNN seasonal model) for Spring with and without including downscaled data

Figure B2: Short term reservoir inlfow forecasts (BNN seasonal model) for Spring with and without including downscaled data